EFFECT OF DRUG PHYSICOCHEMICAL PROPERTIES ON THE RELEASE FROM LIPOSOMAL SYSTEMS IN VITRO AND IN VIVO

Dissertation
zur Erlangung des Grades
„Doktor der Naturwissenschaften“
Im Promotionsfach Pharmazie

am Fachbereich Chemie, Pharmazie und Geowissenschaften
der Johannes Gutenberg-Universität Mainz
im Mainz

Gamal Ahmed

geb. in Assiut, Ägypten

Mainz, den 26.01.2009

Contents

List of abbreviations

Adv. Colloid Interface Sci.	Advances in Colloid and Interface Science
Adv. Drug Delivery Rev.	Advanced Drug Delivery Reviews
AT	Atenolol
BBB	blood brain barrier
Bioch. Biophy. Res. Comm	*Biochemical and Biophysical Research Communications*
Biochim. Biophys. Acta	Biochimica et Biophysica Acta
Biophys. J .	Biophysical Journal
B-NCT	Boron-capture therapy
Braz. arch. biol. technol.	*Brazilian Archives of Biology and Technology*
Canc. Chemo. Pharmaco.	*Cancer Chemotherapy and Pharmacology*
cGPC	Centrifugation gel permeation chromatography
cGPC	Centrifugation gel permeation chromatography
Ci	Curie (a unit of radioactivity)
DDS	Drug Delivery Systems
DLS	dynamic light scattering
DMPC	1,2-Dimyristoyl-sn-glycero-3-phosphatidylcholine
DNS	Dinitrosalicylic acid
Drug Dev. Ind. Pharm.	Drug Development and Industrial Pharmacy
DSPC	1,2-Distearoyl-sn-glycero-3-phosphatidylcholin
DTPA	Diethylenetriaminetetraacetic acid
EE	Encapsulation Efficiency
Er	Erbium
Et	Ethanol
FDA	Food and drug administration
FDG	Fluorodeoxyglucose
FTS	Freeze-thawing sonication

Gd-NCT	Gadolinium-capture therapy
Glu	Glucose
IRT	Indirect radiation therapy
IVIVC	In vitro In vivo Correlation
J. Colloid Interface Sci.	Journal of Colloid and Interface Science
J. Food Sci.	Journal of Food Science
J. Mater. Sci. - Mater. Med.	Journal of Materials Science Materials in Medicine
J. Membr. Biol.	Journal of Membrane Biology
LDA	Laser diffraction Analysis
LUV	Large Unilamellar Vesicle
MAT	Mean absorption time
MBq	megabecquere
MD	Model Distribution
MDT	Mean dissolution time
MLV	Multilamellar Large Vesicle
MRT	Mean residence time
MT	Metoprolol
MWCO	molecular weight cut-off
NCT	neutron capture therapy
PAT	photon activation therapy
PBS	phosphate-buffered saline
PC	Phosphatidyl choline
PCS	Photon Correlation Spectrometry
PD	Pindolol
PDT	photodynamic light therapy
PEG	polymer polyethylene glycol
PET	positron emission tomography
Ph 90H	Phospholipone 90H
Pharm. Res.	Pharmaceutical Research
Pharm. Sci. Technol. Today	Pharmaceutical Science & Technology Today
PIDS	Polarization Intensity Differential Scattering

Pm	Particle diameter
PP	Propranolol
PXT	photodynamic X-ray therapy
QELS	quasi-elastic light scattering
RE	Reverse-phase evaporation
RES	reticuloendothelial system
ROIs	Regions of interests
rpm	rotation per minute
RT	Radiation therapy
SUV	Small Unilamellar Vesicle
Syb	soybean
t½	Elimination half life
Tc	Phase transition temperature
USP	United State Pharmacopoeia
UV	Ultraviolet
WHb	Whole body

Chapter I: Introduction and Aim of thesis

I. Introduction

I.1. Cancer

Cancer (medical term: malignant neoplasm) is a class of diseases in which a group of cells display the traits of uncontrolled growth (growth and division beyond the normal limits), invasion (intrusion on and destruction of adjacent tissues), and sometimes metastasis (spread to other locations in the body via lymph or blood). These three malignant properties of cancers differentiate them from benign tumors, which are self-limited, do not invade or metastasize.

Cancer may affect people at all ages, even fetuses, but risk for the more common varieties tends to increase with age (*Cancer Research UK, 2007*).

Cancer in Europe

In Europe, there were over two million (2 288 100) incident cases of cancer in 2006 and over one million cancer deaths (1 165 500). Cancer is the second frequent cause of death in Europe (*Ferlay, et al., 2007*).

Cancer in Germany

After cardiovascular diseases, cancer is the second killer disease in Germany. As the age of the population increases, the number of cancer patients has increased proportionally. Approximately 424,250 people were diagnosed with cancer, including about 218,250 men and 206,000 women. About 209, 000 of people diagnosed with cancer died (109,631 men and 99,945 women). Among the estimated number of newly diagnosed cancer patients, prostate cancer in men and breast cancer in women are the most frequent cancers, followed by colorectal cancer in both men and women. Lung cancer is the third most frequent form of cancer, both in women and men (*Bertz, et al., 2006*).

I.2. Methods of Cancer treatment

Cancer is treated with surgery, radiation therapy, chemotherapy, hormone therapy, or biological therapy. Patients with cancer are often treated by a team of specialists, which may include a medical oncologist (specialist in cancer treatment), a surgeon, a radiation oncologist (specialist in radiation therapy), and others.

The doctors may decide to use one treatment method or a combination of methods. The choice of treatment depends on the type and location of the cancer, the stage of the disease, the patient's age and general health, and other factors (*http://seniorhealth.about.com/library/conditions/blcancer13.htm*)

Radiation therapy (RT) *(http://www.radiologyinfo.org)*

Radiation therapy is the most effective non-surgical cancer therapy method. Radiation therapy is applied in two general ways:

1. Radiotherapy after surgery and this is used to remove possible residual cancer cells in the environment of a tumour after surgery
2. Radiotherapy to abolish a tumour, which cannot be removed by surgery

Radiation therapy can be applied by two techniques; direct radiation therapy and indirect radiation therapy (IRT).

Indirect radiation therapy (IRT)

Indirect radiation therapy (IRT) inactivates cancer cells by secondary radiation products, evolving from a specific target inside the body upon local absorption of external radiation (*Nawroth, et al., 2007*).

IRT shows three advantages:

1. The higher effectivity resulting from the high number of auger-electrons evolving from a single absorbed neutron or photon (n>>1)

2. The selectivity of the radiation absorption resulting from the high absorption of the target element / isotope
3. The selectivity in absorption location by deposition of the radiation target element / isotope in the area of interest, which enables a combination of target deposition and irradiation methods

There are three possible methods for IRT with incorporated target material as "antenna" for the applied therapeutic beam:

1. with X-ray radiation as "photon activation therapy" PAT, also known as "photodynamic X-ray therapy" PXT
2. with "neutron capture therapy" NCT, which can be divided into Boron-capture therapy B-NCT and Gadolinium-capture therapy Gd-NCT
3. with "photodynamic light therapy" PDT, which is applicable only for tumours of the skin due to the low penetration depth of infra-red light

In each case secondary radiation products result in: free radicals, X-ray- and UV-fluorescence and singulett-oxygen. All these products are effective only nm- and μm-area (*Nawroth, et al., 2007*).

The healing effect of IRT, cell inactivation by secondary radiation products after specific beam absorption, is superimposed by unspecific radiation absorption elsewhere, which may cause later cancer itself by radiation damage and accumulation of DNA lesions (Figure 1).

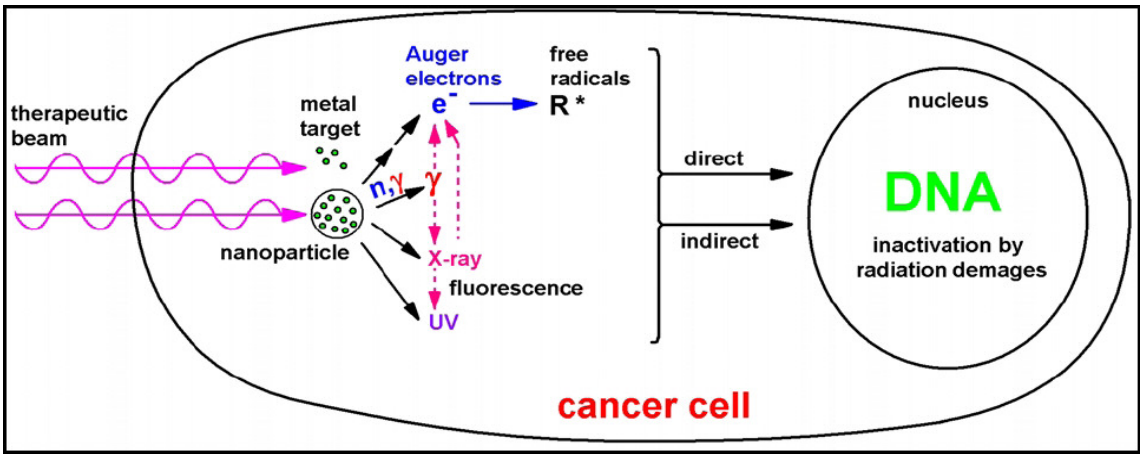

Figure 1: Indirect radiation therapy (IRT) inactivates cancer cells by secondary radiation products of short range upon specific absorption at the target. The tumor DNA is hit directly or indirectly (*Nawroth, et al., 2007*).

The ratio of healing to damage effects can be improved if the target is concentrated in nanoparticles, which can be localized and concentrated at the tumor site by hyperosmotic deposition, magnetic forces or antibodies. These magnetic target nanoparticles are based on two principles (Figure 2).

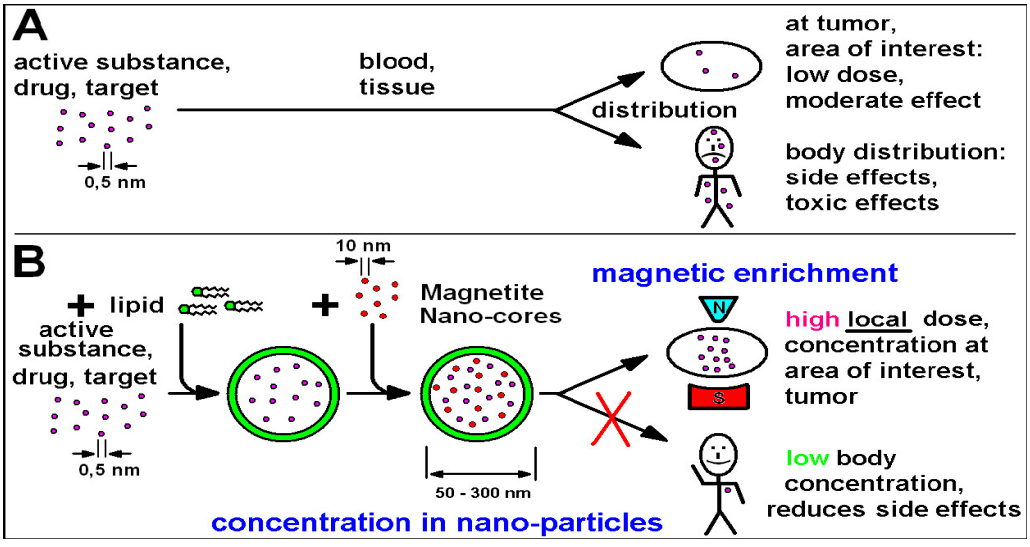

Figure 2: Nanotherapy improves the effect of molecular active substances (drug, target) twice: about 1.000.000 molecules are oncentrated in nanoparticles, which are enriched at the tumor locally. Thus unfavorable side effects of conventional therapy are reduced.

I.3. Drug delivery systems (DDS)

Drug delivery is a way for improving the delivery characteristics of drugs. Drug delivery technologies have many clinical advantages including control of drug concentration in the blood, improved safety and efficacy, improved patient compliance and ease to use, expanded indications, feasibility of incorporation of both hydrophilic and hydrophobic substances and feasibility of variable routes of administration, including oral administration and inhalation (*Gorman et al., 2003; ,Gelperina et al., 2005*). There has been a growing interest in the use of chemical (prodrugs), physical (liposomes, microspheres, polymer conjugates and ferrofluids (Figure 3) and biological methods (monoclonal antibodies) for drug delivery and targeting (*Prescott & Nimmo, 1989*).

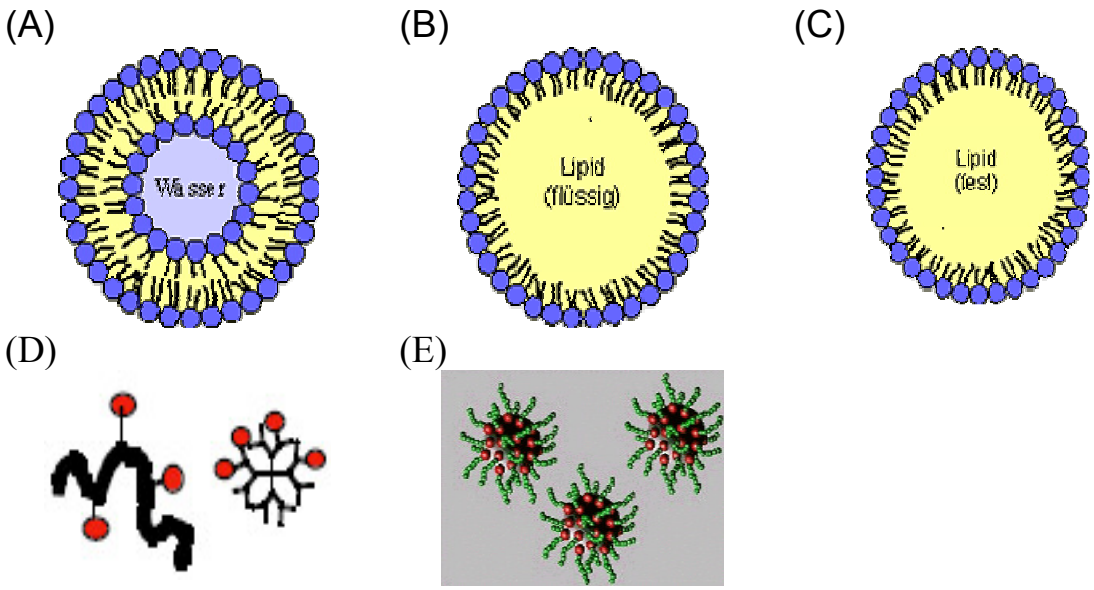

Figure 3: Structure of nanodispersed systems

(A) Liposome (Lipid bilayer enclosing an aqueous core)
(B) Nanoemulsion (Lipid monolayer enclosing a liquid lipid core)
(C) Lipid nanoparticle (Lipid monolayer enclosing a solid lipid core);
(D) Polymer conjugates;
(E) Ferrofluids

I.3.1. Polymer conjugates

Polymer conjugates are becoming established as a new approach towards improved cancer therapy. These water-soluble, hybrid constructs fall into two main categories: polymer-protein conjugates (already available as licensed products), and polymer-drug conjugates (currently in clinical development). Polyethyleneglycol conjugation of proteins is accepted as a means to reduce immunogenicity, prolong plasma half-life and enhance protein stability. Polymer-drug conjugation promotes tumor targeting by the enhanced permeation and retention effect. Eleven polymer-drug conjugates have entered clinical development and activity has already been observed in chemotherapy refractory patients. Certain compounds have also demonstrated a marked reduction in drug toxicity (*Duncan and Thanou, 2003*).

The clinical aims of polymer–drug conjugation are to achieve improved drug targeting to the tumour, to reduce drug toxicity (by limiting access to the sites of toxicity) and to overcome the mechanisms of drug resistance.

First generation conjugates sought to improve the therapeutic index of drugs already in routine clinical use (for example, doxorubicin, camptothecins, paclitaxel and platinates including carboplatin and diaminocyclohexane (DACH)-platinates).

Conjugation to hydrophilic polymeric carriers can also improve the water solubility of hydrophobic drugs such as doxorubicin and paclitaxel, enabling easier formulation and patient administration. The typical structure of polymer–drug conjugates is shown in Figure 3D.

I.3.2. Nanoemulsions

Nanoemulsions can be defined as oil-in-water emulsions with mean droplet diameters ranging from 50 to 1000 nm. Usually, the average droplet size is between 100 and 500 nm. The preparation of nanoemulsions requires high-

pressure homogenization. The particles which are formed exhibit a liquid, lipophilic core separated from the surrounding aqueous phase by a monomolecular layer of phospholipids. The structure of such lecithin stabilized oil droplets can be compared to chylomicrons. Nanoemulsions therefore differ clearly from the liposomes, where a phospholipid bilayer separates an aqueous core from a hydrophilic external phase (Figure 3B) *(Daniels)*.

I.3.3. Lipid nanoparticles

Lipid nanoparticles have a similar structure as nanoemulsions. Their size ranges typically from 50 to 1000 nm. The difference is that the lipid core is in the solid state (Figure 3C). The matrix consists of solid lipids or mixtures of lipids *(Daniels)*

I.3.4. Ferrofluids

Ferrofluids are stable suspensions of colloidal ferromagnetic particles (e.g. magnetite) in suitable, non-magnetic carrier liquids. Typical diameters of the colloidal particles are of the order of 10 nm and are therefore stable against sedimentation.

The colloidal particles are covered with surfactants in order to prevent agglomeration due to attractive Van der Vaals forces. Due to their small size, the colloidal particles can be considered as ferromagnetic mono-domain particles. Since the colloidal particles contain several 1.000 atomic magnetic moments, the ferrofluids are often referred to as 'superparamagnets' (Figure 3E) (http://wwwitp.physik.tu-berlin.de/~ilg/FF_Intro.html).

I.3.5. Liposomes

Liposomes are microscopic spherical vesicles that are formed when phospholipids are hydrated. When phospholipids are mixed in water under low

shear conditions, they arrange themselves in sheets, the molecules aligning side by side in like orientation, "heads" up and "tails" down. These sheets then join tails-to-tails to form a bilayer membrane which encloses some of the water in a phospholipid sphere. Typically, several of these vesicles will form one inside the other in diminishing size, creating a multilamellar structure of concentric phospholipid spheres separated by layers of water (Figure 3A).

Liposomes have been used for more than 30 years as vehicles to improve the delivery of various drugs, such as anticancer drugs (doxorubicin), antibiotics (anthracycline, amphotericin B) or vaccines *(Baldeschwieler, 1997)*.

Liposomes, because of their biphasic character, can act as carriers for both lipophilic and hydrophilic drugs. Depending upon their solubility and partitioning characteristics, the drug molecules are located differently in the liposomal environment and exhibit different entrapment and release properties (Figure 4). Based on these parameters, the drugs can be divided into four classes (1) highly hydrophilic, (2) highly lipophilic, (3) amphiphilic drugs that exhibit good biphasic solubility, and (4) drugs that exhibit biphasic insolubility (*Gulati, et al., 1999*).

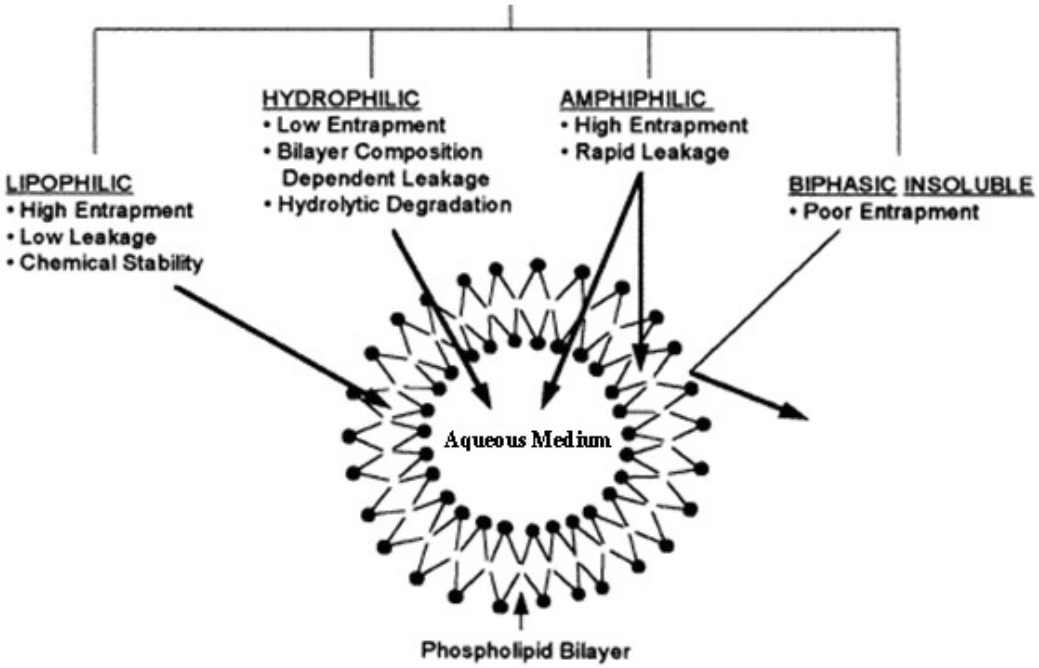

Figure 4: Types of drugs and site of their incorporation into the liposomal vesicle.

I.3.5.1. Advantages of Liposomes

Liposomal drug delivery systems have received considerable attentions due to their specific attractions, including 1) effective encapsulation of both small and large molecules with a wide range of hydrophobicity levels and pKa values; 2) prolonging and targeting release of therapeutic agents by modification of liposome surface and 3) minimising clinical drug dose and reducing toxicity effects (*Prestidge et al., 2005*).

To understand how liposomes can best be used to improve the performance of the enclosed drug, it may be useful to consider the following basic reasons for using liposomes as a drug carrier (*Strom and Crommelin, 1998*).

Direction

Liposomes can direct a drug (1) to the intended site of action (drug targeting, site-specific delivery) and (2) away from those body sites that are particularly sensitive to the toxic action of it (site-avoidance delivery).

Duration

Liposomes can act as a depot form, from which the entrapped compound is slowly released over time.

Protection

Liposomes can protect drugs, which are entrapped in the aqueous interior against the action of detrimental factors (e.g. degradative enzymes) present in the host.

Internalization

Liposomes are able to promote the intracellular delivery of drug molecules that in their ‘free’ form (i.e. non-encapsulated) would not be able to enter the

cellular interior due to unfavorable physicochemical characteristics (e.g. DNA molecules).

Amplification

Liposomes can act as immunological adjuvant in vaccine formulations

I.3.5.2. Classification of Liposomes

I.3.5.2.1. Classification based on pharmaceutical aspects

Liposomes are often distinguished according to their number of lamellae and size. Small unilamellar vesicles (SUV), large unilamellar vesicles (LUV) and large multilamellar vesicles (MLV) or multivesicular vesicles (MVV) are differentiated (Figure 5). SUV show a diameter of 20 to approximately 100 nm. LUV, MLV, and MVV range in size from a few hundred nanometers to several microns. The thickness of the membrane (phospholipid bilayer) measures approximately 5 to 6 nm *(Daniels)*.

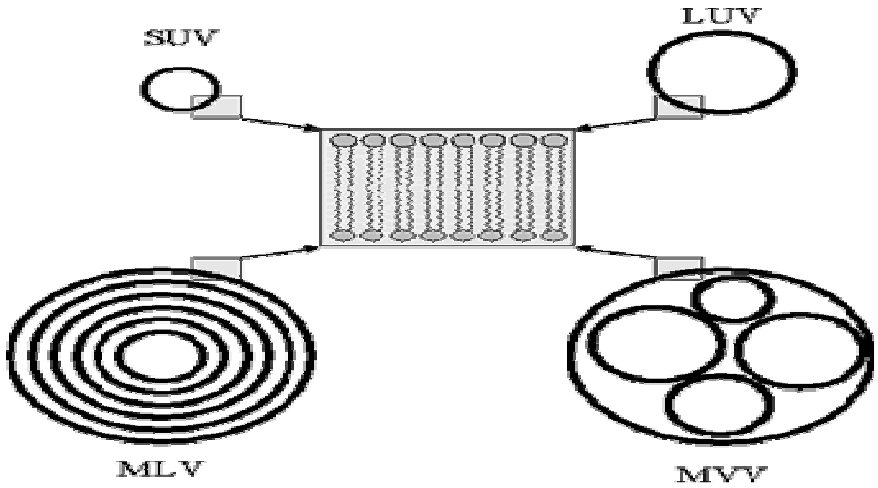

Figure 5: Schematic illustration of different types of liposomes. SUV: Small unilamellar vesicles; LUV: Large unilamellar vesicles; MLV: Multilamellar vesicles; MVV: Multivesicular vesicles *(Daniels)*.

I.3.5.2.2. Classification based on composition

In an attempt to classify the plethora of possible liposome versions, four major liposome types can be broadly distinguished on the basis of composition and *in vivo* application (Figure 6) (*Strom and Crommelin, 1998*).

I.3.5.2.2.1. Conventional liposomes

They are typically composed of only phospholipids (neutral and/or negatively charged) and/or cholesterol. They can vary widely in their physicochemical properties such as size, lipid composition, surface charge and number and fluidity of the phospholipid bilayers. They are characterized by a relatively short blood circulation time. When administered *in vivo* by a variety of parenteral routes (often by intravenous administration), they show a strong tendency to accumulate rapidly in the phagocytic cells of the reticuloendothelial system (RES). Therefore, conventional liposomes may be attractive candidates for drug delivery to RES. The major organs of accumulation are the liver and the spleen. Conventional liposomes have application in macrophage targeting, local depot and vaccination.

I.3.5.2.2.2. Long-circulating liposomes

They were formulated to avoid the short blood circulation time of conventional liposomes and persist for prolonged periods of time in the bloodstream. The most important key feature of long circulating liposomes is that they are able to extravasate at body sites where the permeability of the vascular wall is increased. Fortunately, regions of increased capillary permeability include pathological areas such as solid tumors and sites of infection and inflammation. At present the most popular way to produce long-circulating liposomes is to attach hydrophilic polymer polyethylene glycol (PEG) covalently to the outer surface (Figure 6). Such PEG-coated liposomes are also called ‘stealth’ or ‘sterically stabilized’ liposomes, the former term

referring to their RES-escaping capability, the latter term to the steric stabilization mechanism held responsible for the induction of long (half-life in humans ~48 hr) circulation times. Steric stabilization results from the local surface concentration of highly hydrated PEG groups that create a steric barrier against interactions with molecular and cellular components in the biological environment.

I.3.5.2.2.3. Immunoliposomes

They have specific antibodies or antibody fragments on their surface to enhance target site binding. Although immunoliposome systems have been investigated for various therapeutic applications, the primary focus has been the targeted delivery of anticancer agents *(Vingerhoeds, et al., 1994)*. Successful attempts have been made to prolong the half-life of immunoliposomes after intravenous administration by coating with PEG, thus giving them a greater chance to reach target sites other than RES macrophages.

I.3.5.2.2.4. Cationic liposomes

They represent the youngest member of the liposome family. They are front-line runners among the delivery systems under development for improving the delivery of genetic material *(Lasic and Templeton, 1996 and Mahato, et al., 1997)*. Their cationic lipid components interact with, and neutralize, the negatively-charged DNA, thereby condensing the DNA into a more compact structure. The resulting lipid–DNA complexes, rather than DNA encapsulated within liposomes, provide protection and promote cellular internalization and expression of the condensed plasmid.

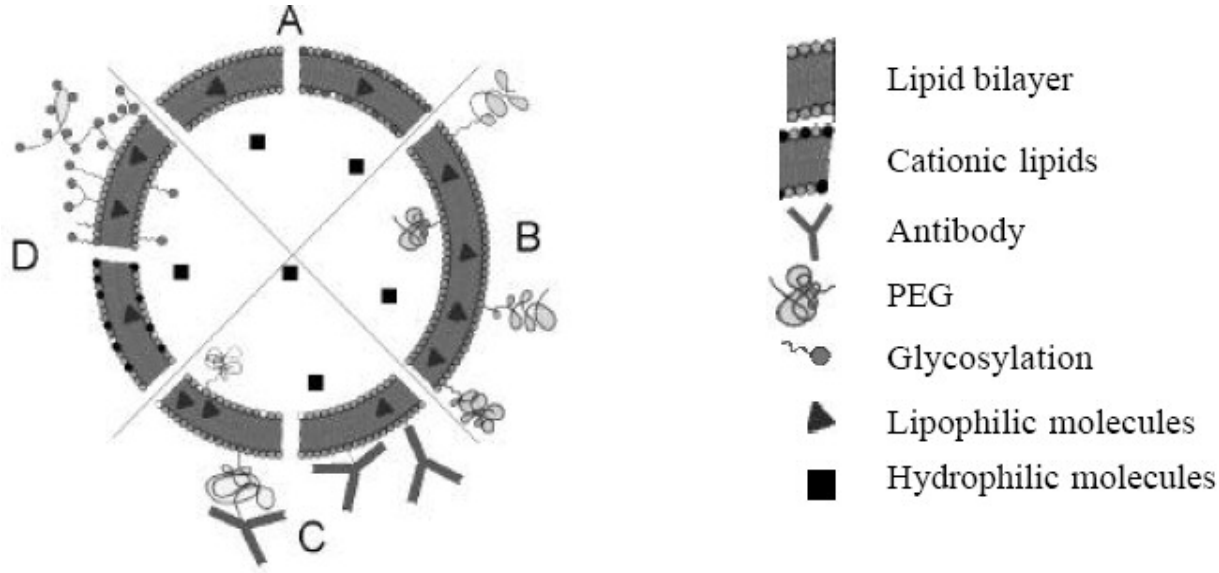

Figure 6: Schematic representation of different liposomes: (**A**) conventional liposomes neutral or negatively charged, (**B**) sterically stabilised ("stealth") liposomes coated with PEG, (**C**) immunoliposomes and (**D**) cationic and glycosylated liposomes (*Strom and Crommelin, 1998*).

I.3.5.3. Pharmaceutical aspects of liposomes

The mechanical and surface properties of liposomes can be modulated by selecting the proper bilayer components. The lipids are predominantly phospholipids which form bilayers similar to those found in biomembranes (Figure 7) (*http://www.dadairs.com/liposomes.htm*). A phospholipid exists of a hydrophilic head group and lipophilic tails (Figure 8) (*http://www.dadairs.com/liposomes.htm*). The polar head can be charged or uncharged and the lipophilic tails are composed of fatty acids chains. The rigidity and permeability of the bilayer strongly depends on the type and quality of PC and additional bilayer lipids used.

The alkyl-chain length and degree of unsaturation play a major role, for example, a C18; saturated alkyl chain produces rigid bilayers with low permeability at body temperature. The presence of cholesterol also tends to

rigidify bilayers. Phosphatidyl choline (PC), the primary lipid used in liposomes, belongs to the group of phosphodiglycerides, which are naturally occurring phospholipids.

The amphiphilic PC is composed of the phosphocholine, a hydrophilic head group, linked to two lipophilic acyl hydrocarbon chains via glycerol (Figure 9).

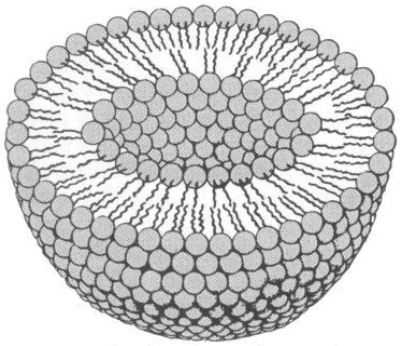

Figure 7: Liposome structure formed from phospholipids

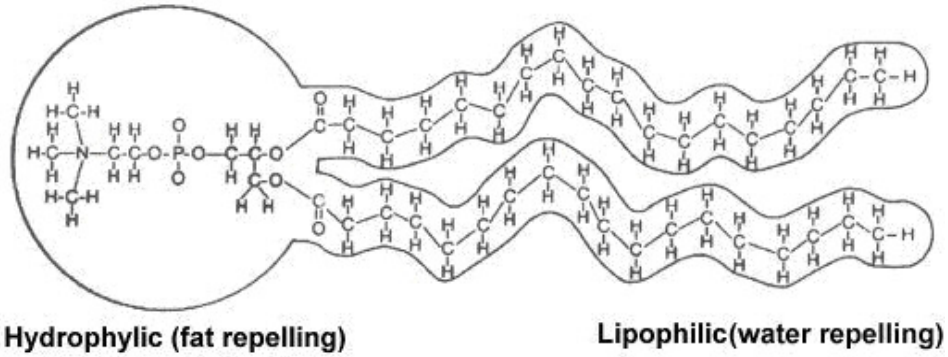

Figure 8: Shape of phospholipid

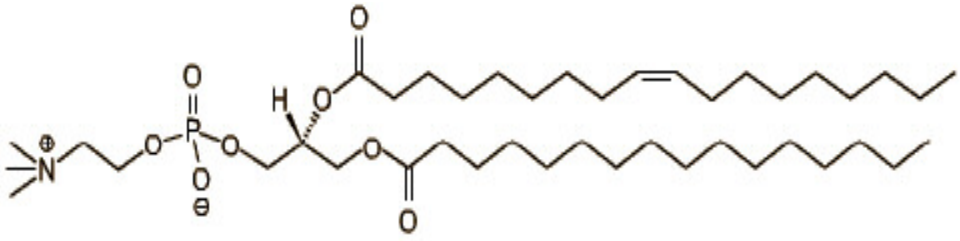

Figure 9: Chemical structure of phosphatidyl choline

I.3.5.4. Methods of the preparation of pharmaceutical liposomes

Table 1 explains classification and sub-classification of methods used for preparation of liposomes and the type of the liposomes produced by these methods (*Knight, 1981; Kawano et al., 2003*).

Table 1: Methods, sub/classification method and type of liposomes obtained

Method	Sub-classification of method	Liposomes obtained
Mechanical dispersion	Hand-shaken method	LUV or MLV
	Pro-liposomes	MLV
	Freeze-drying method	MLV
Physical-hydration (modify or improve characteristics of liposomes)	Micro-emulsification	MLV
	Sonication (cuphorn, bath or probe tip sonicator)	SUV
	French press extrusion	SUV
	Membrane extrusion	LUV
	Dried-reconstitute	LUV or MLV
	Freeze-thawing sonication (FTS)	SUV or LUV
	Dehydration-rehydration vesicle	SUV
	pH-induced vesiculation	SUV or LUV
	Calcium-induced fusion	LUV
Solvent dispersion	Ethanol injection	SUV or LUV
	Ether injection	SUV or LUV
	Double emulsification	SUV or LUV
	Multiple emulsification	LUV
	Reverse-phase evaporation (RE)	LUV
Other methods	Detergent removal/dialysis	SUV or LUV
	Fusion of SUV	LUV
	Film-ultrasonic technique	Dependent on drugs
	Amphiphiles-loading	Dependent on drugs

I.3.5.5. Storage of liposomes

Liposomes can be stored in a buffer at pH 7.4 and at approximately 4°C for 5-7 days. Storage time depends on a number of factors including temperature, pH, medium, etc. Liposomes suspensions should not be frozen as the freezing process could fracture or rupture the vesicles leading to a change in size distribution and loss of internal contents.

I.3.5.6. Determinations of liposomal size

The liposomal size not only influences the liposome's in-vitro characteristics such as drug loading capacity, aggregation and sedimentation but also the pharmacokinetics and biodistribution of the carrier is strongly size-dependent. There are several techniques suitable for determining the size of liposome preparations.

I.3.5.6.1. Photon Correlation Spectroscopy (PCS)

PCS is also known as dynamic light scattering (DLS) or quasi-elastic light scattering (QELS). It provides a mean diameter of the particle and its distribution. PCS can also distinguish whether the particle population is uniformly distributed around a mean value or more complicated particle size distributions e.g. unimodal vs. bimodal are present.

Theory of DLS

Schematic diagram for the dynamic light scattering equipment is shown in the following Figure

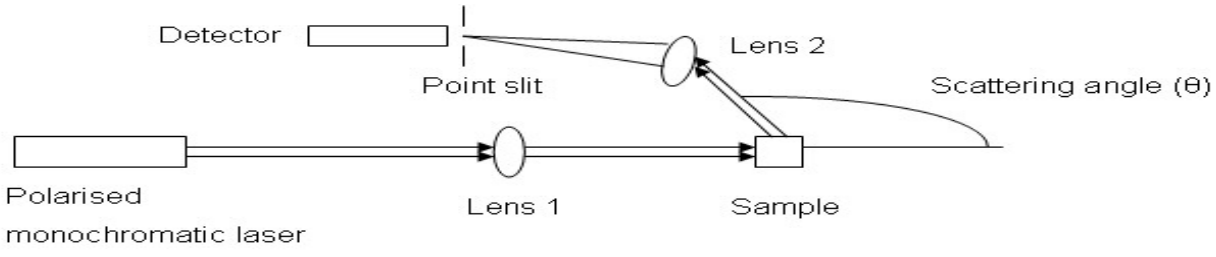

Figure 10: Schematic representation of the dynamic light scattering equipment.

The following schematic diagrams (Figures 11 to 15) explain the theory of dynamic light scattering

(*http://www.malvern.co.uk/common/downloads/campaign/MRK656-01.pdf*)

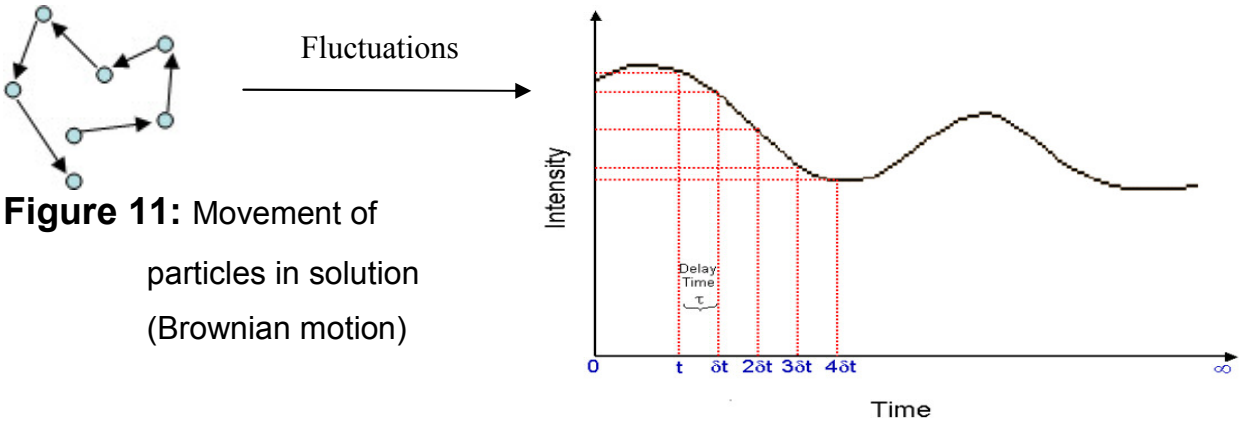

Figure 11: Movement of particles in solution (Brownian motion)

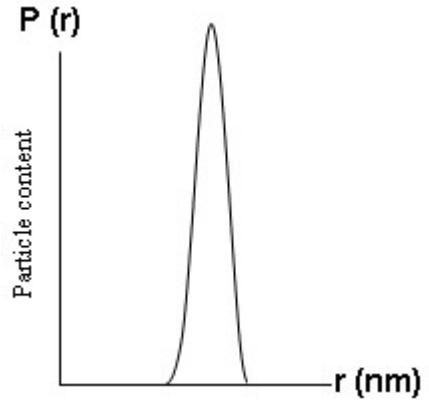

Figure 15: Axis exchange by diffusion law

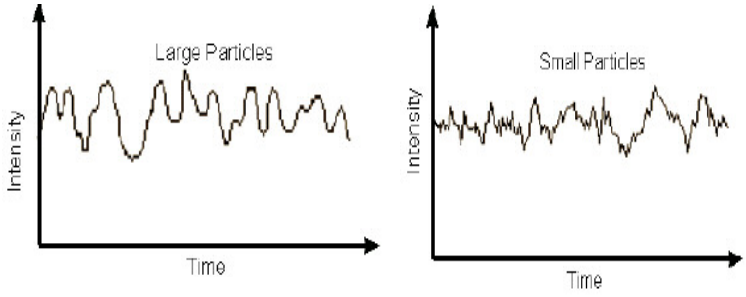

igure 12: Fluctuations in the intensity of scattered Light as a function of time

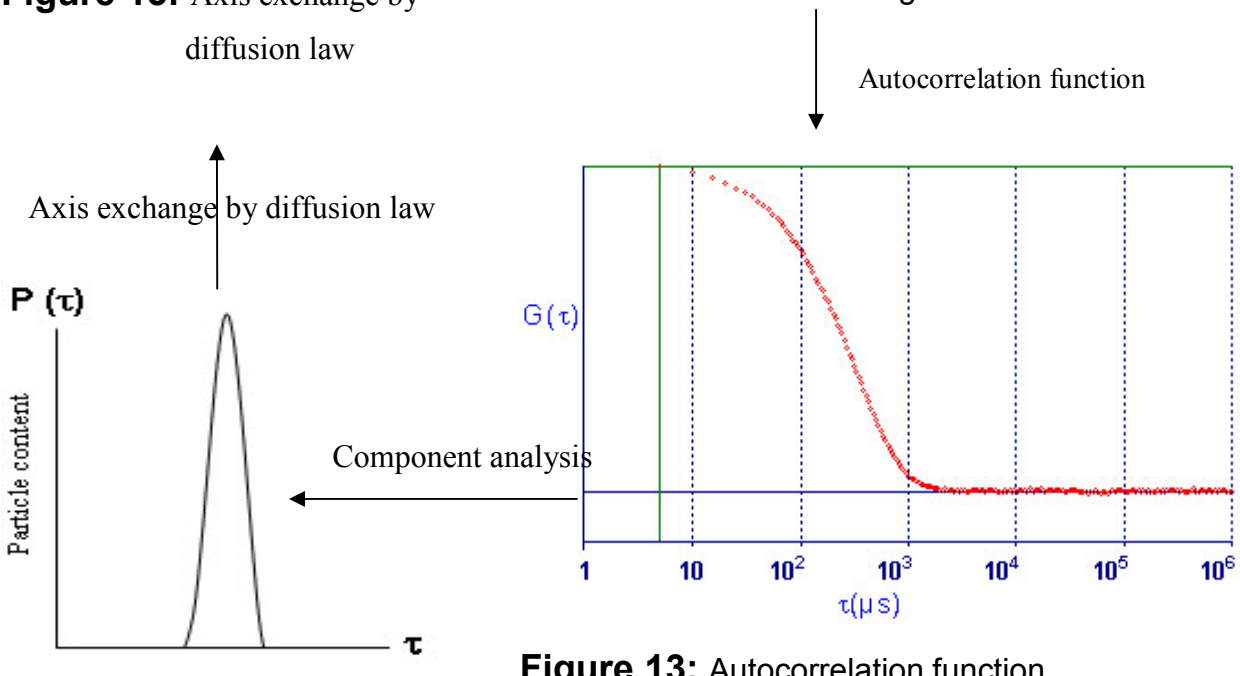

Figure 14: Component analysis

Figure 13: Autocorrelation function

It has been seen that particles in dispersion are in a constant, random Brownian motion and that this causes the intensity of scattered light to fluctuate as a function of time. The correlator used in PCS instrument will construct the correlation function G(τ) of the scattered intensity:

$$G(\tau) = \langle I(t).I(t+\tau)\rangle$$

Where τ =the time difference (the sample time) of the correlator.

For monodisperse particles in Brownian motion, the correlation function (given the symbol [G]) is an exponential decaying function of the correlator time delay τ (*Chu, 1991*):

$$G(\tau) = A[1 + B\exp(-2\Gamma\tau)$$

Where A = the baseline of the correlation function, B = intercept of the correlation function.

$$D = \frac{\Gamma}{q^2}$$

Where D = translational diffusion coefficient

$$q = \frac{4\pi n_0}{\lambda_0}\sin(\theta/2)$$

Where n = refractive index of dispersant, λo = wavelength of the laser, θ = scattering angle.

For polydisperse samples, the equation can be written as:

$$G(\tau) = A[1 + Bg^{1}(\tau)^2]$$

Where $g^1(\tau)$ = is the sum of all the exponential decays contained in the correlation function.

The hydrodynamic radius d_h of a sphere is calculated from the translational diffusion coefficient by using the Stokes-Einstein equation;

$$d_h = \frac{KT}{3\pi\eta D}$$

Where d_h = hydrodynamic diameter, k is Boltzmann's constant, T is the temperature in K, and η is the solvent viscosity.

The diameter that is measured in DLS is a value that refers to how a particle diffuses within a fluid so it is referred to as a hydrodynamic diameter. The diameter that is obtained by this technique is the diameter of a sphere that has the same translational diffusion coefficient as the particle.

I.3.5.6.2. Laser diffraction analysis

The technique of laser diffraction depends on the fact that particles passing through a laser beam scatter light at an angle that is inversely proportional to their size (small particles scatter light at high angles whereas large particles scatter light at low angles). It is therefore possible to calculate particle size distributions if the intensity of light scattered from a sample is measured as a function of angle. This angular information needs to be compared with a scattering model (Mie theory) in order to calculate the size distribution.
The laser diffraction technique is flexible in terms of the type of samples that can be measured. Particles can be dispersed in a liquid medium (wet laser diffraction) or as solid particles dispersed in an air stream (dry laser diffraction). Measurements are also possible on aerosol-based systems such as liquid atomizers and pharmaceutical inhalers. For wet analysis samples require dilution to be measured
(*http://www.malvern.co.uk/LabEng/support/technologies.htm*).

Laser diffraction analyzer (Beckman Coulter LS 13320 with liquid module) was used in this study.

Measurement principle

Laser diffraction is based on the phenomenon that particles scatter light in all directions with an intensity pattern that is dependent on particle size.

A typical light scattering instrument consists of a light beam (usually a laser), a particulate dispersion device, a detector for measuring the scattering pattern and a computer for both control of the instrument and calculation of the particle size distribution.

Laser diffraction has advantages of its ease of use and fast operation; its high reproducibility; and an extremely broad dynamic size range, spanning almost five orders of magnitude, from nanometers to millimetres (http://www.beckmancoulter.com/coultercounter/homepage_tech_laserdiff.jsp)

Figure 16 shows the generic setup of a laser diffraction instrument and the major functions of each element.

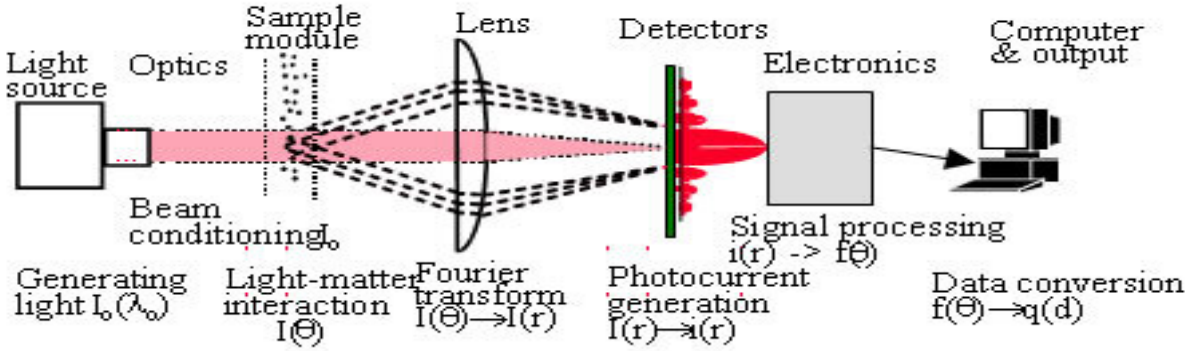

Figure 16: Schematic representation of a laser diffraction instrument

I.3.5.7. Entrapment model drugs and metals

I.3.5.7.1. Lanthanide chelates

Numbers of lanthanides are used as medical useful radionuclides. Lanthanides emit γ-rays, which can in most cases (depending on their energy) be used for

imaging with a gamma camera to follow the biodistribution and allow dosimetry (*Beyer, et al., 2004*).

The desired high target absorption can be obtained by using biocompatible Lanthanide complexes (lanthanide-DTPA). As erbium is easy to measure, it was chosen as an example for therapeutic heavy metals e.g. gadolinium and lutetium (Figure 17).

Furthermore, liposomes can be used for encapsulation of metal targets and magnetic cores for IRT.

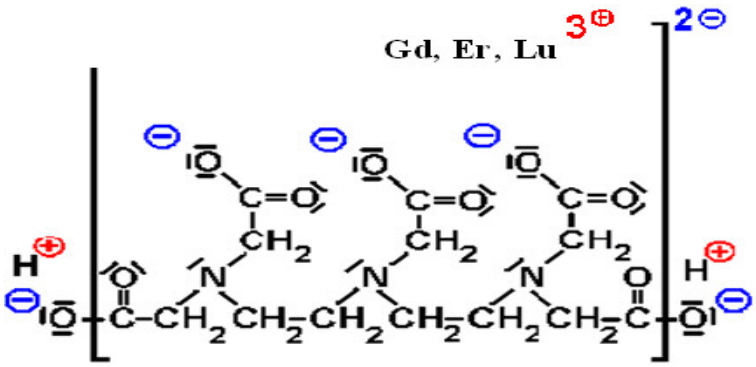

Figure 17: Lanthanide, heavy metal-DTPA complexes are biocompatible targets for radiation therapy and imaging with synchrotron X-rays, neutrons, photobiology or MRI.

I.3.5.7.2. β-Adrenoceptor antagonists

β-adrenoceptor antagonists are used as model drugs for toxic chemotherapeutic agents e.g. tamoxifen and doxorubicin. Four β-adrenoceptor antagonists e.g. propranolol, metoprolol, pindolol and atenolol were chosen as model drugs.

β- adrenoceptor antagonists are amphiphilic drugs i.e. containing both hydrophilic and lipophilic parts (Figure 18) (*Lee, et al., 2006)*.

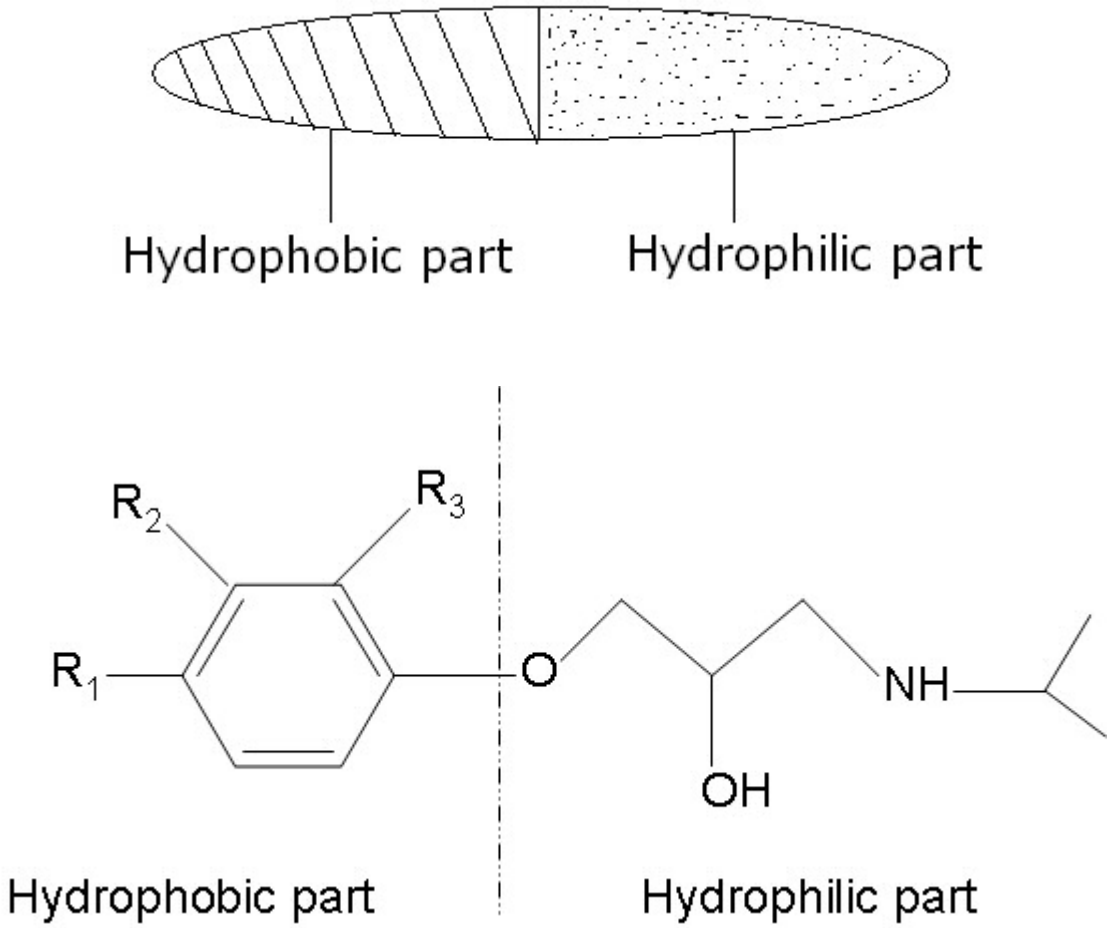

Figure 18: Schematic representation of amphiphilic molecule and general structure of β- adrenoceptor antagonists used

Chemical structures and physicochemical properties of the selected β- adrenoceptor antagonists

Table 2 explains the chemical structures and physicochemical properties of the selected β- adrenoceptor antagonists (*Yoshikazu, et al., 2001*).

Table 2: Chemical structures and physicochemical properties of the selected β- adrenoreceptor antagonists (*Yoshikazu, et al., 2001*)

Drug	Structure			M.W. (free base)	pK_a	Log P(37 °C)		Ionization (mol%, pH 7.4)
	R_1	R_2	R_3			Nonionic	Ionic (pH 7.4)	
Propranolol	H	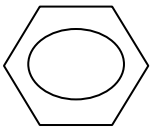		259	9.45	3.54	1.49	99.1
Metoprolol	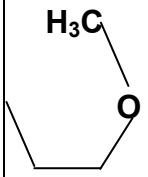	H	H	267	9.70	2.49	0.20	99.5
Atenolol	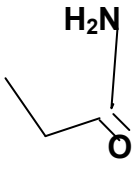	H	H	266	9.55	2.04	- 0.11	99.33
Pindolol	H	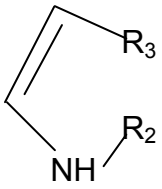		248	8.80	1.57	0.08	96.2

I.4. Positron emission tomography

Positron emission tomography (PET) is a nuclear medicine imaging technique which produces a three-dimensional image or map of functional processes in the body (Figures 19 and 20). The system detects pairs of gamma rays emitted indirectly by a positron-emitting radioisotope (tracer), which is introduced into the body on a biologically active molecule. Images of tracer concentration in 3-dimensional space within the body are then reconstructed by computer analysis.

In modern scanners, this reconstruction is often accomplished with the aid of a CT X-ray scan performed on the patient during the same session, in the same machine (*http://en.wikipedia.org/wiki/Positron_emission_tomography*).

If the biologically active molecule chosen for PET is FDG, a derivative of glucose, the concentrations of tracer imaged then give tissue metabolic activity, in terms of regional glucose uptake. Although use of this tracer results in the most common type of PET scan, other tracer molecules are used in PET to image the tissue concentration of many other types of molecules of interest.

Figure 19: Image of a typical positron emission tomography (PET) facility *(http://en.wikipedia.org/wiki/Positron_emission_tomography)*

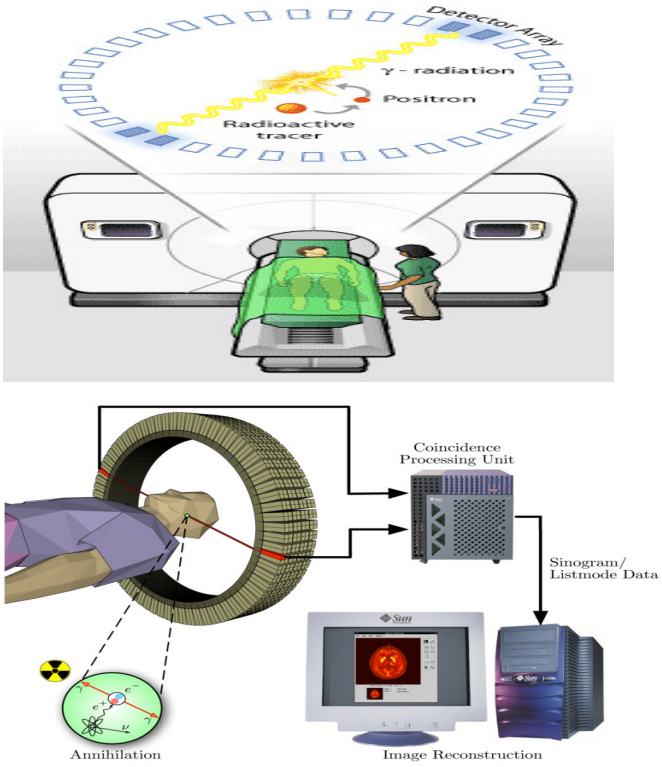

Figure 20: Diagram of PET Scan Process (http://www.scq.ubc.ca/looking-inside-the-human-body-using-positrons/) (http://en.wikipedia.org/wiki/Positron_emission_tomography

Fluorodeoxyglucose (FDG)

FDG is most commonly used in the medical imaging modality positron emission tomography (PET): the fluorine in the FDG molecule is chosen to be the positron-emitting radioactive isotope fluorine-18, to produce ^{18}F-FDG. After FDG is injected into a patient, a PET scanner can generate images of the distribution of FDG within the body. The images can be assessed by a nuclear medicine physician or radiologist to provide diagnoses of various medical conditions.

Mechanism of action and metabolic fate of FDG

FDG, as a glucose analog, is taken up by high-glucose-utilizing cells such as brain, kidney, and cancer cells, where phosphorylation prevents the glucose from being released intact. The oxygen in the 2-position in glucose is needed for further glycolysis, so that (in common with 2-deoxy-D-glucose) FDG cannot be further metabolized in cells, and therefore the FDG-6-phosphate formed does not undergo glycolysis before radioactive decay. As a result, the distribution of ^{18}F-FDG is a good reflection of the distribution of glucose uptake and phosphorylation by cells in the body.

Before FDG decays, it is inhibited from metabolic degradation or use, because of the fluorine at the 2' position in the molecule. However, after FDG decays radioactively, its fluorine is converted to ^{18}O, and after picking up a H^+ from the environment, it becomes glucose-6-phosphate labeled with harmless nonradioactive "heavy oxygen" (oxygen-18) at the 2-position, and is thereafter metabolized normally in the same way as ordinary glucose (*Quon and Gambhir, 2005*).

Applications

In Position Emission Tomography (PET) imaging, ^{18}F-FDG can be used for the assessment of glucose metabolism in the heart and in the brain. It is also used for imaging tumours in oncology. FDG-PET can be used for diagnosis, staging, and monitoring treatment of cancers. In body-scanning applications in searching for tumor or metastatic disease, a dose of FDG in solution (typically 5 to 10 millicuries (1 Ci = 3.7×10^{10} Bq) or 200 to 400 MBq) is used.

I.5. In vitro-In vivo Correlation (IVIVC)

I.5.1. Introduction

Correlations between in vitro and in vivo data (IVIVC) are often used during pharmaceutical development in order to reduce development time and optimize the formulation. A good correlation is a tool for predicting in vivo results based on in vitro data. IVIVC allows dosage form optimization with the fewest possible trials in man (*Cardot, et al., 2007*).

IVIVC is a predictive mathematical model describing the relationship between an in vitro property of a dosage form and a relevant in vivo response. Generally, the in vitro property is the rate or extent of drug dissolution or release while the in vivo response is the plasma drug concentration or amount of drug absorbed (*Emami, 2006)*.

I.5.2. Correlation levels

Five correlation levels have been defined in the IVIVC FDA guidance (*Guidance for industry, 1997*).

Level A Correlation

This level of correlation is the highest category of correlation and represents a point-to-point relationship between in vitro dissolution rate and in vivo input

rate of the drug from the dosage form (*USP, 2008*). It is also a predictive model for the relationship between the entire in vitro release time course and the entire in vivo response time course (*Gillespie, 1997*).

Level B Correlation

In this level of correlation, the mean in vitro dissolution time (MDT_{vitro}) of the product is related to either mean in vivo residence time (MRT) or the mean in vivo dissolution time (MDT_{vivo}) (*Guidance For Industry, 1997; USP, 2008*).

Level C Correlation

At this level of correlation, one dissolution time point (t_{50}%, t_{90}%, etc.) is compared to one mean pharmacokinetic parameter such as AUC, t_{max} or C_{max}.

Therefore, it represents a single point correlation and does not reflect the entire shape of the plasma drug concentration time curve, the latter being a good indicative of the performance of modified-release products (*Guidance For Industry, 1997; USP, 2008*).

Multiple-level C correlation

A multiple level C correlation relates one or several pharmacokinetic parameters of interest (C_{max}, AUC, or any other suitable parameters) to the amount of drug dissolved at several time points of the dissolution profile (*Emami, 2006*).

Level D correlation

Level D correlation is a rank order and qualitative analysis and is not considered useful for regulatory purposes. It is not a formal correlation but serves as an aid in the development of a formulation or processing procedure (*Emami, 2006*).

I.6. Aim of the Thesis

The aim of this doctoral thesis was to

1. Prepare different types of liposomes e.g. MLV, LUV, and SUV containing model drugs (e.g. β-adrenoceptor antagonists e.g. propranolol, metoprolol, atenolol, and pindolol, metal chelates e.g. Er-DTPA, glucose as well as 18-fluorodeoxyglucose (^{18}F-FDG) in liposomes.
2. Study the effect of liposomal type e.g. MLV, LUV, and SUV and lipid type used e.g. Phospholipone 90H, Distearoylphosphatidylcholine (DSPC), Dimyrisoylphosphatidylcholine (DMPC) and 1:1 mixture of Distearoylphosphatidylcholine and Dimyrisoylphosphatidylcholine on the in vitro release characteristics of incorporated drug.
3. Study the effect of lipid concentration, in vitro release method, drug lipophilicity and temperature on the in vitro release characteristics of liposomes.
4. Characterize the prepared liposomes by determination of encapsulation efficiency (%) and determination of particle size and particle size distribution.
5. Study the possible relationship between in vitro and in vivo release using FDG –containing liposomes by positron emission tomography (PET).

Chapter II: Materials and methods

II.1. Materials

II.1.1. Reagents

Materials used in this study are detailed in Table 3. All chemical reagents were of analytical grade.

Table 3: Materials used in this study

Name	Purity	Abbreviation	Source
Propranolol	> 95%	PP	Sigma-Aldrich Chemie GmbH, Germany
Metoprolol	> 95%	MT	
Atenolol	> 95%	AT	
Pindolol	> 95%	PD	
Erbium DTPA solution, pH 7		Er-DTPA	Sigma-Aldrich Chemie GmbH, Germany
Lecithin from Soybean Phospholipid		SBL	SERVA GmbH, Germany
Diethylenetriaminepentaacetic acid		DTPA	Fluka Chemie, Germany
Citric acid			Merck, Germany
2-amino-2-(hydroxymethyl)-1, 3-propanediol		Tris	Boehringer GmbH, Geermany
Sephadex^{TM} G-25 medium			GE Healthcare Bioscience AB, Germany
3,5-Dinitrosalicylic acid		DNS	Sigma-Aldrich Chemie GmbH, Germany
Sodium Sulfite			Riedel-deHaẽn, Germany
Phenol			Merck KGaA, Germany
Sodium hydroxide			Merck KGaA, Germany
Ethanol		Et	VWR International GmbH, Darmstadt, Germany
D (+) Glucose Monohydrate	> 99%	Glu	E. Merck, Germany
[^{18}F]Fluoro-2-deoxy-D.glucose		FDG	PET NET GmbH, Germany

Table 3: continued

Phospholipon 90H® (A mixture of hydrogenated soybean phosphatidylcholine, 95%, and lyso-phosphatidylcholine, max. 4%, with a fatty acid composition of about 85% stearic acid and 15% palmitic acid)	> 99%	Ph90H	Phospholipid GmbH, Germany
1,2-Dimyristoyl-*sn*-Glycero-3-Phosphocholine 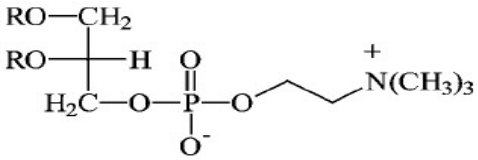 **R = $CH_3(CH_2)_{12}$-C=O**	-	DMPC	Avanti Polar Lipids, Germany
1,2-Distearoyl-*sn*-Glycero-3-Phosphocholine 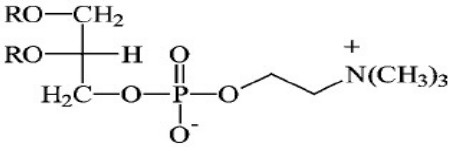 **R = $CH_3(CH_2)_{16}$-C=O**	-	DSPC	Avanti Polar Lipids, Germany
Sodium dihydrogen phosphate monohydrate	> 99%	NaH_2PO_4,H_2O	E. Merck, Germany
Phosphate buffered saline	-	PBS Dulbecco's w/o Ca and Mg)	Biochrom AG, Germany
Triton® X-100 $C_{34}H_{62}O_{11}$ **Synonyms:** octyl phenol ethoxylate, polyoxyethylene Octyl phenyl ether	> 98%		Merck KGaA, Germany
Acetonitril HPLC grade	> 99.9%	CH_3CN	Fisher Scientific, UK
Isotonic saline solution			Fresenius Kabi Deutschland GmbH

II.1.2. Equipment

Equipment used in this study is detailed in Table 4.

Table 4: Equipment used in this study

Equipment	Type	Source
Balance	Precisa Balance (XR 205SM-DR)	Precisa Instruments Ltd., Switzerland
Cryovials	Cryovial®	VWR International GmbH, Darmstadt, Germany
Vials	Nunc Cryotube ™ Vials	VWR International GmbH, Darmstadt, Germany
Rotator	Neolab-Reagenzglas-Mischer	Neolab migge Laborbedarf-Vertriebs GmbH, Germany
Vortex	VIBROFIX VF1	JANKE & KUNKEL IKA®–WERK GmbH & CO.KG, Germany
Water Bath	Julabo HC	ERWEKA® Appaeatebau GmbH, Germany
Test tubes	CELLSTAR®	Greiner bio-one, Germany
Microcentrifuge tube	CELLSTAR®, Greiner bio-one, Germany	VWR International GmbH, Darmstadt, Germany
Spectrophotometer	PERKIN ELMER UV/VIS Lambda 20	Perkin-Elmer GmbH, Germany
Oven	ECOCELL	MMM-Group, Medcenter Einrichtungen GmbH, Germany
Extruder	LiposoFast-Basic TM	Avestin Europe GmbH, Germany
Polycarbonate membranes	LFM-100nm	Avestin Europe GmbH, Germany
Probe tip Sonicator	UP 200S Tip	Dr. Hielscher GmbH, Germany
Laser diffraction analyzer	Beckman-Coulter LS 13 320	Beckman-Coulter, U.S.A.
Shaker and incubator	GFL 3032	LABOTEC, Germany
Centrifuge	Eppendorf 5804R centrifuge	Eppendorf, Germany
HPLC (Merck-Hitachi HPLC)	HPLC System Manager Chromatography Data Station Software® Modell D- 7000; interface D-7000; Programmable L-7250; Pump L-7100; Detector L-7420; column Lichrospher®100 RP-18e (5µm)	Merck-Hitachi, Germany
Cuvettes	Suprasil cuvettes, diameter 10 mm	QS Hellma, Mülheim

Table 4: continued

Dialysis membrane	SERVAPOR® (regenerated cellulose, MWCO 12 000-14000, diameter 6 mm)	SERVA Electrophoresis GmbH, Heidelberg, Germany
Photon Correlation Spectroscopy (PCS)	ALV 3000 correlator	ALV-Laser Vertriebsgesellschaft m-b.H., Germany
Clean bench (Skan)	VFC-120	Skan AG, Germany
Penefsky columns (*Roberts, et al., 1996*)	Centrifugation columns for medium speed with glass frit of pore size A_3	HWS Labortechnik, Mainz, Germany
FDG dose calibrator	VDC-405 dose calibrator (Detector unit and VDC-405 software for PC)	Veenstra Instruments, Germany

II.2. Methods

II.2.1. Preparation of liposomes

II.2.1.2. Preparation of multilamellar vesicles (MLV)

A schematic diagram for the preparation of MLV containing β-adrenoceptor antagonists or glucose by the freeze-thawing method is depicted in Figure 21 (*Port, et al., 2006*). The amounts of the lipids and drugs used are summarized in Table 5.

Table 5: Lipids used for formulation of liposomes (w/w)

	DSPC	DMPC	DSPC/DMPC (1:1)	Ph 90H		SBL
Propranolol:Lipid (w/w)	19: 50	19:50	19:50	19:50	19: 100	-
Metoprolol:Lipid (w/w)	19: 50	19:50	19:50	19:50	19: 100	-
Atenolol:Lipid (w/w)	19: 50	19:50	19:50	19:50	19: 100	-
Pindolol:Lipid (w/w)	19: 50	19:50	19:50	19:50	19: 100	-
Glucose:Lipid (w/w)	500:50	500:50	500:50	500:50	-	500:50
FDG:Lipid (MBq of FDG and mg of lipid/ml)	-	-	-	-		200:50
Er-DTPA:lipid (molarity of Er-DTPA and mg of lipid/ml)	-	-	-	-		0.3:50

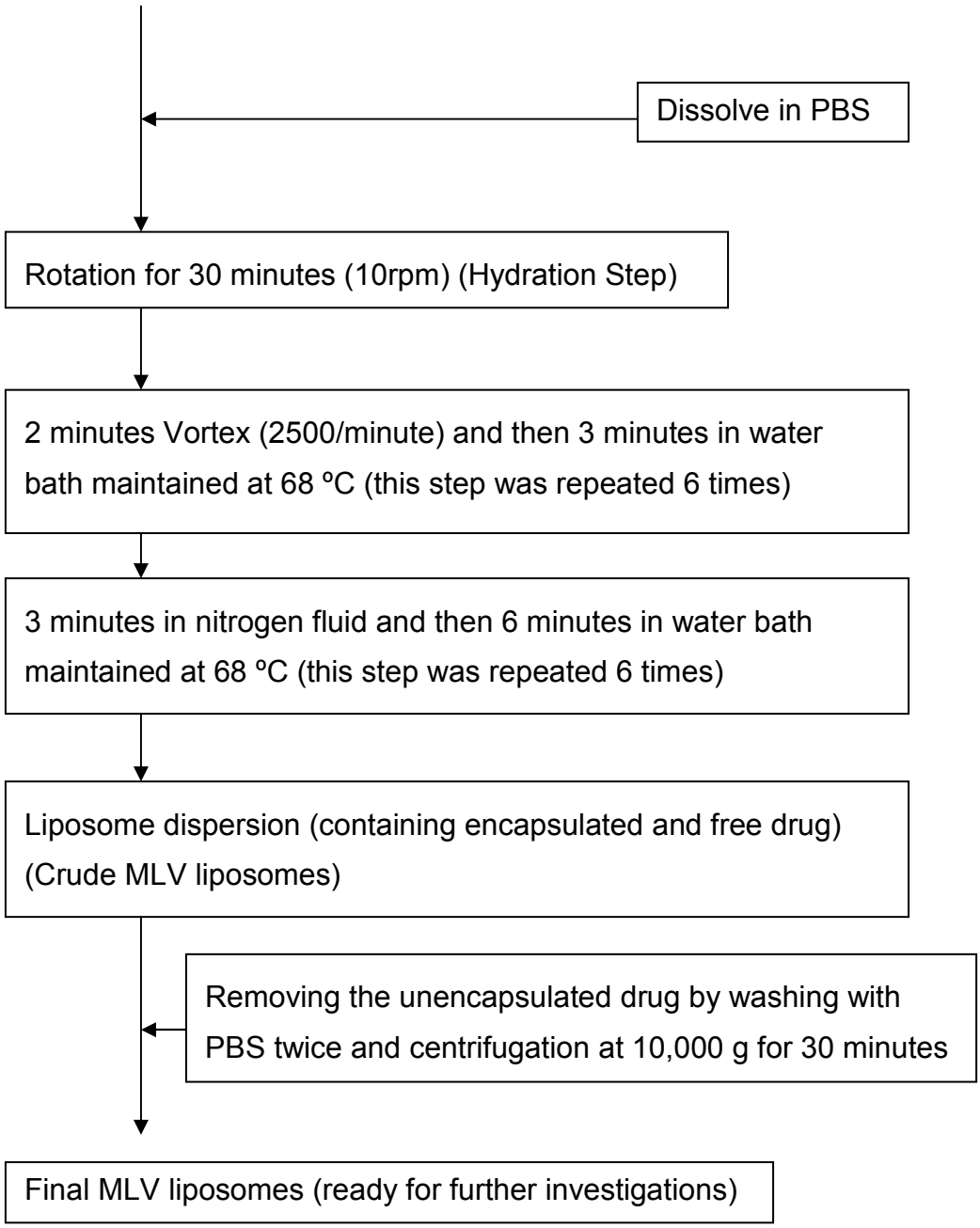

Figure 21: A schematic presentation for the preparation of MLV containing β-adrenoceptor antagonists or glucose by freeze-thawing method

The process of thawing is used to help break up multilamellar vesicles and to promote the mixing of the enclosed contents with the exterior solution (*Patty and Frisken, 2003*). But the freezing process is used to help the encapsulation

of the drug inside liposomes. The two processes help to increase the encapsulation efficiency.

II.2.1.3. Preparation of large unilamellar vesicles (LUV)

Figure 22 presents the schematic preparation method of large unilamellar vesicles containing β-adrenoceptor antagonists or glucose from MLV.

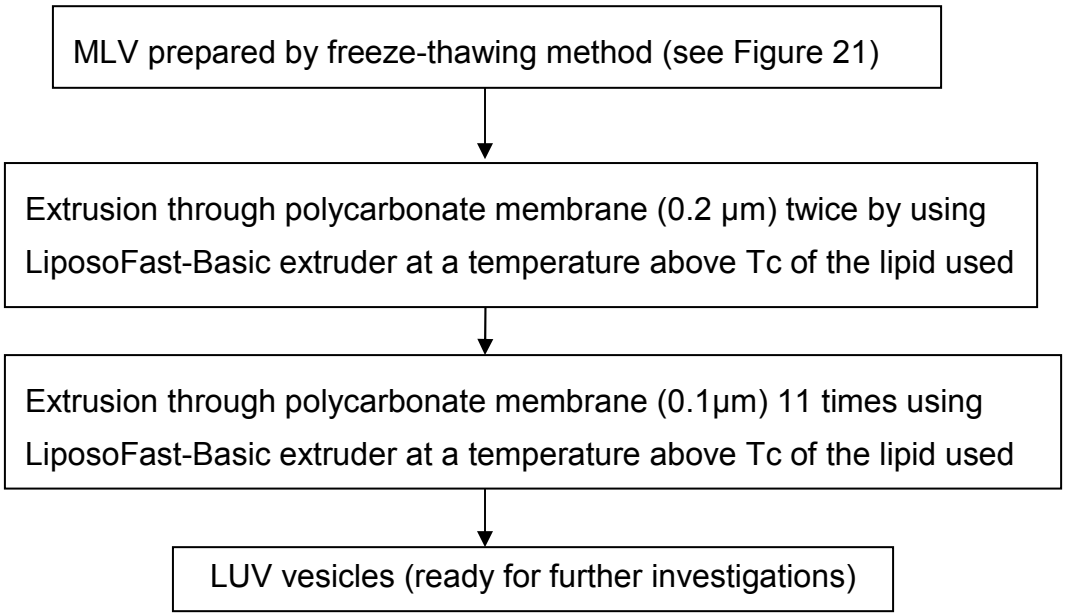

Figure 22: A schematic presentation for the preparation of LUV containing β-adrenoceptor antagonists or glucose

The odd number of extrusion steps was done to avoid contamination of the sample by large vesicles which might not have passed through the filter (*Hope, et al., 1985; MacDonald, et al., 1991; Yoshiyuki, et al., 2006*).

The extrusion was done first with 0.2 nm to prevent blocking and damage of the polycarbonate membrane

The phase transition temperatures of the used lipids are listed in Table 6.

Table 6: Phase transition temperatures (Tc) of the lipids used

	DSPC	Ph90H	DMPC	SBL
Phase transition temperature (Tc)	53 °C	54 °C	23 °C	~ -20

II.2.1.4. Preparation of small unilamellar vesicles (SUV)

Figure 23 exhibits the method of preparation of small unilamellar vesicles containing β-adrenoceptor antagonists or glucose from MLV.

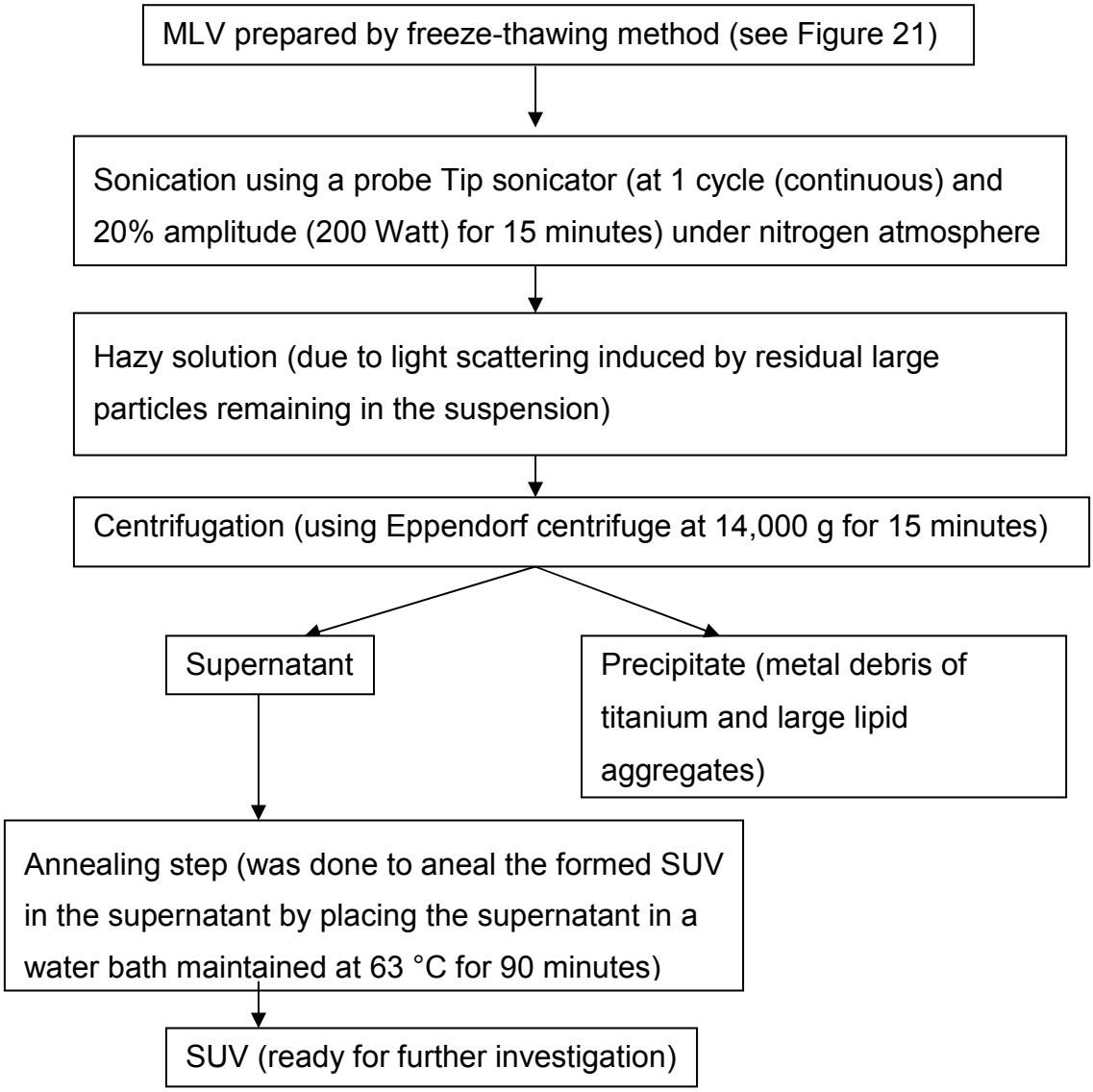

Figure 23: A schematic presentation for the preparation of SUV containing β-adrenoceptor antagonist or glucose

The centrifugation was done at 14.000g for 15 minutes to remove larger lipid aggregates and to remove the metal debris of the titanium tip (*Pitcher and Huestis, 2002)*.

The nitrogen atmosphere was used to prevent oxidation of the lipid during sonication.

II.2.1.5. Preparation of FDG-containing liposomes

II.2.1.5.1. Preparation of FDG-containing MLV

Figure 24 explains the schematic procedures for preparing MLV liposomes containing FDG.

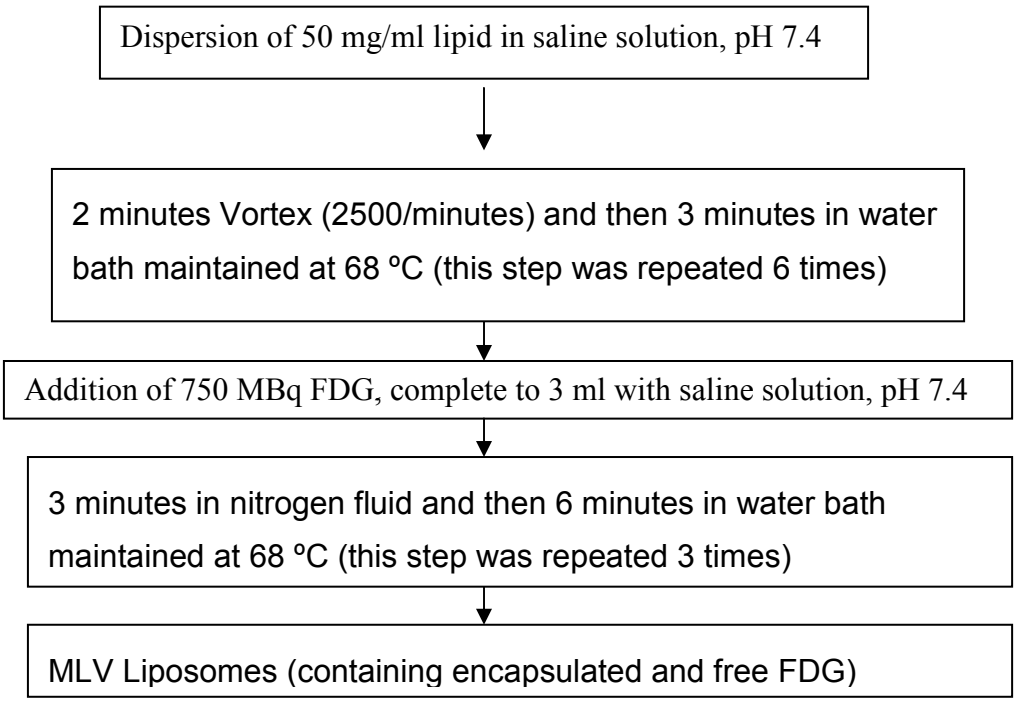

Figure 24: A schematic presentation for the preparation of MLV containing FDG

II.2.1.5.2. Preparation of FDG-containing LUV

Figure 25 explains the schematic diagram for preparing LUV liposomes containing FDG.

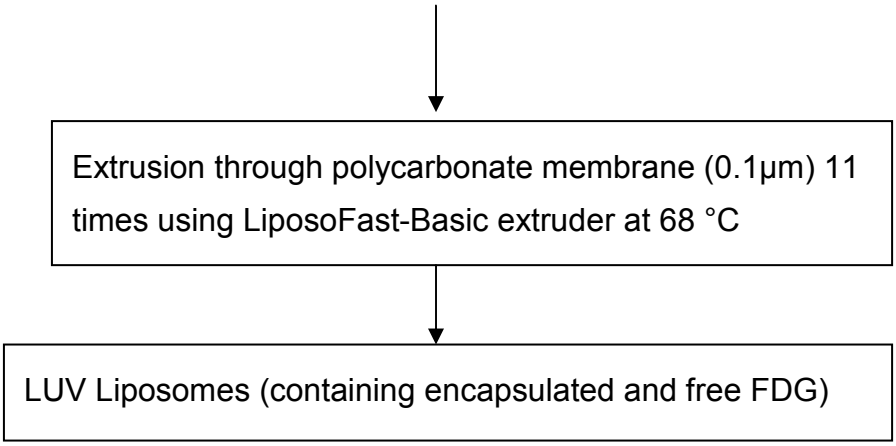

Figure 25: A schematic presentation for the preparation of LUV containing FDG

II.2.1.5.3. Preparation of FDG-containing SUV

Figure 26 explains the schematic diagram for preparing SUV liposomes containing FDG.

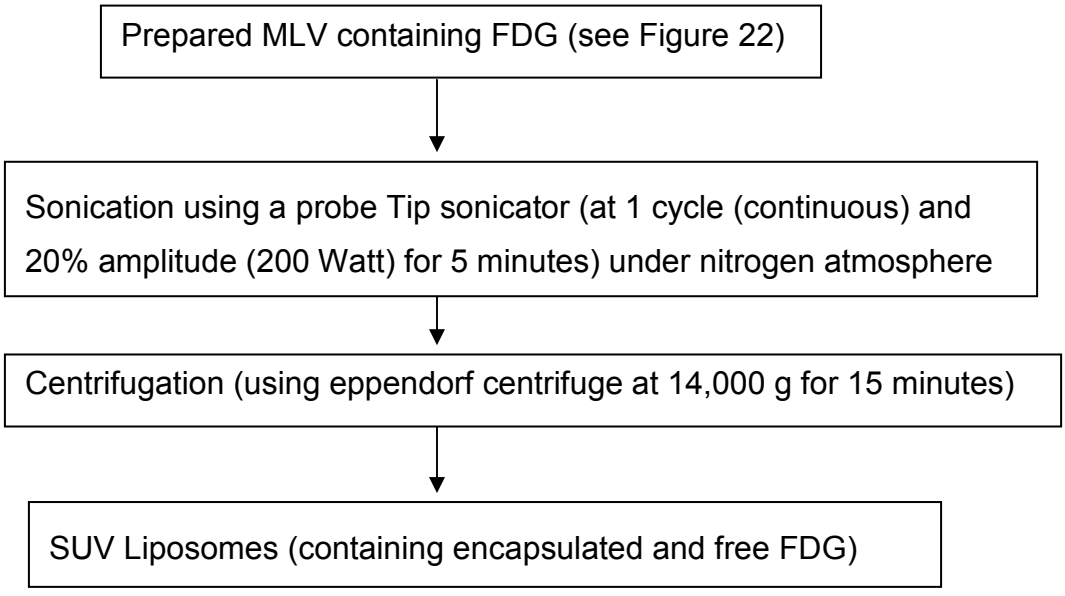

Figure 26: A schematic presentation for the preparation of SUV containing FDG

II.2.1.6. Preparation of small unilamellar vesicles containing Er-DTPA

Figure 27 shows the schematic procedures for preparing liposomes containing Er-DTPA. All procedures were done under sterilization conditions in clean pinch.

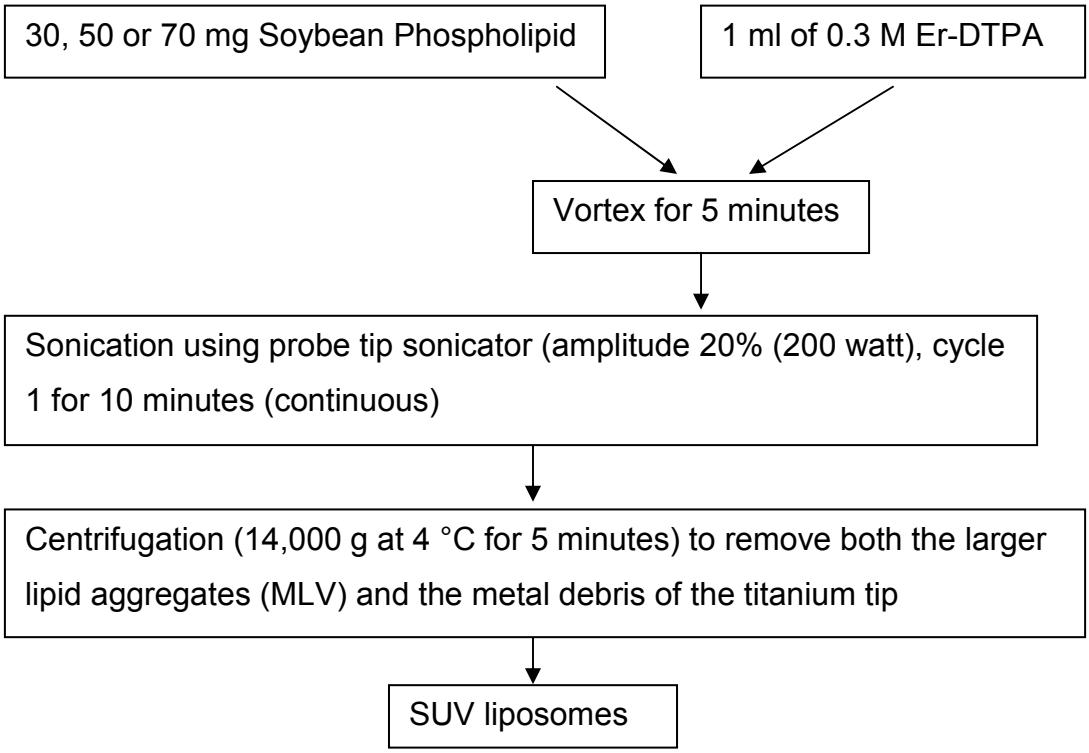

Figure 27: A schematic presentation for the preparation of SUV containing Er-DTPA

During sonication the sample has to be cooled by putting the tube in a water bath in order to avoid deterioration of the soybean phospholipid. Also the mixture is fumigated with nitrogen gas using sterile syringe and sterile filter (0.2 μm, cellulose acetate).

II.2.2. Characterization of the prepared liposomes (*Dhe-Paganon, et al., 1994*)

II.2.2.1. Preparation of cGPC columns

II.2.2.1.1. Swelling of dry GPC material (Sephadex G-25 M)

10g of GPC material (sephadex G-25 M) was weighed into a sterile bottle and 50 ml sterile swelling buffer (PBS) was added; the lid was closed and suspended by gentle shaking. The preparation was suspended again after 5 and 10 minutes, and then allowed to stand for 2 hours followed by suspension again by gentle shaking. The preparation was left for 10 minutes, and then the supernatant containing fine particles was discarded from the semi-solid Sephadex precipitate (sephadex bed).

II.2.2.1.2. Preparation of the GPC slurry

To the sephadex bed 20 % of PBS was added and the lid was closed and suspended by gentle shaking. The shaking was repeated frequently during use.

II.2.2.1.3. Preparation of the cGPC colums

cGPC columns were put into centrifuge tubes. The head of a 1ml filter tip was cut for a wide opening. The cGPC columns were filled with freshly suspended slurry (e.g. 4.5 ml/ column). The columns then were centrifuged at ~100g for 10 seconds using Eppendorf centrifuge. The gap at the columns was filled with slurry up to 2 mm to the top and then centrifuged again at ~100g for 10 seconds. The eluate was then removed.

II.2.2.1.4. Washing cGPC columns with GPC-buffer

Pre-washings: 500 µl of PBS was added to each column followed by a waiting period of 5-10 seconds, and then another 500 µl was added to each column. The columns were centrifuged at ~100g for 10 seconds (low speed, short time) and the eluate was removed. This washing was repeated 4 times.

Final washing: The columns were flushed as above with 2x 10% of bed volume with PBS (1 ml) and then centrifuged at 800g for 1 minute.

II.2.2.1.5. Sample run (loading the liposomes)

80 % of the threshold volume sample (250 µl for 5 ml columns) was applied to each column. The columns then were centrifuged at ~800g for exactly 1 minute (Eppendorf centrifuge) and the eluate was removed.

II.2.2.1.6. Reusing cGPC columns

If used columns have to be recycled, cGPC columns were washed 7 times to remove the retained drug completely. Recycling will be successful for up to 4 times.

II.2.2.2. Separation of the free drug

Figure 28 represents the separation of the free β-adrenoceptor antagonists and glucose from the prepared MLV. The summary of the conditions of HPLC required for analysis of β-adrenoceptor antagonists are listed in Table 7.

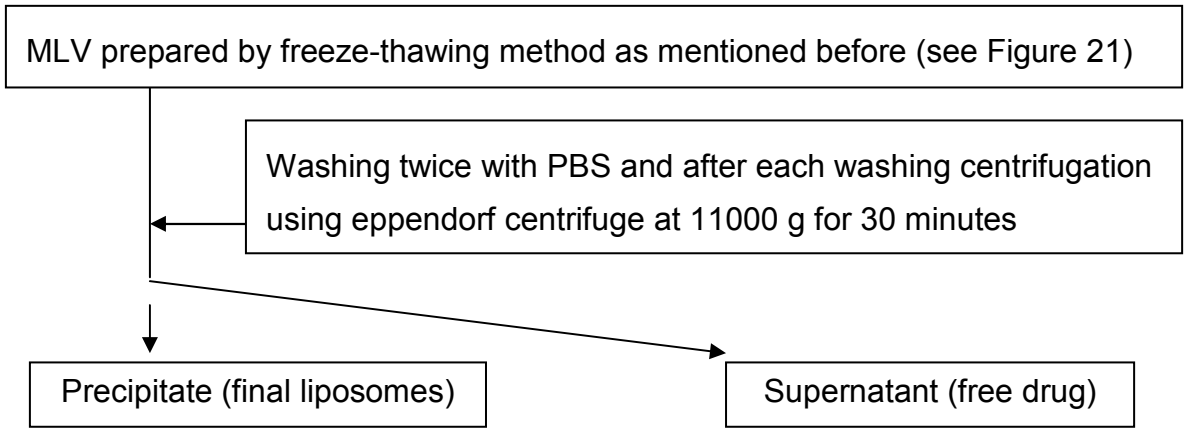

Figure 28: Schematic presentation of the separation of the free β-adrenoceptor antagonists and glucose from MLV

A schematic representation of the separation of free glucose, free FDG and free Er-DTPA from MLV, LUV and SUV is exhibited in Figure 29.

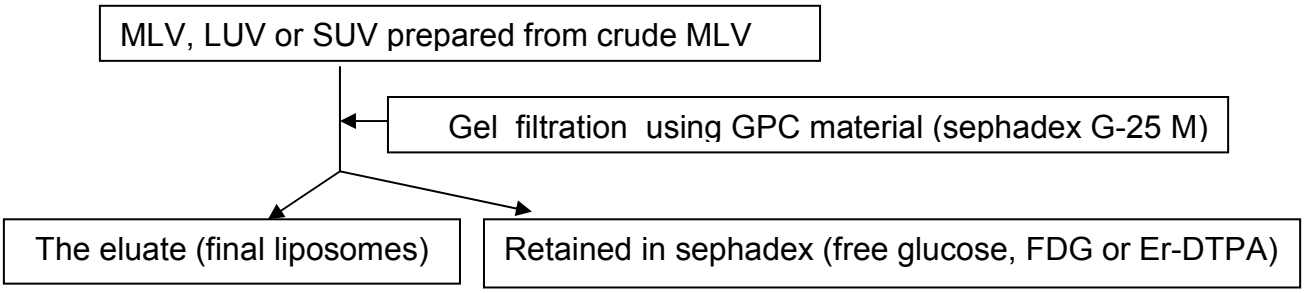

Figure 29: A schematic representation for the separation of the free Er-DTPA, free FDG and free glucose from MLV, LUV or SUV

II.2.2.3. Determination of entrapment efficiency (EE)

II.2.2.3.1. EE of MLV

A schematic representation of the procedures for determination of the entrapment efficiency of β-adrenoceptor antagonists and glucose in MLV is shown in Figure 30.

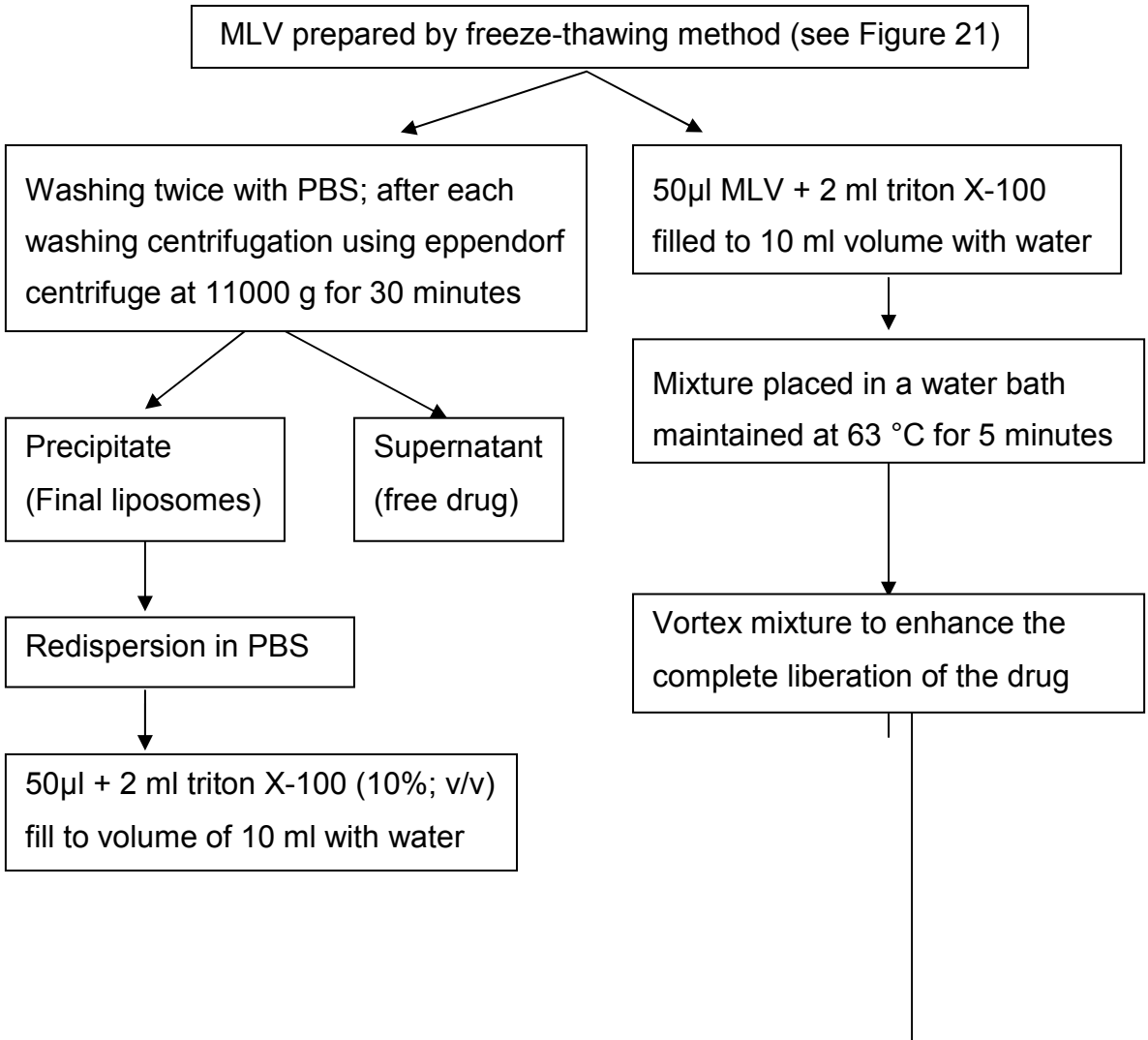

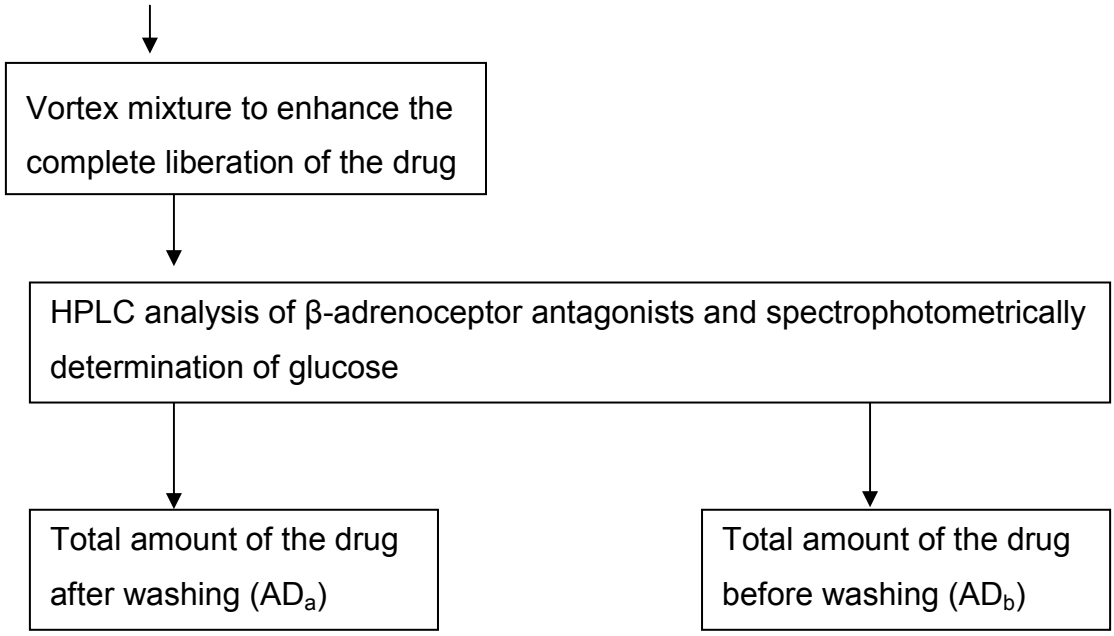

Figure 30: A schematic presentation for the procedures for EE determination of β-adrenoceptor antagonists and glucose from MLV

The entrapment efficiency (%) of the drug was determined by the following equation

$$EE = \frac{AD_a}{AD_b}.100$$

Where AD_a and AD_b are the drug amounts in liposome after and before washing respectively

II.2.2.3.2. EE of LUV and SUV

A schematic representation of the procedures for determination of the encapsulation efficiency of glucose in LUV or SUV and Er-DTPA in SUV are presented in Figure 31.

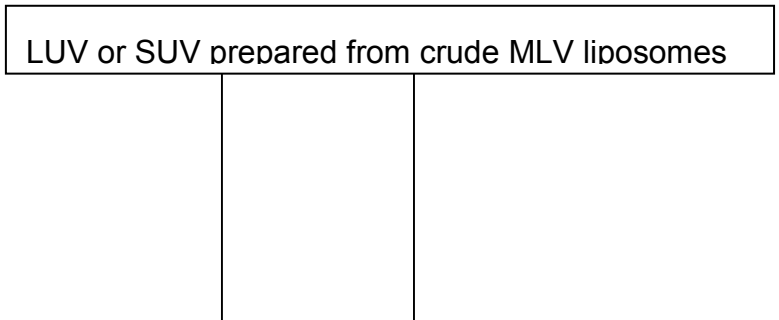

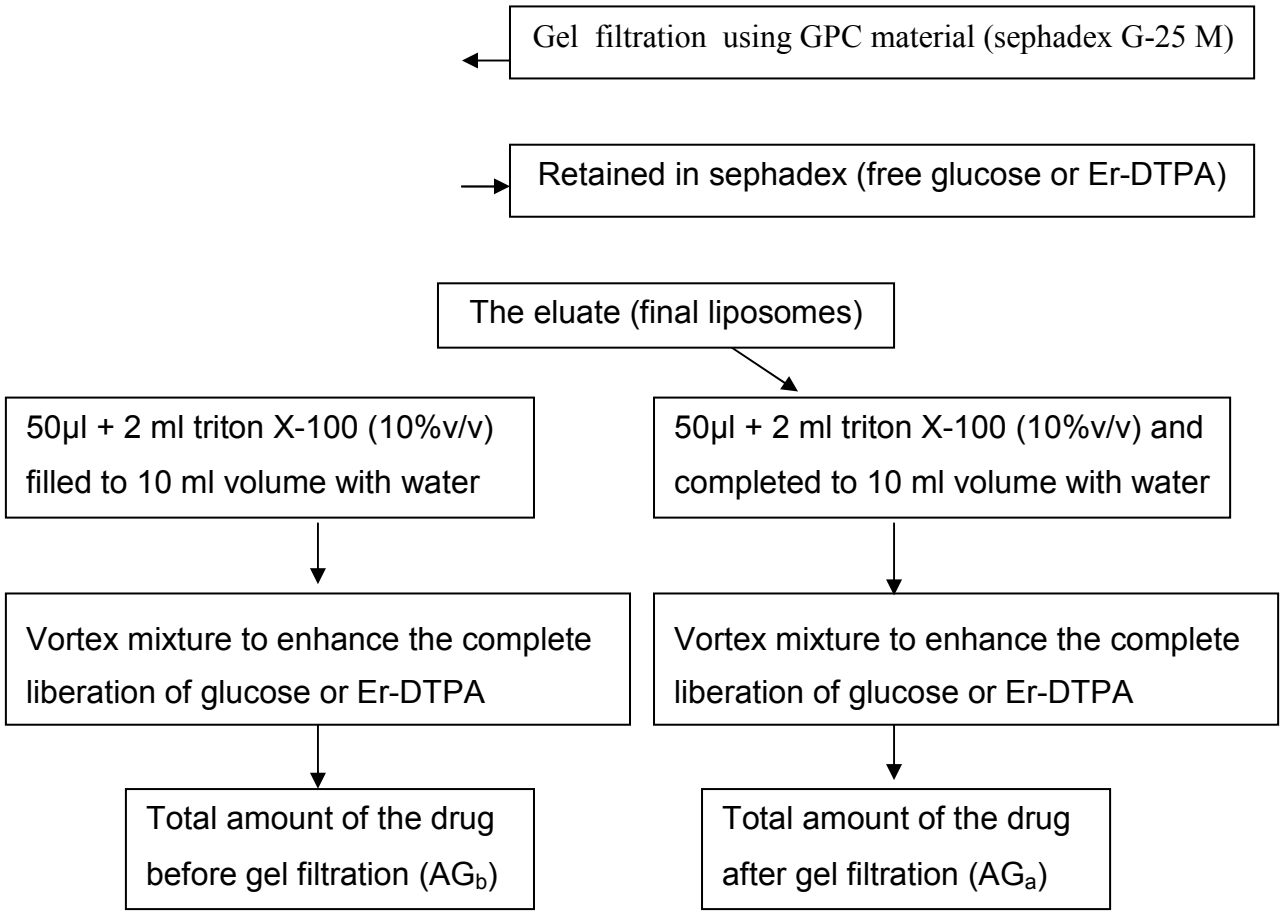

Figure 31: Procedures for EE determination of glucose in LUV or SUV and Er-DTPA in SUV

The entrapment efficiency (%) of the drug was determined by the following equation

$$EE = \frac{AG_a}{AG_b}.100$$

Where AG_a and AG_b are the drug amounts in liposome after and before gel filtration respectively

II.2.2.4. Chromatographic analysis of β-adrenoceptor antagonists

II.2.2.4.1. Calibration Curves

The calibration curves of β-adrenoceptor antagonists were done by accurately weighing 1mg of each drug and dissolving in 1 ml PBS. Dilutions were made to obtain different concentrations corresponding to 0.025, 0.05, 0.075, 0.1, 0.125 and 0.15 mg/ml of each drug. The drug concentration was determined by HPLC.

II.2.2.4.2. HPLC methods

The drug content in the dissolution fluid was analyzed using a Merck-Hitachi HPLC system, consisting of an HPLC System Manager Chromatography Data Station Software® Model D- 7000, a D-7000 interface, a programmable L-7250 autosampler, a pump model L-7100 and a detector model L-7420 (MERCK HITACHI, Germany). The method was a reversed-phase chromatography. The conditions employed for each model drug are given in Table 7.

Table 7: Summary of HPLC conditions used for analysis of the β-adrenoceptor antagonists

β-adrenoceptor antagonists	Mobile phase (%;v/v)		Injection volume (µl)	Flow rate (ml/minute)	wavelength (nm)
	Phosphate buffer* (pH 7.4)	Acetonitril			
Propranolol	50	50	20	1.2	294
Metoprolol	50	50	20	1.0	224
Atenolol	70	30	20	0.8	224
Pindolol	70	30	20	1.0	264

*Phosphate buffer is composed of 0.067 M $NaH_2PO_4.H_2O$ with 0.2 % triethylamine

II.2.2.5. Spectrophotometric determination of glucose

II.2.2.5.1. Method

Glucose was determined using a dinitrosalicylic acid colorimetric method according to (*Hsieh, et al., 2002*) with some modifications. This method involves the oxidation of the aldehyde functional group present in glucose. 3,5-dinitrosalicylic acid (DNS) is reduced to 3-amino,5-nitrosalicylic acid under alkaline conditions:

$$\text{Aldehyde} \xrightarrow{\textit{Oxidation}} \text{Carboxyl group}$$

$$\text{3,5-dinitrosalicylic acid} \xrightarrow{\text{Re}\textit{duction}} \text{3-amino-5-nitrosalicylic acid}$$

Because the dissolved oxygen can interfere with glucose oxidation, sulfite, which itself is not necessary for the colour reaction, is added in the reagent to absorb the dissolved oxygen.

II.2.2.5.2. Procedure

A mixture of 100 µl of liposomal preparation and 200 µl of tritonX-100 10% was heated in a water bath for 15 minutes and then vortexed to completely release the entrapped glucose. To this mixture 300 µl of a 1:1 mixture of DNS solution (Dinitrosalicylic acid 10 g, Phenol 2 g, Sodium sulfite 0.5 g, Sodium hydroxide 10 g, water ad 1 liter) and potassium sodium tartrate solution (40%; w/v) was added. The mixture was heated at 90º C for 15 minutes to develop the red-brown colour. After cooling to room temperature, the absorbance was recorded spectrophotometrically at 575 nm.

II.2.2.5.3. Calibration curve of glucose

The calibration curve of glucose was done by accurately weighing 1mg of glucose and dissolving in 1 ml PBS. Dilutions were made to obtain different concentrations corresponding to 0.005, 0.01, 0.015, 0.02, 0.025, 0.03 and

0.035 mg/ml of glucose. Glucose was determined spectrophotometrically at 575 nm using the same dilution medium without glucose as a blank.

II.2.2.6. Analysis of the erbium content

The amount of erbium was measured by UV spectrophotometry. The measurement was done between 700 nm to 300 nm using brain-key buffer as a blank.

Preparation of brain key buffer (Buffer Key1)

117.30 g of Tris (base) and 65.06 g of citric acid monohydrate were dissolved in 550 ml sterile water. The pH of the solution was adjusted to 7.2 with 2 M citric acid and then completed to 600 mL with sterile water. The obtained solution was filtered with sterile filter membrane (0.2 μm) in a sterile flask under the laminar flow.

II.2.2.7. Determination of the particle size

II.2.2.7.1. Determination of the particle size of liposomes containing β-adrenoceptor antagonists

II.2.2.7.1.1. Dynamic light scattering (DLS)

Dynamic light scattering (DLS) was performed at 20 °C utilizing an ALV 3000 correlator, an ALV-SP86 goniometer equipped with an ALV High QE APD Avalanche photodiode fiber optical detection system, and a He-Ne laser (Uniphase, 22 mW, λ = 632.8 nm). DLS was performed at seven different angles ($30° < \theta < 150°$) i.e. 30, 50, 70, 90, 110, 130 and 150º. Diffusion coefficients were determined by a non-linear fitting (Simplex algorithm) of the field autocorrelation function by applying mono- or biexponential fit functions. Dynamic light scattering was conducted from $\theta = 30°$ to $\theta = 150°$ in steps of 5 degrees. PBS (previously filtered through Millex LCR filters (0.45 μm diameter) containing one drop of the prepared liposomes (1.0 mg/mL)

was put into dust free cylindrical suprasil cuvettes (diameter 10 mm, 540.110 QS Hellma, Mülheim) under the flow box. Autocorrelation function of the intensity was analyzed to obtain the average diffusion coefficient, D, of the particles. The hydrodynamic radii were calculated by applying the Stokes-Einstein equation ($D_h = k_B T/3\pi\eta$ D, where k_B = Boltzmann constant ($1.3807*10^{-23}$ J/K), T= Temperature (K) (room temp=298K), D = diffusion coefficient (in m^2/s) and η is the viscosity of the medium (*Khelfallah, et al., 2005*).

II.2.2.7.1.2. Laser diffraction analysis (LDA)

Laser diffraction was performed using a Beckman-Coulter LS 13320 (Beckman-Coulter, U.S.A.) configured with a universal liquid module. Run conditions were as follows: sample refractive index, 1.33; circulation speed, 50%; measurement time, 90 seconds; carrier fluid, water. The sample was put in the receptacle of the sampler unit for dispersion and delivery to the flow cell. Volume particle size distribution was plotted using a computer program supplied by the manufacturer.

II.2.2.7.2. Determination of the particle size of liposomes containing glucose

The particle size distribution of glucose-containing liposomes was determined using laser diffraction on a Beckman-Coulter LS 13 320 (Beckman-Coulter, U.S.A.) configured with a universal liquid module.

II.2.2.7.3. Determination of the particle size of Er-DTPA SUV

The liposomal size distribution was measured using laser diffraction analyzer. The effects of soybean concentration, temperature and storage time on the particle size were studied.

II.2.3. In vitro release characteristics

II.2.3.1. In vitro release of β-adrenoceptor antagonists from liposomes

II.2.3.1.1. Dialysis method

In this method, a volume of 0.5 ml of liposome preparation was put in a dialysis bag (Dialysis tubing: regenerated cellulose, MWCO 12,000-14,000, SERVA Electrophoresis GmbH, Heidelberg), and both the ends were tied. The dialysiswas suspended in a bottle containing 25 ml of PBS, pH 7.4. The bottle was shaken at 200 rotations/minute in an incubator (GFL 3032 Shaker, LABOTEC, Germany) maintained at 37°C ± 0.5°C. At certain time intervals, 1 ml samples were drawn and replaced by 1 ml of fresh PBS. The amount of drug released was determined using HPLC (Table 5). All experiments were conducted in triplicate. This method was used for in vitro release of all types of the prepared liposomes (MLV, LUV and SUV).

II.2.3.1.2. Dispersion method

In this method, 0.5 ml of liposomes was dispersed in a bottle containing 25 ml of PBS, pH 7.4. The bottle was shaken at 200 rotations/minute in an incubator (GFL 3032 Shaker, LABOTEC, Germany) maintained at 37°C ± 0.5°C. At defined time intervals, 0.25 ml of the dispersion was withdrawn and replaced by 0.25 ml of fresh PBS. The sample was centrifuged (Eppendorf centrifuge, Eppendorf, Germany) at 14000 g for 30 minutes. The supernatant was analysed for the drug released using HPLC (Table 5). All experiments were conducted in triplicate. This method was used only for in vitro release of β-adrenoceptor antagonists from MLV.

II.2.3.2. In vitro release of glucose from liposomes using a dispersion method

The in vitro release of glucose from different liposomes was studied using the dispersion method. 1 ml of liposomal dispersion was diluted to 2 ml with PBS in Eppendorf tubes. The tubes were rotated using a rotator 25 rpm (Neolab laborbedarf-Vertriebs GmbH, Germany) in an incubator (GFL 3032 Shaker, LABOTEC, Germany) maintained at 37°C ± 0.5°C. At predetermined time intervals, 0.3 ml of the dispersion was withdrawn and replaced with 0.3 ml of fresh PBS.

The sample was filtered through gel filtration using GPC material (sephadex G-25 M). The amount of glucose was determined as mentioned above. All experiments were conducted in triplicate.

II.2.3.3. In vitro release of FDG from MLV, LUV and SUV using a dispersion method

One ml of MLV, LUV and SUV was diluted to 2 ml with PBS in Eppendorf tubes. The tubes were rotated using a rotator at 25 rpm and maintained at 37°C ± 0.5°C. At defined time intervals, 0.2 ml of the dispersion was withdrawn and replaced with 0.2 ml of fresh PBS. The sample was filtered by gel filtration using GPC material (sephadex G-25 M). The activity of FDG was measured.

II.2.3.4. Calculation of the half life ($t_{1/2}$) of the in vitro release

The release half life ($t_{1/2}$) of β-adrenoceptor antagonists and glucose from liposomes can be calculated by determined the maximum cumulative percentage of amount released using Lineweaver-Burk plot (called also the double-reciprocal plot), which is a plot of 1/cumulative percentage of drug release (1/R) against 1/time to yield a straight line that intersects the Y-axis at 1/maximum cumulative percentage of amount released ($1/R_{max}$) (Figure 32).

The cumulative percentage of amount remaining can be calculated using the maximum percentage of amount released. The half life ($t_{1/2}$) can be calculated from the slope of the resulting curve by plotting the ln (cumulative percentage remaining) against time (Figure 33).

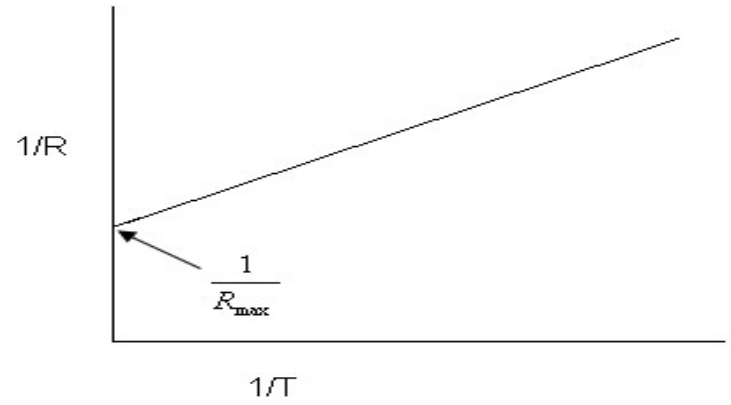

Figure 32: Double-reciprocal plot of drug release

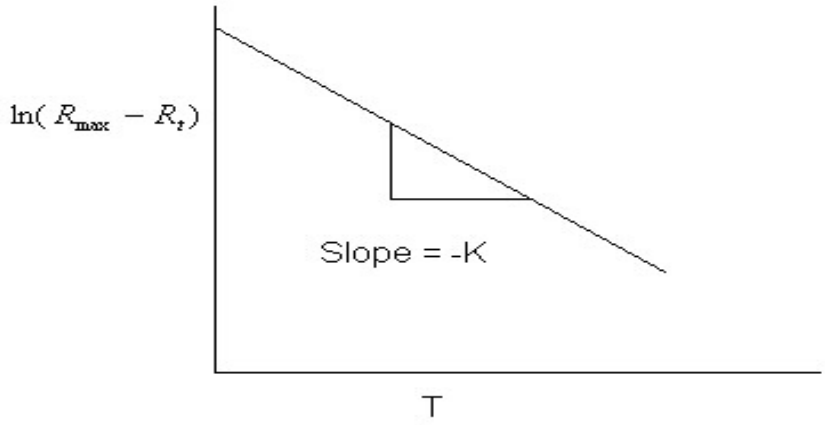

Figure 33: Semi-logarithmic presentation of drug release in case of a single exponential release

II.2.4. Stability of the liposomes containing Er-DTPA

II.2.4.5. Effect of storage temperatures

The stability of erbium-containing liposomes was determined by monitoring erbium release from the vesicles at three different temperatures; 4, 25, and 37 °C. The prepared liposomes after removing free erbium were divided into

samples of 300 µl. The divided samples were stored at 3 three different temperatures; 4, 25, and 37 °C. At predetermined time intervals, 1, 24, 48, 72, and 98 hours, the sample was taken and filtered using gel filtration to remove the released erbium. The eluate was taken and the amount of erbium retained in liposomes was analysed by UV analysis.

II.2.4.6. Effect of lipid concentration

Three preparations of liposomes with three different concentrations of soybean lipid (e.g. 30, 50 and 70 mg) were prepared and the release of erbium was monitored at three temperatures (4, 25 and 37 °C). The unencapsulated erbium was removed using cGPC and the filtered liposomes were divided into samples of 300 µl. Then the samples were stored at three different temperatures; 4, 25, and 37 °C. At predetermined time intervals, 1, 24, 48, 72, and 98 hours, the sample was taken and filtered using gel filtration to remove the released erbium. The eluate was taken and amount of erbium retained in liposomes was analysed by UV analysis.

II.2.5. In vivo animal imaging of FDG using PET

Two healthy Wister male rats (210 g) were scanned by the microPET studies. The rats were anesthetized by intraperitoneal injection with pentobarbital (40 mg/Kg). Thereafter the rats were injected with MLV containing 14.5 MBq ^{18}F-FDG intraperitoneally. Dynamic scanning of FDG for the whole body was done up to 120 minutes. The control rats were anesthetized by intraperitoneal injection with pentobarbital (40 mg/Kg) and then were injected with 18 MBq of unencapsulated ^{18}F-FDG in saline solution intraperitoneally. The scanning by microPET was done 30, 60, 90 and 120 minutes following the injection.

Chapter III: Results

III.1. Analysis of the model drugs

III.1.1. Standard calibration curves of β-adrenoceptor antagonists

The peak area of serial concentrations of propranolol, metoprolol, atenolol and pindolol was measured using HPLC. The average peak area of three measurements was calculated for each concentration. The standard calibration curves of the average peak area as a function of β-adrenoceptor antagonists concentration were constructed and are shown in Figure 34. All calibration curves have a linear relationship with a correlation coefficient (*r*) of ≥ 0.999 for all β-adrenoceptor antagonists.

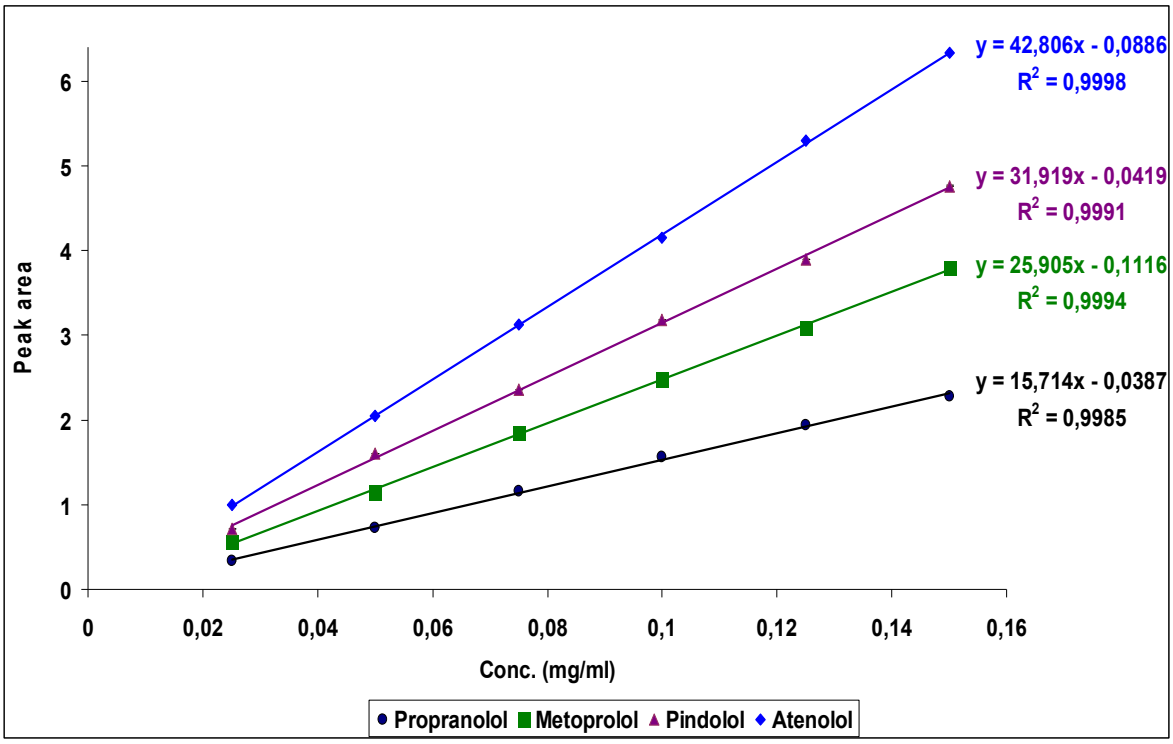

Figure 34: Standard calibration curves of the peak area as a function of β-adrenoceptor antagonists concentrations using HPLC

III.1.2. Retention times of the β-adrenoceptor antagonists

The retention time of propranolol, metoprolol, atenolol and pindolol was read from the chromatogram obtained from HPLC of each drug. Figure 35(A-D) exhibits the HPLC chromatograms of β-adrenoceptor antagonists with retention times. The retention times are listed in Table 8.

Table 8: Retention times of β-adrenoceptor antagonists

	Propranolol	Metoprolol	Atenolol	Pindolol
Retention time (minutes)	2.86	2.46	2.23	3.69

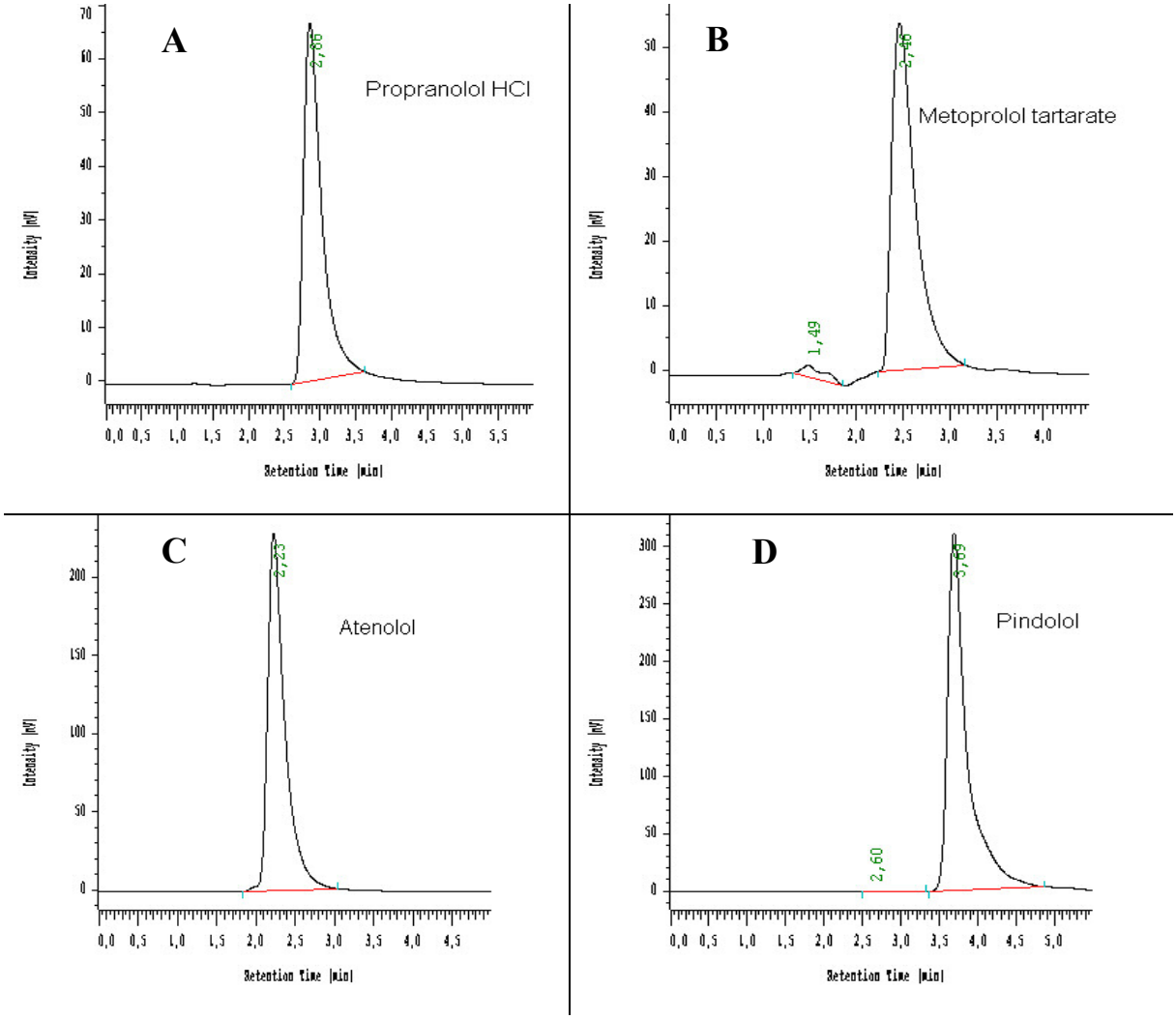

Figure 35: HPLC Chromatograms of β-adrenoreceptor antagonists A: Propranolol (1mg/ml), B: Metoprolol (1mg/ml), C: Atenolol (1mg/ml), D: Pindolol (1mg/ml)

III.1.3. Standard calibration curve of glucose

The absorbance of serial concentrations of glucose was determined spectrophotometrically in triplicates at 575 nm. The average absorbance of measurements for each concentration was plotted against glucose concentration to obtain a calibration curve which is exhibited in Figure 36.

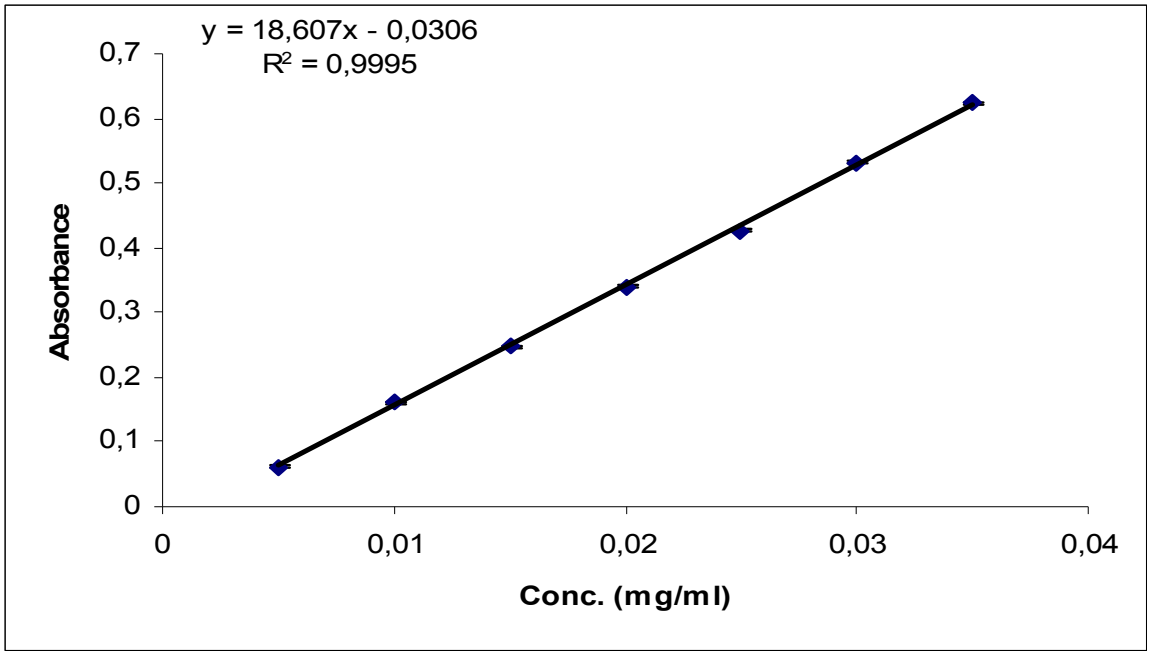

Figure 36: The standard calibration curve of the absorbance as a function of glucose concentration at 575 nm on the visible spectrophotometer

III.1.4. Analysis of the erbium content

Figure 37 depicts the UV spectrum of pure erbium DTPA (0.3 M) in key buffer solution. It was found that the baseline in case of pure erbium DTPA was at zero. The baseline for liposomes with erbium DTPA was above zero which, was due to the light scattering of the liposomes (Figure 38).

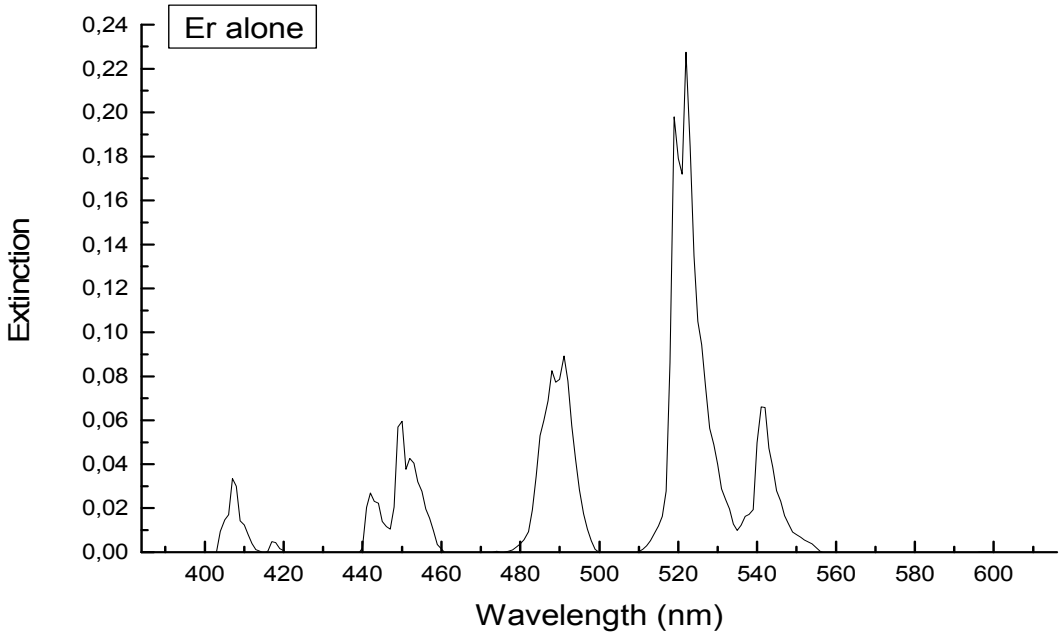

Figure 37: UV/Visible spectrum of Er-DTPA in key buffer solution (0.3 M)

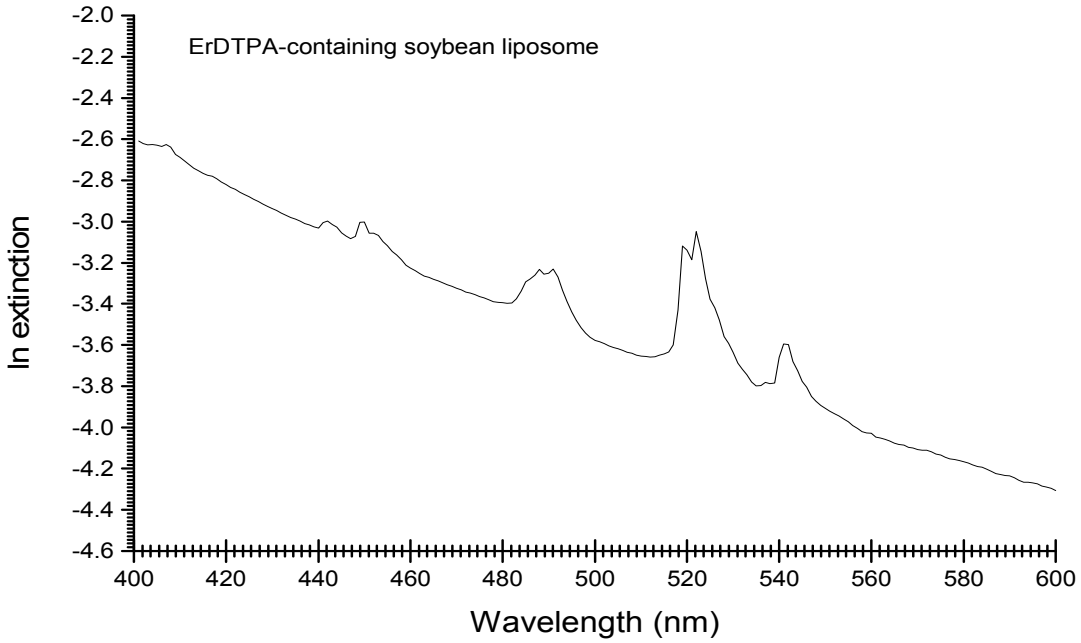

Figure 38: UV/Visible spectrum of Er-DTPA-containing soybean liposomes (0.3 M Er-DTPA /50 mg soybean lipid)

III.2. Determination of entrapment efficiency

III.2.1. Entrapment efficiency (EE) of β-adrenoceptor antagonists

The EE of β-adrenoceptor antagonists in MLV is shown in Figure 39. It was found that the EE differs from one lipid to another. Regarding propranolol and metoprolol, the EE was in the following order Ph90H > DSPC > DSPC/DMPC (1:1) > DMPC. The highest value of EE was in case of Ph90H (95.4 and 83.6 % for propranolol and metoprolol, respectively) and the lowest value was in case of DMPC (58 and 31 % for propranolol and metoprolol respectively). In case of atenolol and pindolol, the EE was in the following order DSPC > Ph90H > DSPC/DMPC (1:1) > DMPC. The highest value of EE was in case of DSPC (68.1 and 43.9 % for atenolol and pindolol, respectively) and the lowest value was in case of DMPC (2.7 and 28.5 % for atenolol and pindolol, respectively).

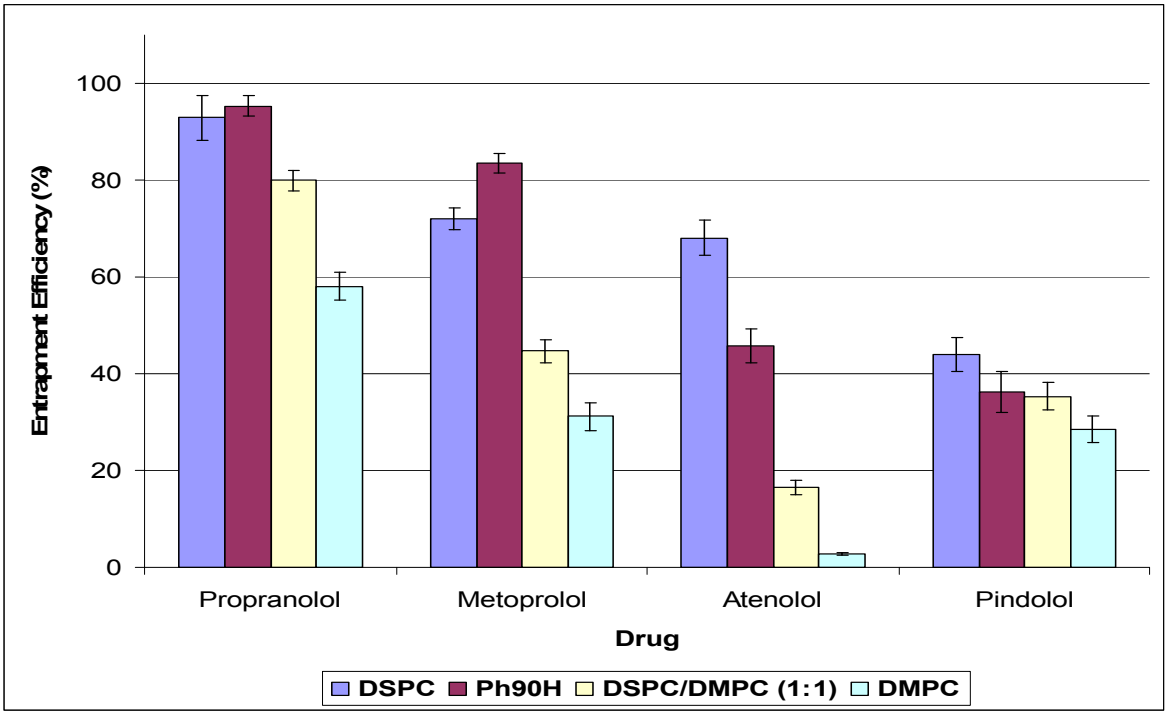

Figure 39: Entrapment efficiency (EE) of β-adrenoceptor antagonists in MLV prepared rom different lipids e.g. Ph90H, DSPC, DSPC/DMPC (1:1) and DMPC (concentration of lipid to drug is 19:50 mg/ml). Mean ± S.D., *n* = 3.

III.2.2. Entrapment efficiency (EE) of glucose

Figure 40 depicts the EE of glucose in MLV, LUV and SUV. It was found that the EE was in the following order SUV > MLV > LUV for all lipids used.

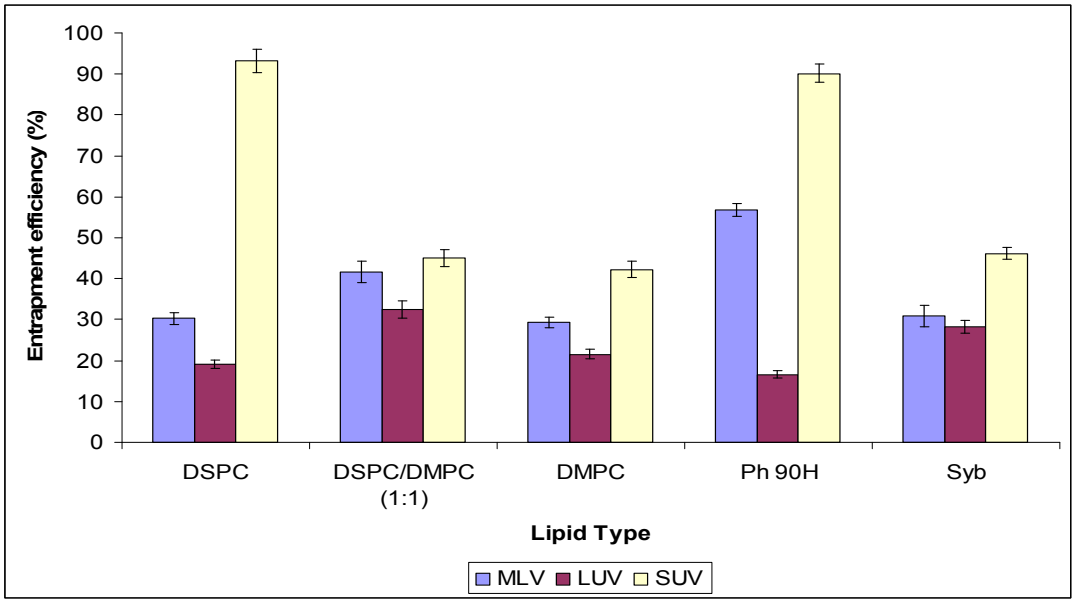

Figure 40: Entrapment efficiency (EE) of glucose in MLV, LUV and SUV prepared from different lipids e.g. DSPC, DMPC, DSPC/DMPC (1:1), Syb and Ph 90H. Mean ± S.D., *n* = 3.

III.2.3. Entrapment efficiency (EE) of Er-DTPA

Entrapment efficiency (EE) of Er-DTPA complex in SUV liposome with different concentrations of soybean lipid was calculated and is shown in Figure 41.

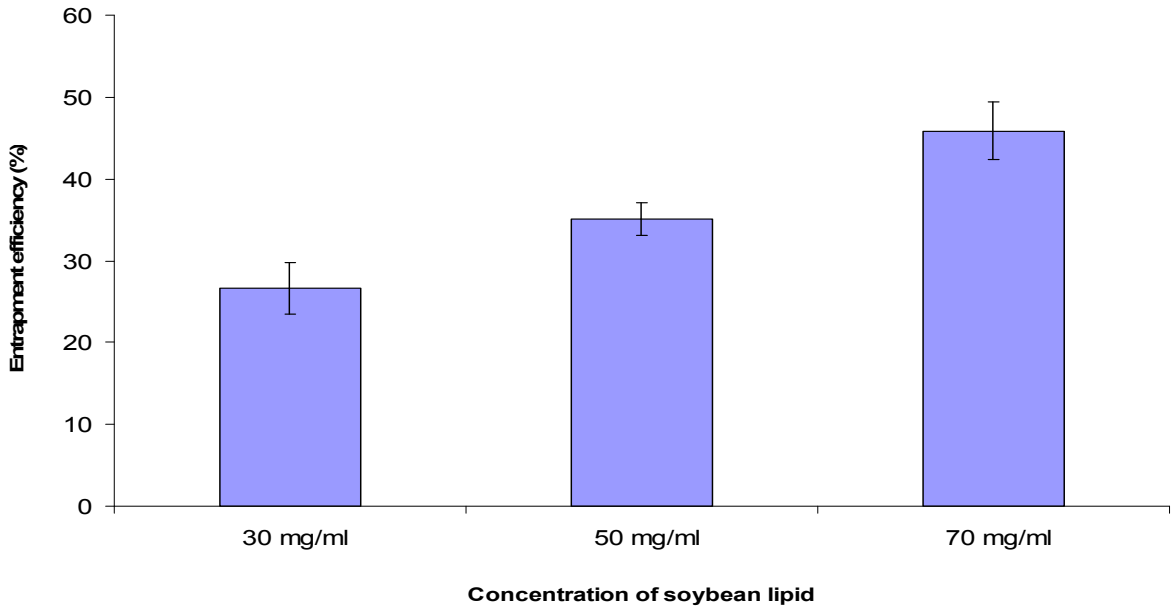

Figure 41: Encapsulation efficiency (EE) of Er-DTPA in liposomes prepared from soybean lipid of different concentrations (30, 50 and 70 mg/ml). Mean ± S.D., *n* = 3.

III.3. Determination of the particle size

III.3.1. Determination of the particle size of liposomes containing β-adrenoceptor antagonists

III.3.1.1. Determination of the particle size of β-adrenoceptor antagonists liposomes using dynamic light scattering (DLS)

The apparent particle size diameters of the MLV, LUV, and SUV of β-adrenoceptor antagonists liposomes with different lipids are shown in Table 9 and Figure 42.

Table 9: Average particle diameters of the liposomes containing β-adrenoceptor antagonists

Liposomal Type		Average Particle Size (μm)			
		Propranolol	**Metoprolol**	**Pindolol**	**Atenolol**
MLV	**DSPC**	2.691	5.967	3.466	4.268
	Ph 90H	3.332	11.889	7.387	3.191
	DSPC/DMPC (1:1)	0.956	2.289	2.327	3.322
	DMPC	0.694	5.967	1.315	1.834
LUV	**DSPC**	0.231	0.258	0.200	0.228
	Ph 90H	0.393	0.196	0.211	1.315
	DSPC/DMPC (1:1)	0.166	0.123	0.138	0.434
	DMPC	0.331	0.136	0.130	0.147
SUV	**DSPC**	0.389	0.184	0.316	1.662
	Ph 90H	0.182	0.246	0.234	0.490
	DSPC/DMPC (1:1)	0.207	0.79	0.226	0.583
	DMPC	0.638	0.952	0.450	0.106

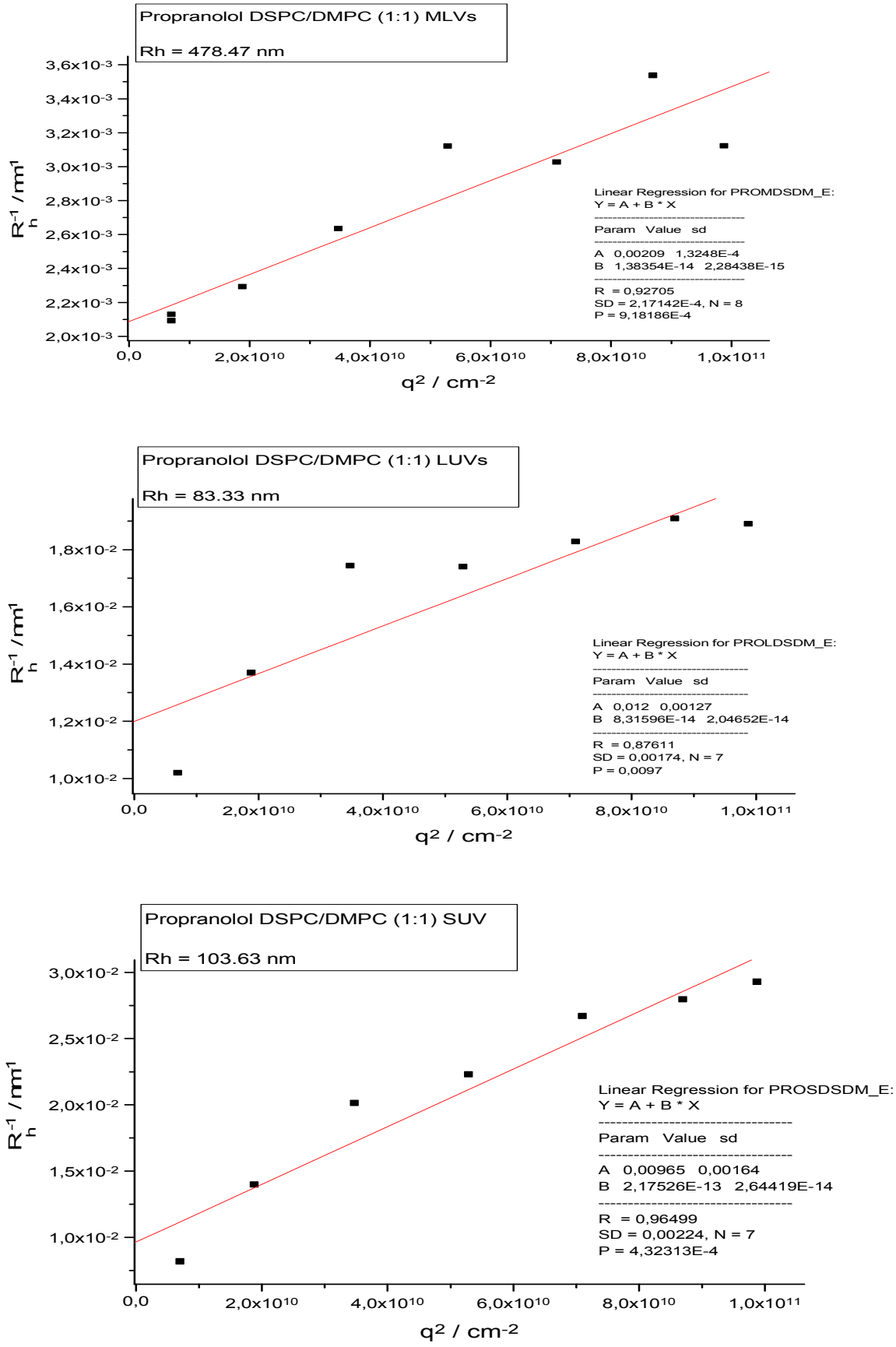

Figure 42: Reciprocal of radius plotted against scattering vector of the prepared propranolol-containing liposomes

III.3.1.2. Determination of the particle size of β-adrenoceptor antagonists liposomes using laser diffraction analysis (LDA)

The particle size distribution analysis obtained from laser diffraction analyzer is shown in Table 10 and Figure 43.

Table 10: Particle size distribution of the liposomes containing β-adrenoceptor antagonists

Lipo. type	Lipid Type / Drug		Propranolol					Metoprolol					Pindolol					Atenolol				
			Volume of particles (%) having particle diameter < (µm)																			
			10 %	25 %	50 %	75 %	90 %	10 %	25 %	50 %	75 %	90 %	10 %	25 %	50 %	75 %	90 %	10 %	25 %	50 %	75 %	90 %
MLV	DSPC	Particle diameter < (µm)	3.0	4.6	7.8	16.7	57.0	4.4	6.4	9.6	13.9	19.8	4.0	5.7	8.5	12.8	22.3	4.1	6.0	9.1	13.1	18.0
		Model distribution	Trimodal distribution					Trimodal distribution					Multimodal distribution					Bimodal distribution				
	Ph 90H	Particle diameter < (µm)	3.9	5.5	8.15	11.7	16.7	3.7	5.7	8.1	10.8	13.8	1.2	3.1	5.6	8.3	10.9	5.5	7.8	11.2	15.6	20.8
		Model distribution	Bimodal distribution					Bimodal distribution					Trimodal distribution					Unimodal distribution				
	DSPC/ DMPC (1:1)	Particle diameter < (µm)	2.6	3.8	6.0	9.6	21.8	3.7	5.4	8.2	11.9	16.5	3.0	5.00	8.09	11.9	16.3	3.5	5.9	9.8	16.7	68.3
		Model distribution	Trimodal distribution					Bimodal distribution					Bimodal distribution					Bimodal distribution				
	DMPC	Particle diameter < (µm)	0.7	0.9	1.4	1.8	2.1	3.1	5. 1	7. 7	10.8	13.8	3.8	6.2	10.0	17.0	130	4.5	9.6	99.3	164	232
		Model distribution	Bimodal distribution					Bimodal distribution					Multimodal distribution					Trimodal distribution				
LUV	DSPC	Particle diameter < (µm)	2.8	4.7	8.8	14.5	26.8	0.1	0.1	0.1	0.5	0.6	0.1	0.1	0.5	0.6	0. 7	0.1	0.1	0.1	0.2	0.2
		Model distribution	Multimodal distribution					Trimodal distribution					Trimodal distribution					Unimodal distribution				

LUV	**Ph 90H**	**Particle diameter < (µm)**	0.4	0.5	0. 6	1.9	2.2	0.1	0.1	0.11	0.2	0.2	0.1	0.1	0.1	0.1	0.2	2. 4	3. 4	4.6	6.0	7.4
		Model distribution	**Trimodal distribution**					**Bimodal distribution**					**Trimodal distribution**					**Bimodal distribution**				
	DSPC/ DMPC (1:1)	**Particle diameter < (µm)**	0.1	0.1	0.1	0.2	0.2	0.1	0. 1	0.1	0.1	0.2	0.1	0.7	0.1	0.1	0.2	3.1	4.9	7. 8	11.6	17.0
		Model distribution	**Unimodal distribution**					**Multimodal distribution**					**Trimodal distribution**					**Trimodal distribution**				
	DMPC	**Particle diameter < (µm)**	0. 1	0.5	0.6	0.7	1.9	0.1	0.1	0.1	0.2	0.2	0.1	0.1	0.2	0.2	0. 2	10.6	70.8	139	182	278
		Model distribution	**Trimodal distribution**					**Unimodal distribution**					**Unimodal distribution**					**Multimodal distribution**				
SUV	**DSPC**	**Particle diameter < (µm)**	0.1	0.1	0.2	0.5	0. 6	0.1	0.1	0.1	0.5	0.6	0.1	0.4	0.8	1.7	2.1	1.8	5.4	11.7	36.2	93.1
		Model distribution	**Trimodal distribution**					**Trimodal distribution**					**Trimodal distribution**					**Trimodal distribution**				
	Ph 90H	**Particle diameter < (µm)**	0.4	0.4	0.5	0.5	0.5	0. 1	0.1	0.1	0. 2	0.2	0.1	0.1	0.1	0.1	0.1	0.1	0.1	0.1	0.1	0.2
		Model distribution	**Unimodal distribution**					**Bimodal distribution**					**Bimodal distribution**					**Bimodal distribution**				
	DSPC/ DMPC (1:1)	**Particle diameter < (µm)**	3.1	10.8	76.3	170	238	0. 1	0.1	0.2	1. 7	2.1	0.1	0.1	0.1	0.1	0.2	34.1	84.3	132	172	215
		Model distribution	**Multimodal distribution**					**Multimodal distribution**					**Bimodal distribution**					**Bimodal distribution**				
	DMPC	**Particle diameter < (µm)**	0.1	0.6	0.8	1.9	2.2	1.9	2.9	3.9	5. 2	6.3	0.1	0.5	1.1	1.8	2.1	3.7	6.4	10.7	19.6	141
		Model distribution	**Trimodal distribution**					**Bimodal distribution**					**Trimodal distribution**					**Multimodal distribution**				

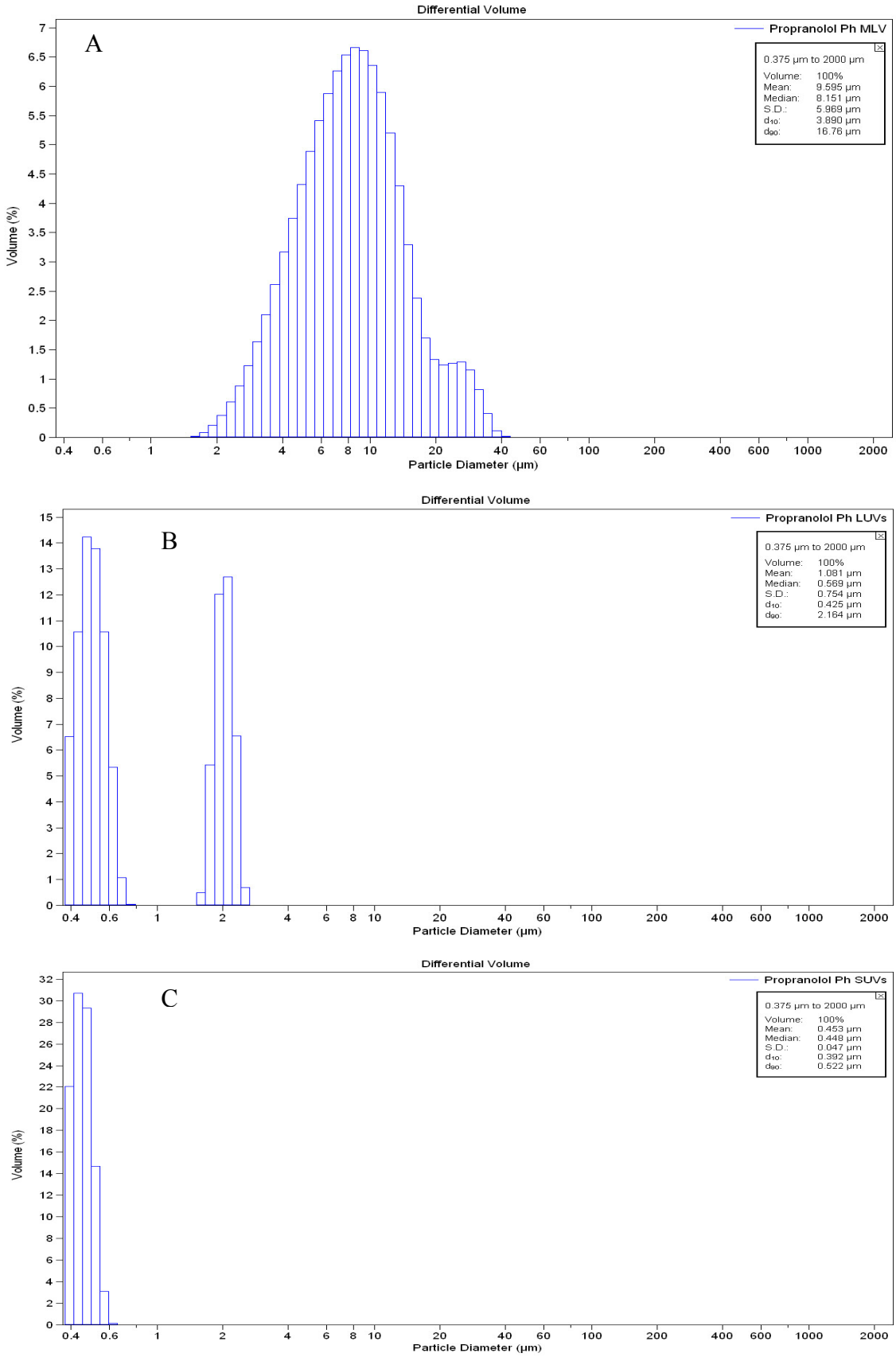

Figure 43: Particle size distribution of propranolol-containing liposomes, A: MLV, B: LUV, C: SUV

III.3.2. Determination of the particle size of glucose-containing liposomes

The particle size distribution analysis of liposomes containing glucose obtained from laser diffraction analyzer is shown in Table 11. It was found that there is a different broad size distribution ranging from 0.04 µm to 18.2 µm. This broad size distribution depends on the lipid and the liposomal types. Figure 44 shows particle size distribution of Ph90H liposomes as examples of glucose-containing liposomes.

Table 11: Particle size distribution of the liposomes containing glucose

Lipo. type	Lipid type / % Particle Volume / Pm and MD		Volume of particles (%) having particle diameter < (µm)				
			10%	25%	50%	75 %	90%
MLV	DSPC	Particle diameter < (µm)	2.385	3.510	5.461	8.438	12.72
		Model distribution	Trimodal distribution				
	Ph 90H	Particle diameter < (µm)	1.841	2.565	3.778	5.507	7.441
		Model distribution	Unimodal distribution				
	DSPC/DMPC (1:1)	Particle diameter < (µm)	2.159	4.250	7.433	11.90	18.16
		Model distribution	Unimodal distribution				
	DMPC	Particle diameter < (µm)	2.002	5.515	9.553	13.15	16.43
		Model distribution	Trimodal distribution				
	Syb	Particle diameter < (µm)	0.062	0.082	0.512	0.677	1.883
		Model distribution	Multimodal distribution				
LUV	DSPC	Particle diameter < (µm)	0.048	0.054	0.064	0.265	0.496
		Model distribution	Trimodal distribution				
	Ph 90H	Particle diameter < (µm)	0.050	0.057	0.065	0.076	0.181
		Model distribution	Bimodal distribution				
	DSPC/DMPC (1:1)	Particle diameter < (µm)	0.106	0.121	0.158	1.578	2.154
		Model distribution	Bimodal distribution				
	DMPC	Particle diameter < (µm)	0.113	0.122	0.133	0.146	0.158
		Model distribution	Unimodal distribution				
	Syb	Particle diameter < (µm)	0.113	0.122	0.133	0.145	0.157
		Model distribution	Unimodal distribution				
SUV	DSPC	Particle diameter < (µm)	0.048	0.054	0.061	0.071	0.180
		Model distribution	Bimodal distribution				
	Ph 90H	Particle diameter < (µm)	0.050	0.057	0.067	0.091	0.624
		Model distribution	Multimodal distribution				
	DSPC/DMPC (1:1)	Particle diameter < (µm)	0.058	0.075	0.653	1.853	2.279
		Model distribution	Bimodal distribution				
	DMPC	Particle diameter < (µm)	0.083	0.498	1.306	1.831	2.130
		Model distribution	Trimodal distribution				
	Syb	Particle diameter < (µm)	0.043	0.047	0.054	0.068	0.454
		Model distribution	Bimodal distribution				

Pm: Particle diameter (µm), MD: Model distribution

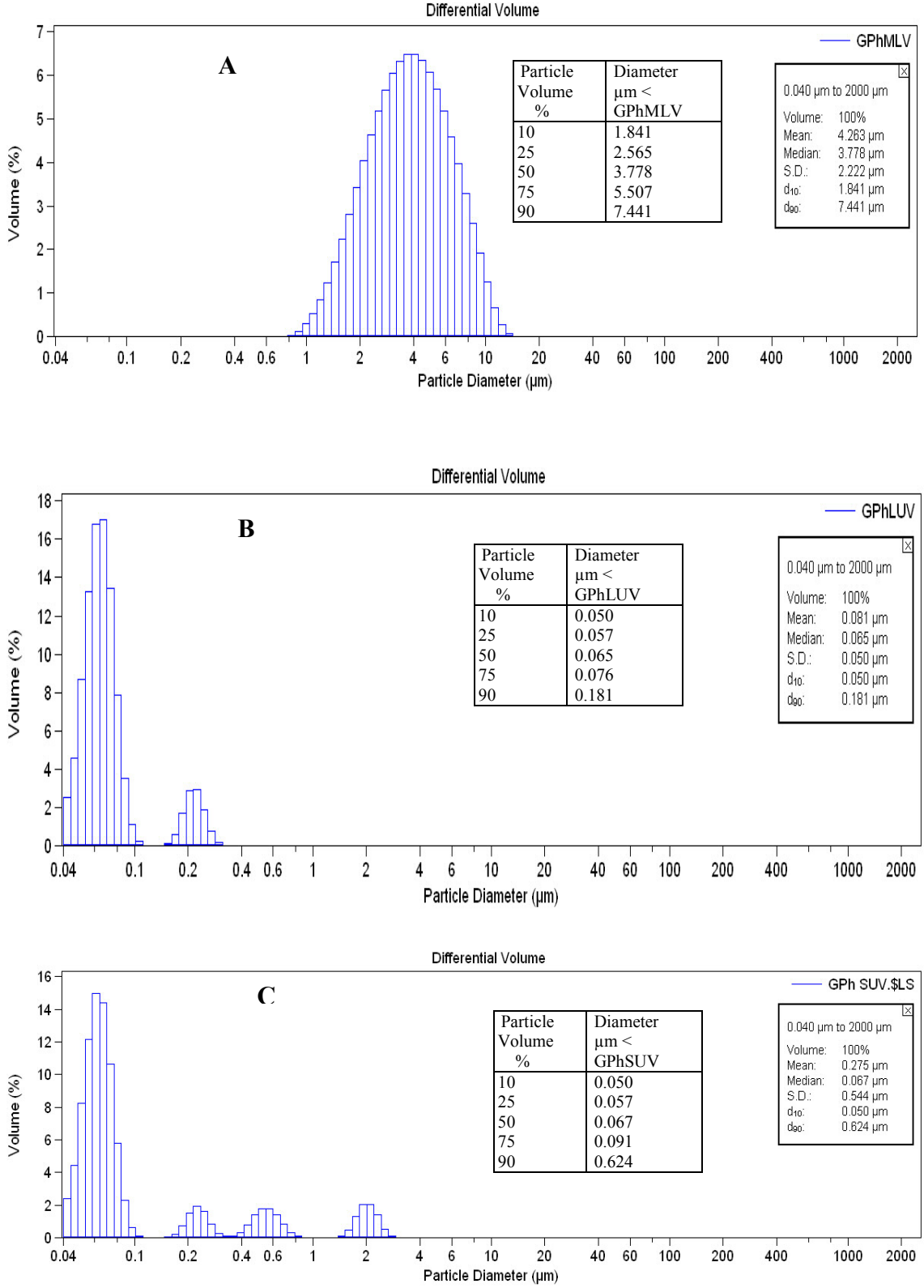

Figure 44: Effect of liposomal structure on particle size and particle size distribution of glucose-containing liposomes, A: MLV, B: LUV, C: SUV

III.3.3. Determination of the particle size of Er-DTPA liposomes

The particle size distribution analysis of Er-DTPA SUV was determined by laser diffraction analyzer and is displayed in Figures 45, 46 and 47. Figure 45 exhibits the effect of soybean lipid content on the diameter of liposomal particles. Figure 46 shows the effect of storage temperature on the particle diameter of liposomes. The effect of storage time on the stability of liposomes containing Er-DTPA is depicted in Figure 47.

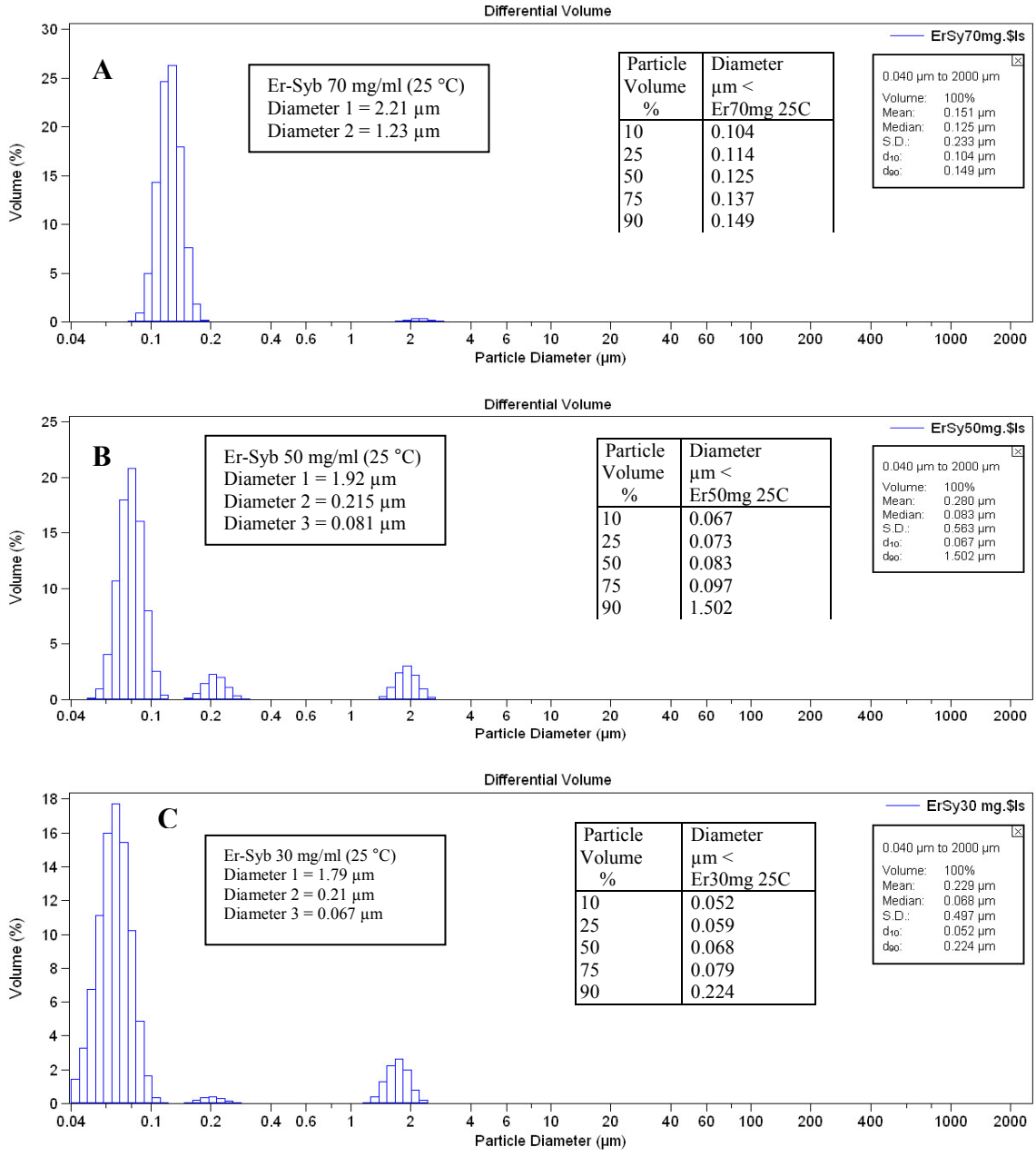

Figure 45: Effect of soybean concentration on the average particle size and size distribution of Er-DTPA-containing SUV, A: 70 mg/ml, B: 50 mg/ml, C: 30 mg/ml

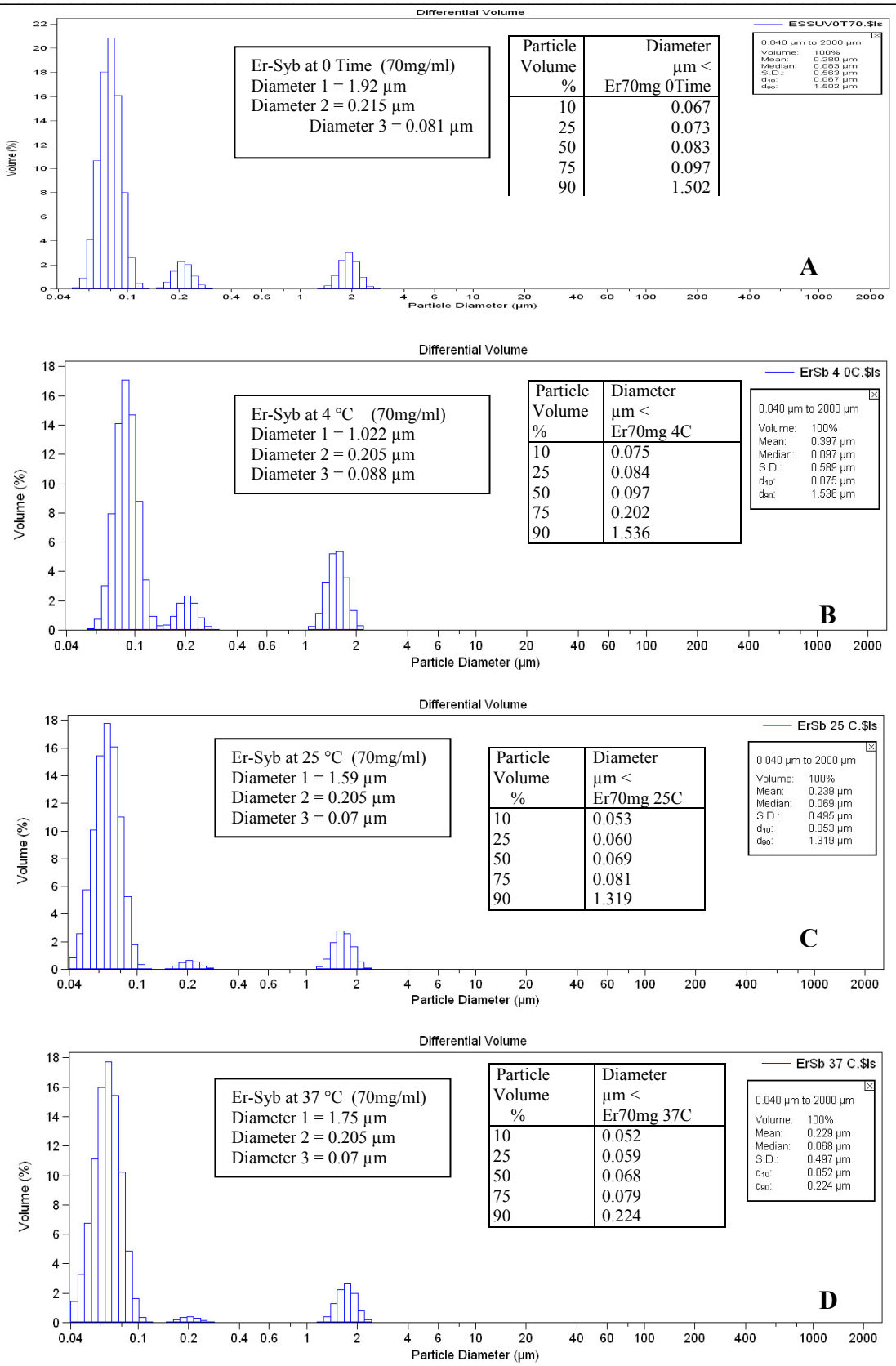

Figure 46: Effect of storage temperature (after one month storage) on the average particle size and size distribution of Er-DTPA-containing SUV, A: Initial value at zero time, B: at 4 °C, C: at 25 °C, D: at 37 °C

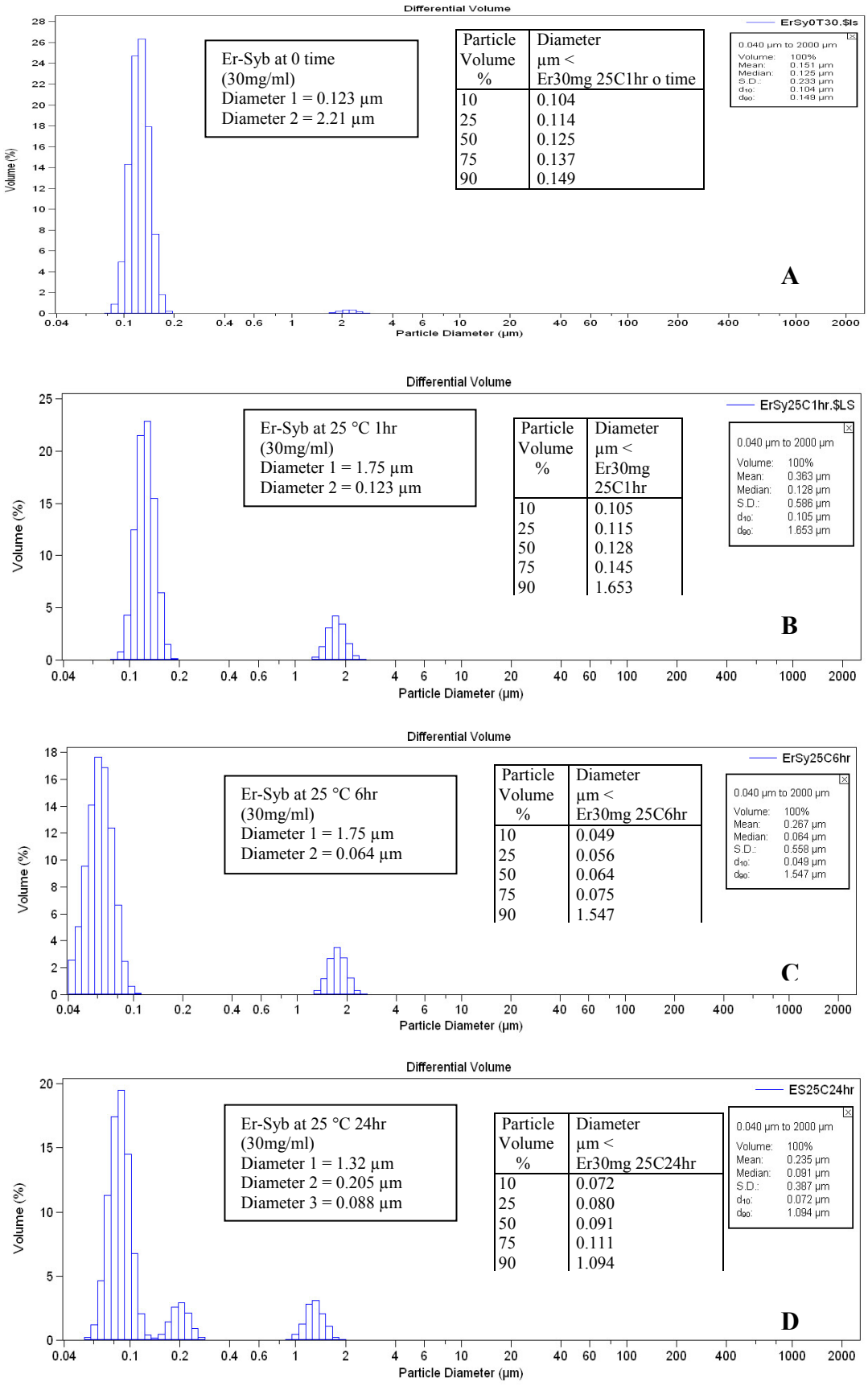

Figure 47: Effect of storage time on the average particle size and size distribution of Er-DTPA-containing SUV, A: Initial value at 0 time, B: 1hr, C: 6 hr, D: 24 hr

III.4. In vitro release of β-adrenoceptor antagonists from liposomes

III.4.1. In vitro release of β-adrenoceptor antagonists from liposomes using a dialysis method

III.4.1.1. In vitro release of β-adrenoceptor antagonists from MLV

III.4.1.1.1. In vitro release of propranolol from MLV

Figure 48 shows the release profiles of unencapsulted propranolol and propranolol MLV formulations prepared from different lipids (DSPC, DMPC, DSPC/DMPC (1:1) or Ph90H) into PBS, pH 7.4 at 37± 0.5 °C. The results were illustrated by plotting the percentage cumulative amount released of propranolol versus time. From the release profiles, it was found that the unencapsulated propranolol diffuses completely (100 %) through the membrane into the release medium in about one hour. Concerning encapsulated propranolol, it was found that the formulations made from DSPC, Ph90H and DMPC lipids exhibited an initial burst drug release during the first four hours (36, 23, and 37 %, respectively) followed by a plateau for over 336 hours. In case of DSPC/DMPC (1:1), there was rapid increase of the propranolol concentration in the dissolution medium up to 85% within 4 hours followed by slightly increase in the propranolol release.

III.4.1.1.2. In vitro release of metoprolol from MLV

The release profiles of unencapsulated metoprolol and metoprolol MLV formulations prepared from different lipids (DSPC, DMPC, DSPC/DMPC (1:1) or Ph90H) into PBS, pH 7.4 at 37± 0.5 °C is exhibited in Figure 49. From the release profiles, it was found that the unencapsulated metoprolol diffuses completely (100 %) across the dialysis membrane into the release medium in about one hour. In case of the formulation containing Ph90H, the release of metoprolol increases gradually until reaching 100 % after 336 hours. But in case of DSPC MLV, the release rate slightly increases, which

is then followed by a plateau for over 72 hours, then increases again. In case of DSPC/DMPC, the release rate of metoprolol increased gradually and it reached 100 % after 168 hours. Although DMPC has short acyl chain and the low Tc (23 °C), the release of metoprolol was very slow and constant up to 672 hours.

III.4.1.1.3. In vitro release of atenolol from MLV

The percentage cumulative amount released of atenolol versus time from MLV prepared from different lipids (DSPC, DSPC/DMPC (1:1), DMPC or Ph90H) into PBS, pH 7.4 at 37± 0.5 °C is shown in Figure 50. The results were illustrated by plotting the cumulative percentage of drug released versus time. It was found that the release rate of atenolol was in the following order DMPC > DSPC/DMPC (1:1) > Ph90H > DSPC until 4 hours, DSPC/DMPC (1:1) > Ph90H > DMPC > DSPC after 4 hours and until 48 hours, and finally the order Ph90H > DSPC/DMPC (1:1)> DSPC > DMPC until 504 hours. The release rate of atenolol from DMPC liposomes is characterized by a sharp initial burst release during the first 4 hours followed by a plateau up to 504 hours.

III.4.1.1.4. In vitro release of pindolol from MLV

The release profiles of pindolol MLV formulations prepared from different lipids (DSPC, DMPC, DSPC/DMPC (1:1), or Ph90H) into PBS, pH 7.4 at 37± 0.5 °C are illustrated in Figure 51. It was found that the release rate of pindolol was in the following order DSPC > Ph90H > DSPC/DMPC (1:1) > DMPC. After 6 hours, the release rate of pindolol from the formulation containing DSPC, Ph90H, DSPC/DMPC (1:1) and DMPC was 100 %, 74 %, 66.02 % and 45 % respectively.

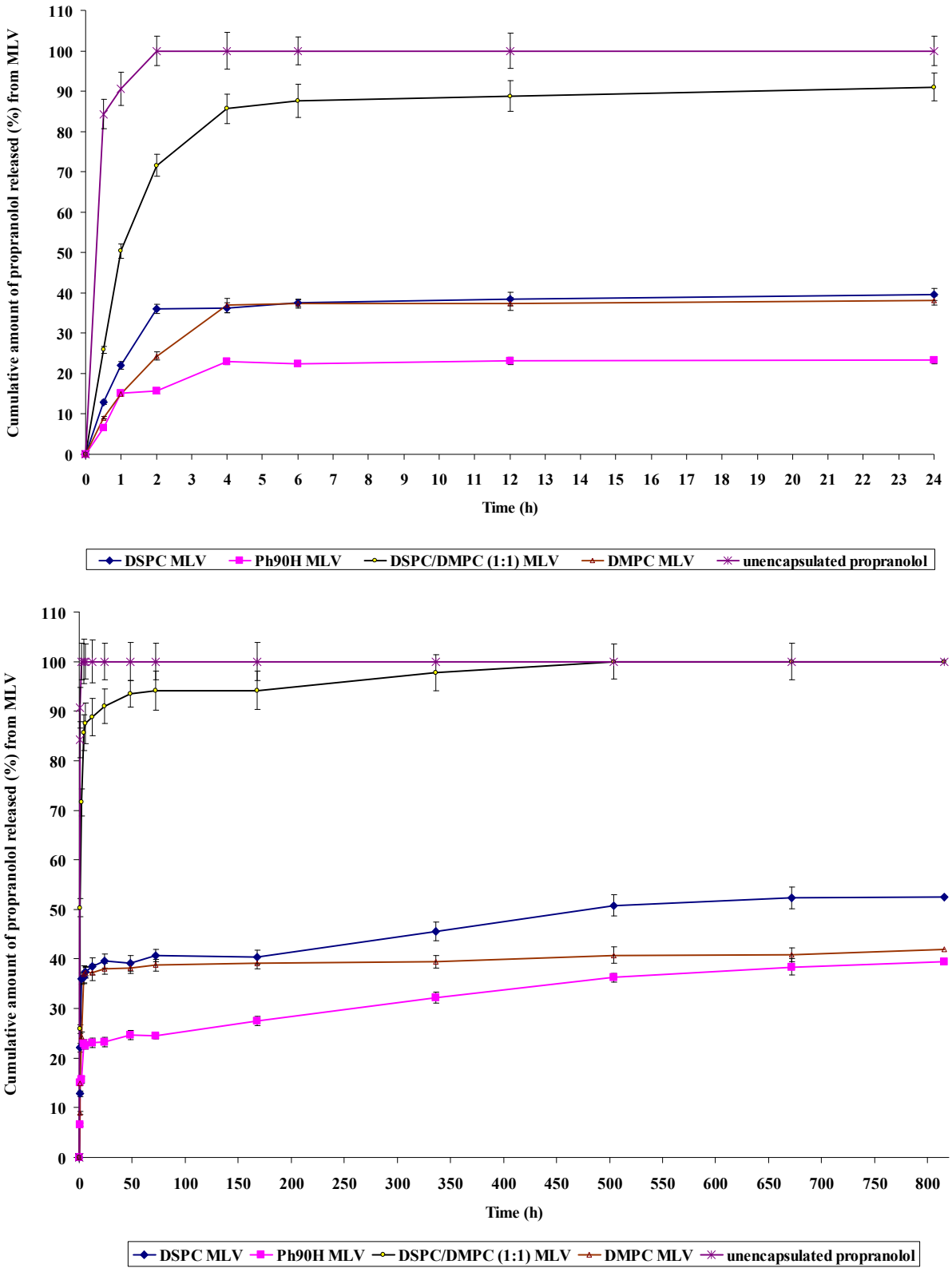

Figure 48: Release pattern of unencapsulated propranolol and propranolol from MLV liposomes of different lipid compositions into PBS, at pH 7.4, at 37 ± 0.5 °C using dialysismethod. Mean ± S.D., *n* = 3.

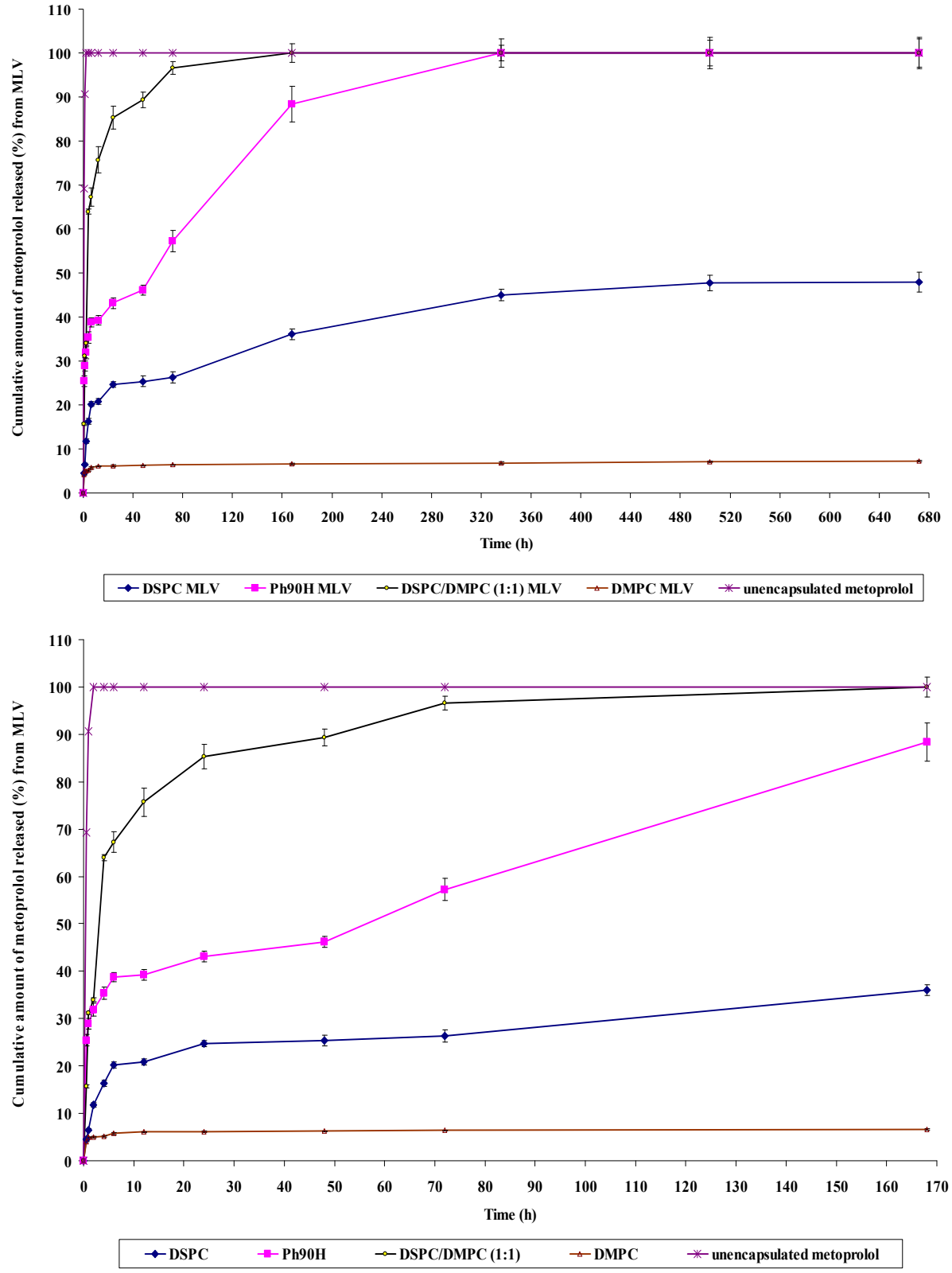

Figure 49: Release pattern of unencapsulated metoprolol and metoprolol from MLV liposomes of different lipid compositions into PBS, at pH 7.4, at 37 ± 0.5 °C using dialysismethod. Mean ± S.D., *n* = 3.

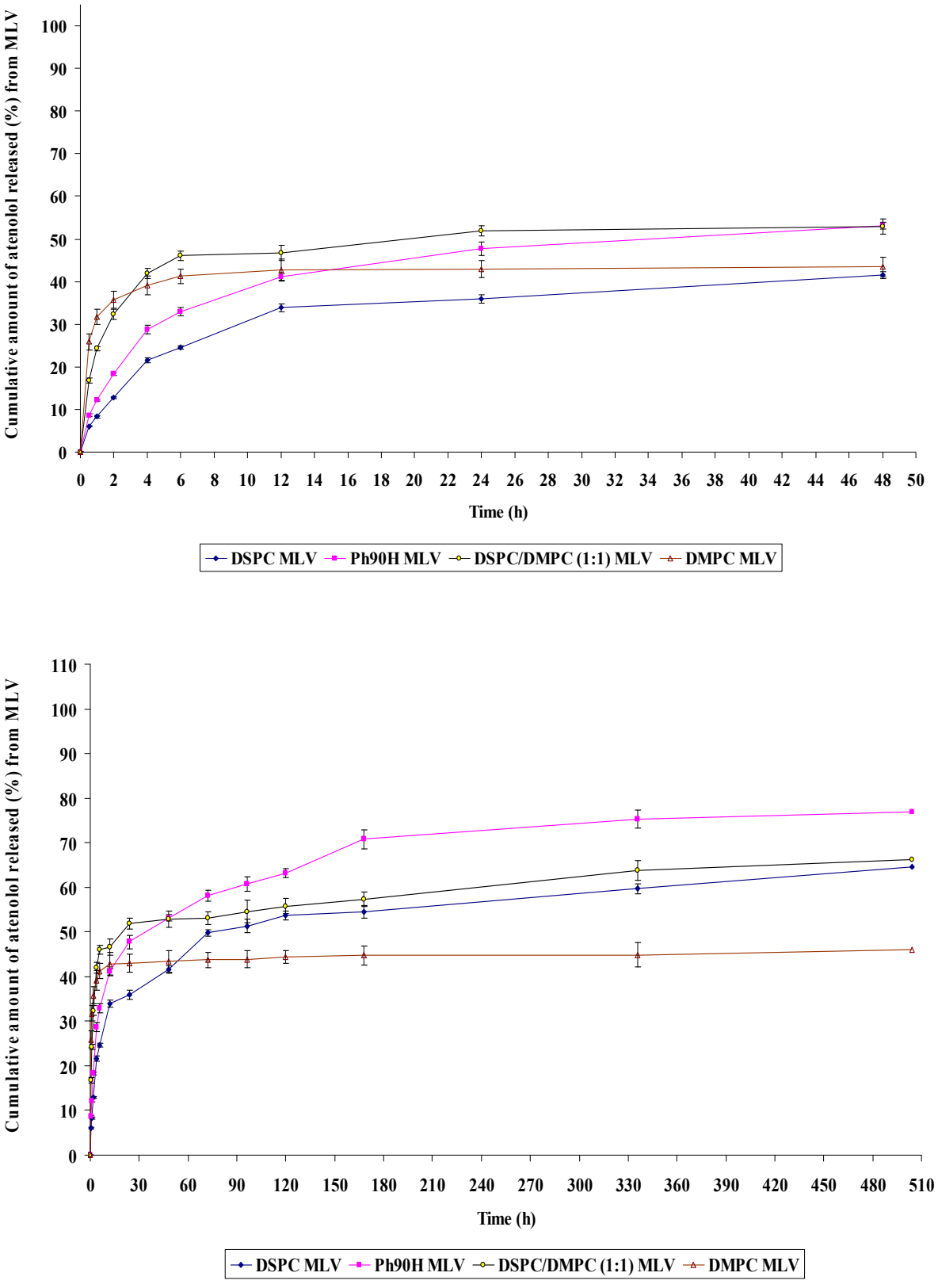

Figure 50: Release pattern of atenolol from MLV liposomes of different lipid compositions into PBS, at pH 7.4, at 37 ± 0.5 °C using dialysismethod. Mean ± S.D., *n* = 3.

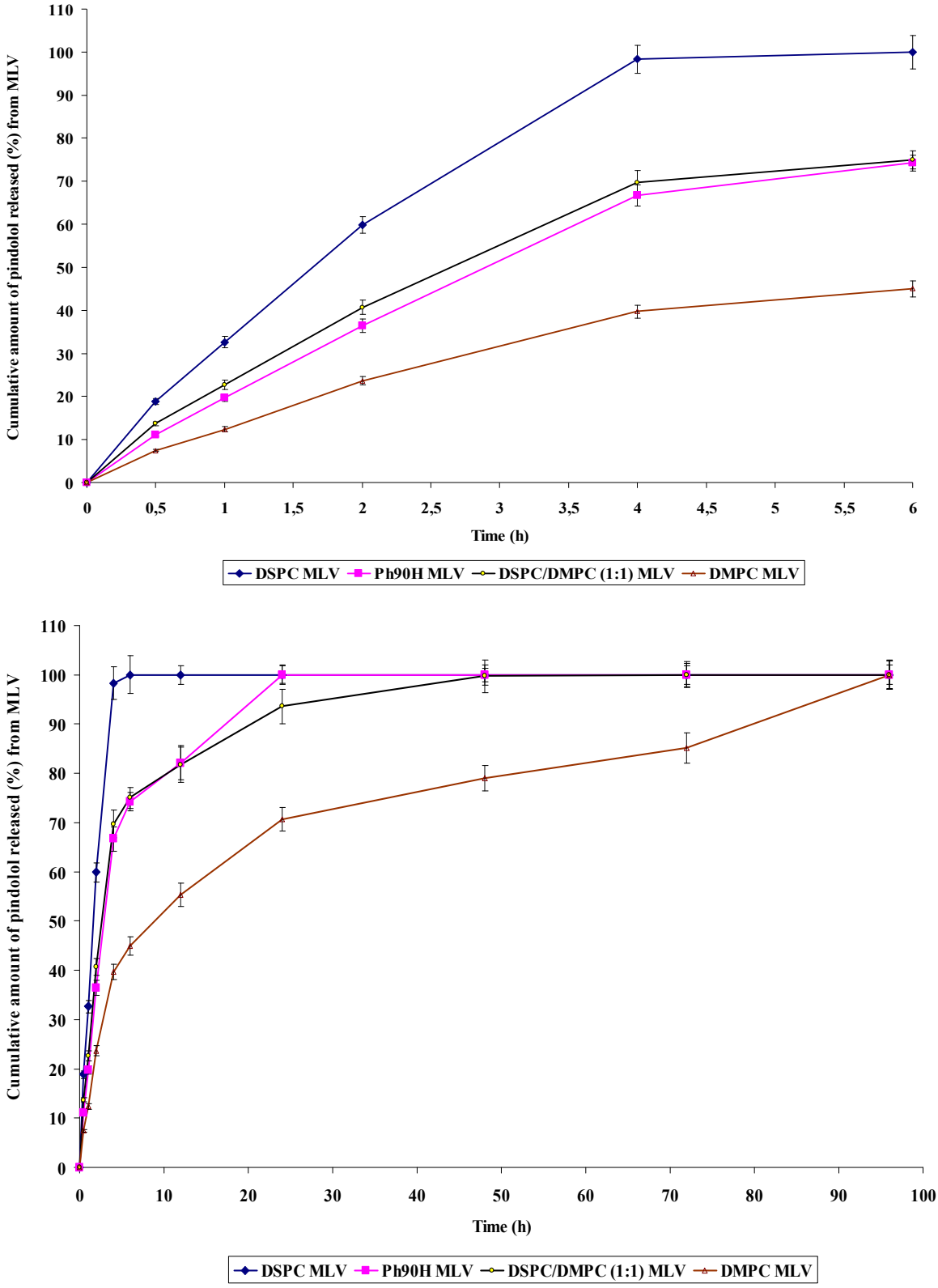

Figure 51: Release pattern of pindolol from MLV liposomes of different lipid compositions into PBS, at pH 7.4, at 37 ± 0.5 °C using dialysismethod. Mean ± S.D., *n* = 3.

III.4.1.2. In vitro release of β-adrenoceptor antagonists from LUV

III.4.1.2.1. In vitro release of propranolol from LUV

The release profiles, illustrated by plotting the percentage cumulative amount released of propranolol versus time, of propranolol from LUV formulations prepared from different lipids (DSPC, DMPC, DSPC/DMPC (1:1) or Ph90H) into PBS, pH 7.4 at 37± 0.5 °C are shown in Figure 52. From these data it was found that the release rate of propranolol was slower in case of the formulation made from DMPC than the formulations made from DSPC, DSPC/DMPC (1:1) or Ph90H. The release of propranolol from formulations made from either DSPC or Ph90H was higher (100%) than the release rate from the formulation made from DSPC/DMPC (1:1) (80%) after 6 hours.

III.4.1.2.2. In vitro release of metoprolol from LUV

The percentage cumulative amount released versus time of metoprolol from LUV liposomes prepared from different lipids (DSPC, DMPC, DSPC/DMPC (1:1) or Ph90H) into PBS, pH 7.4 at 37± 0.5 °C are depicted in Figure 53. It was noticed that the greatest cumulative percentage of metoprolol release was exhibited by Ph90H (100%), followed by DSPC (97.4%), DSPC/DMPC (1:1) (73.04%) and DMPC (5.31%) after 4 hours.

III.4.1.2.3. In vitro release of atenolol from LUV

Figure 54 shows the release pattern (illustrated by plotting the percentage cumulative amount released versus time) of atenolol from LUV formulations prepared from different lipids (DSPC, DMPC, DSPC/DMPC (1:1) or Ph90H) into PBS, pH 7.4 at 37± 0.5 °C.

It was found that the greatest cumulative amount released (%) of atenolol was exhibited from Ph90H liposomes (100%), followed by DSPC (80 %), DSPC/DMPC (1:1) (65%) and DMPC (45%) after 24 hours.

III.4.1.2.4. In vitro release of pindolol from LUV

The in vitro release data, which are exhibited by plotting the percentage cumulative amount released versus time, of pindolol from LUV formulations prepared from different lipids (DSPC, DMPC, DSPC/DMPC (1:1), Ph90H), into PBS, pH 7.4 at 37± 0.5 °C are shown in Figure 55. It was found that the release rate of pindolol was in the following order DSPC/DMPC (1:1) > DSPC > DMPC > Ph90H before 4 hours. But after 4 hours, 100% of pindolol was obtained from DSPC, Ph90H, DSPC/DMPC (1:1) and DMPC.

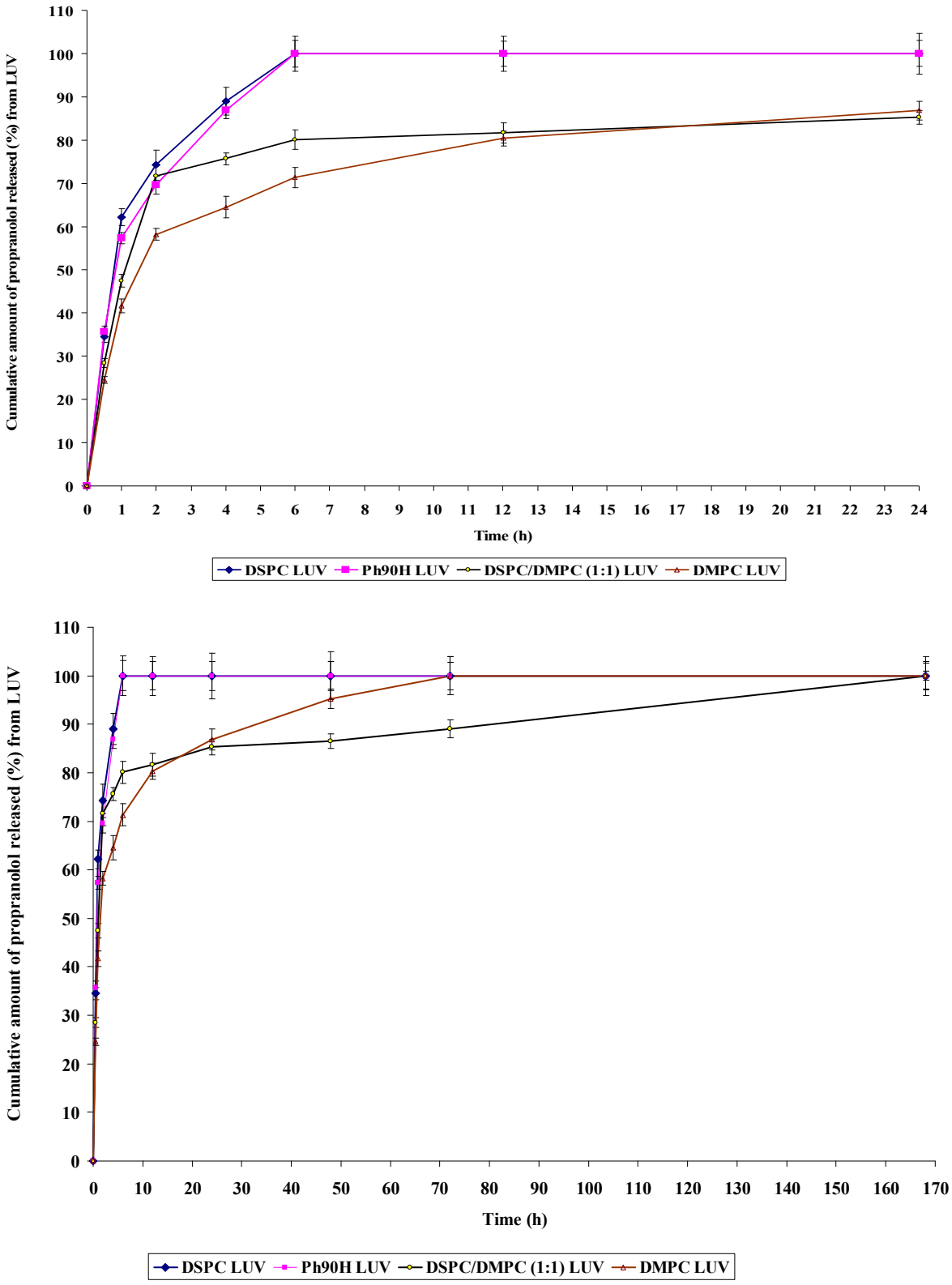

Figure 52: Release pattern of propranolol from LUV liposomes of different lipid compositions into PBS, at pH 7.4, at 37 ± 0.5 °C using dialysismethod. Mean ± S.D., *n* = 3.

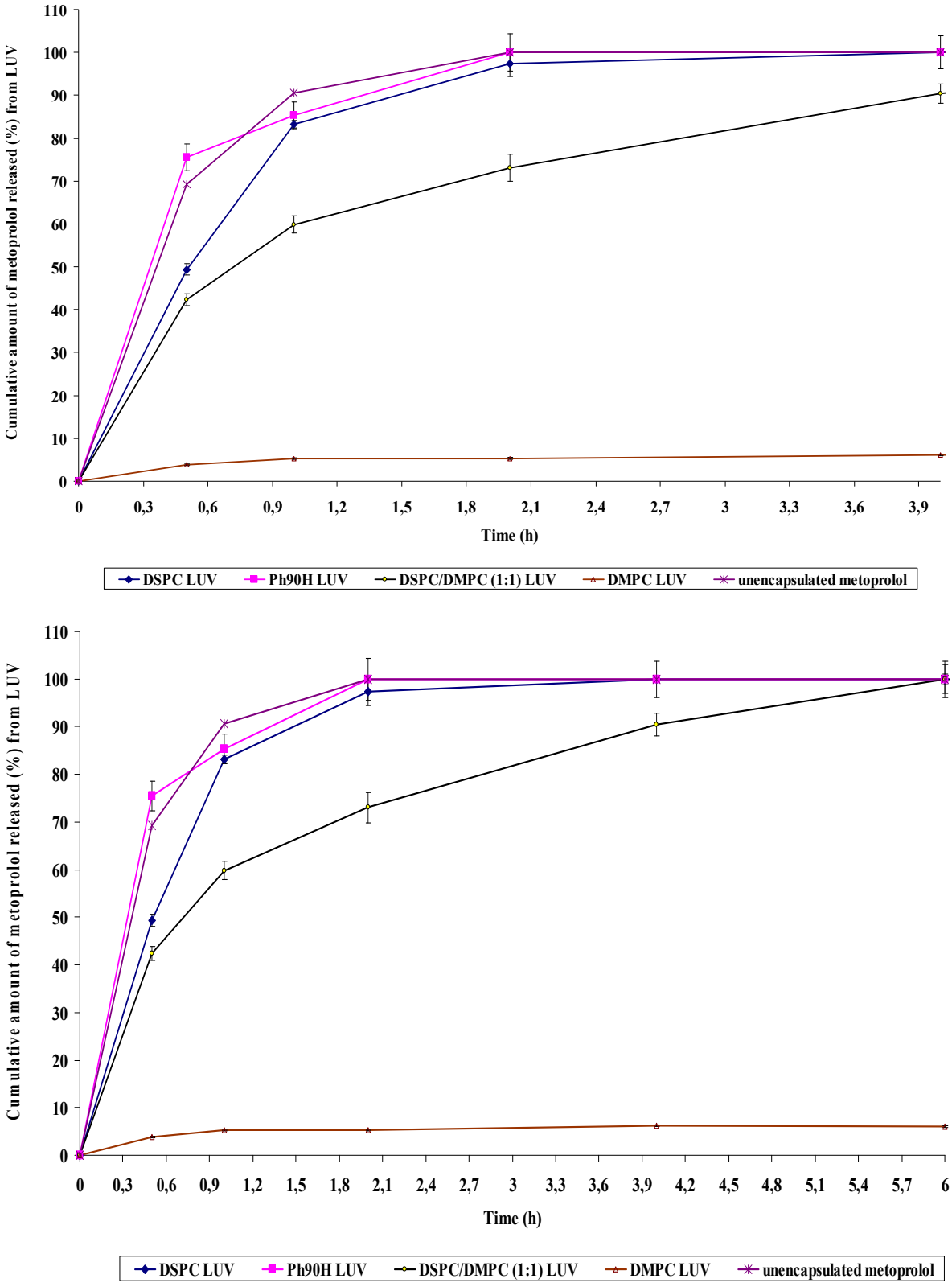

Figure 53: Release pattern of metoprolol from LUV liposomes of different lipid compositions into PBS, at pH 7.4, at 37 ± 0.5 °C using dialysismethod. Mean ± S.D., *n* = 3.

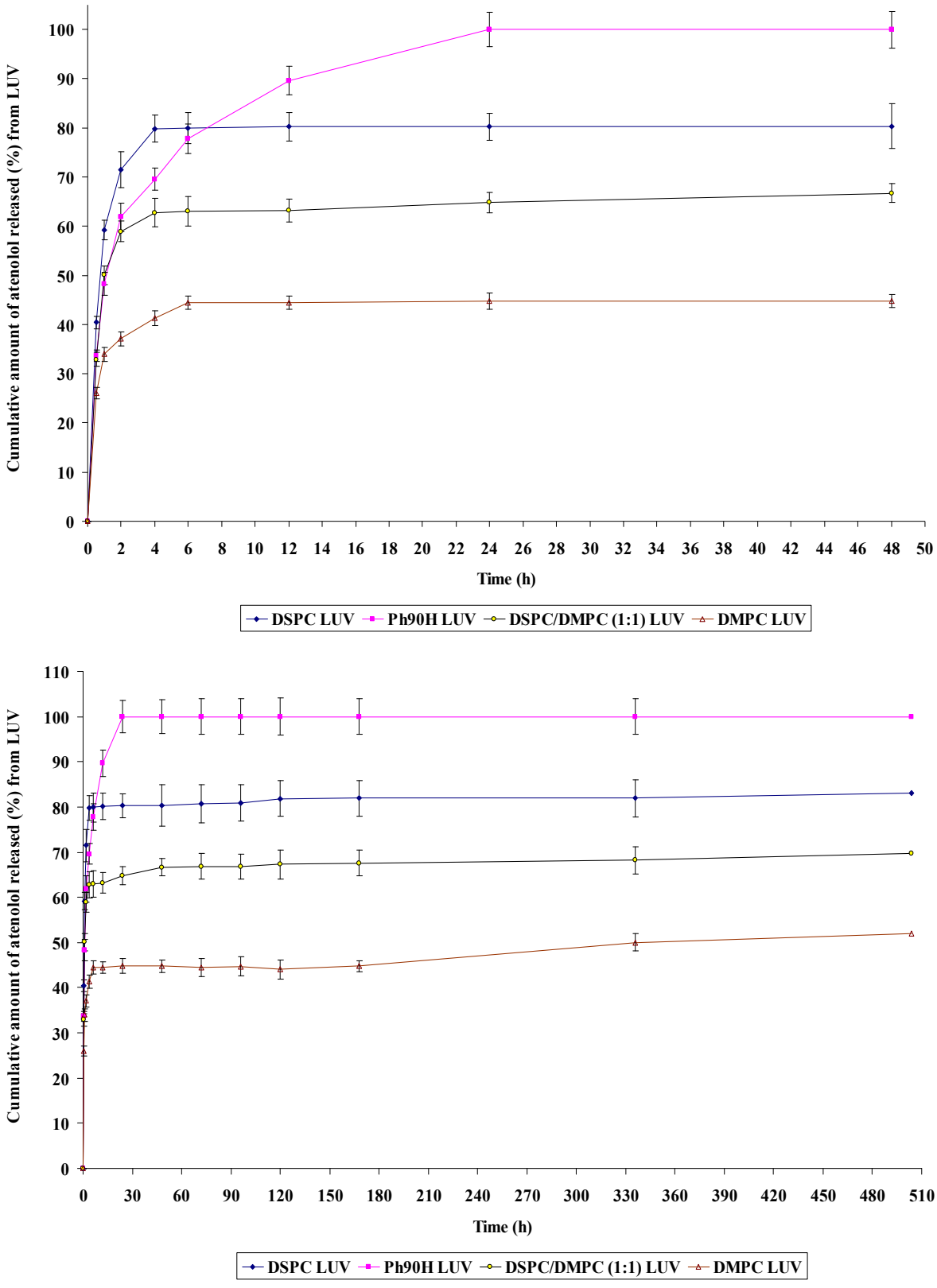

Figure 54: Release pattern of atenolol from LUV liposomes of different lipid compositions into PBS, at pH 7.4, at 37 ± 0.5 °C using dialysismethod. Mean ± S.D., *n* = 3.

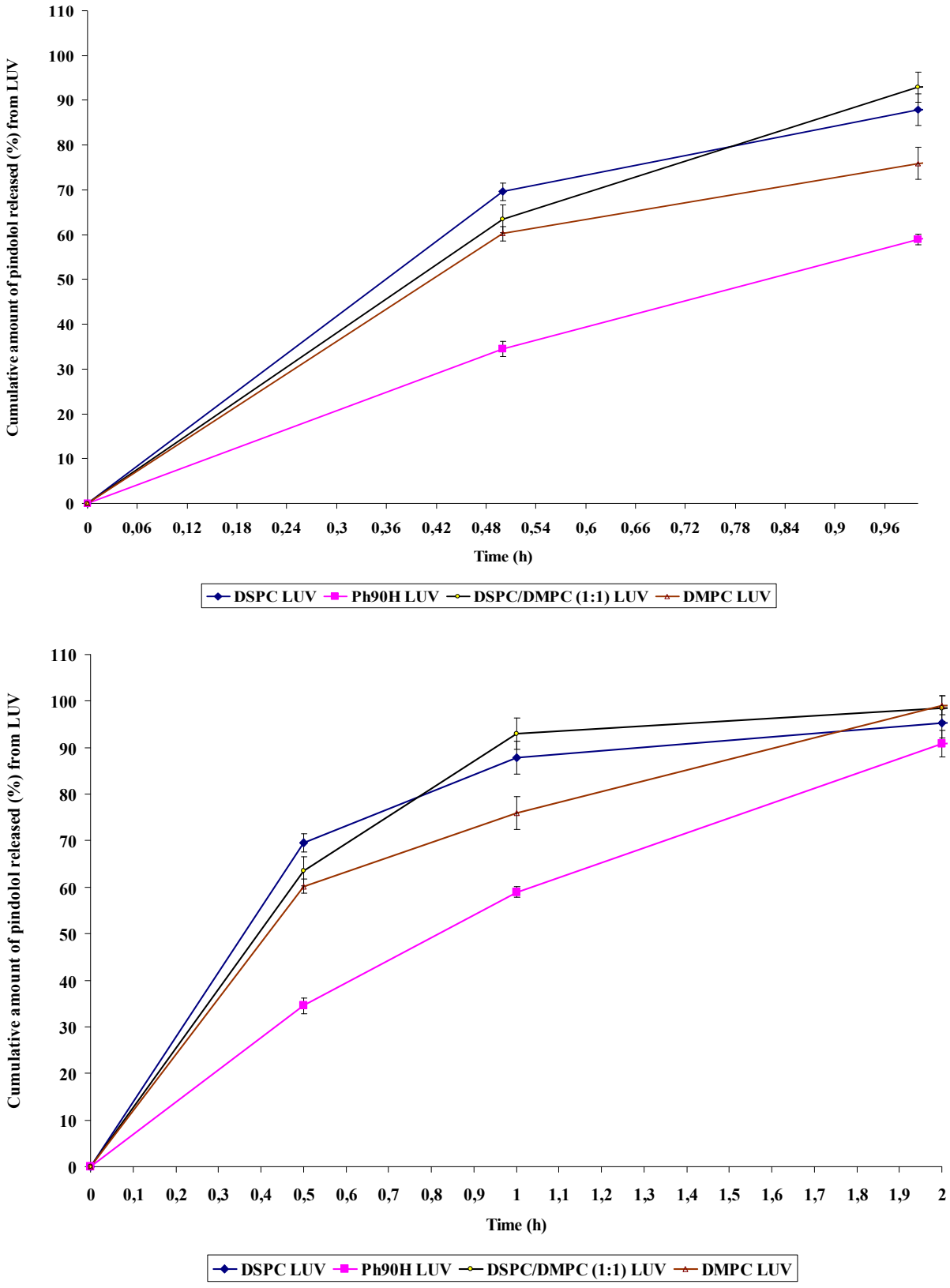

Figure 55: Release pattern of pindolol from LUV liposomes of different lipid compositions into PBS, at pH 7.4, at 37 ± 0.5 °C using dialysismethod. Mean ± S.D., *n* = 3.

III.4.1.3. In vitro release of β-adrenoceptor antagonists from SUV

III.4.1.3.1. In vitro release of propranolol from SUV

Figure 56 depicts the release data (presented by plotting the cumulative percentage versus time) of propranolol from SUV prepared from different lipids (DSPC, DMPC, DSPC/DMPC (1:1) or Ph90H) into PBS, pH 7.4 at 37± 0.5 °C. It was found that the greatest cumulative percentage of propranolol released was exhibited by liposomes prepared from Ph90H (100%), followed by DSPC (96%), DSPC/DMPC (1:1) (93%) and DMPC (59 %) after 4 hours. The lowest cumulative percentage of propranolol was released from the formulation made from DMPC.

III.4.1.3.2. In vitro release of metoprolol from SUV

The release profile (illustrated by plotting the cumulative percentage versus time) of metoprolol from SUV liposomes prepared from different lipids (DSPC, DMPC, DSPC/DMPC (1:1) or Ph90H) into PBS, pH 7.4 at 37± 0.5 °C is exhibited in Figure 57. It was found that the greatest cumulative percentage of metoprolol release was exhibited by DSPC/DMPC (1:1) (100%) followed by Ph90H (94.65%), DSPC (90.30%), and DMPC (15.11%) after 1 hour.

III.4.1.3.3. In vitro release of atenolol from SUV

The in vitro release, which is constructed by plotting the cumulative percentage versus time, of atenolol from SUV liposomes prepared from different lipids (DSPC, DMPC, DSPC/DMPC (1:1) or Ph90H) into PBS, pH 7.4 at 37± 0.5 °C is showen in Figure 58. The cumulative percentage of atenolol release was in the following order DSPC/DMPC (1:1) > Ph90H > DSPC > DMPC. In case of DSPC/DMPC, the release rate of atenolol was 100 % after 4 hours.

III.4.1.3.4. In vitro release of pindolol from SUV

The in vitro release data, presented by plotting the cumulative percentage versus time, of pindolol from SUV liposomes prepared from different lipids (DSPC, DMPC, DSPC/DMPC (1:1) or Ph90H) into PBS, pH 7.4 at 37± 0.5 °C is exhibited in Figure 59. It was found that 100 % of pindolol was released from all preparations after 4 hours.

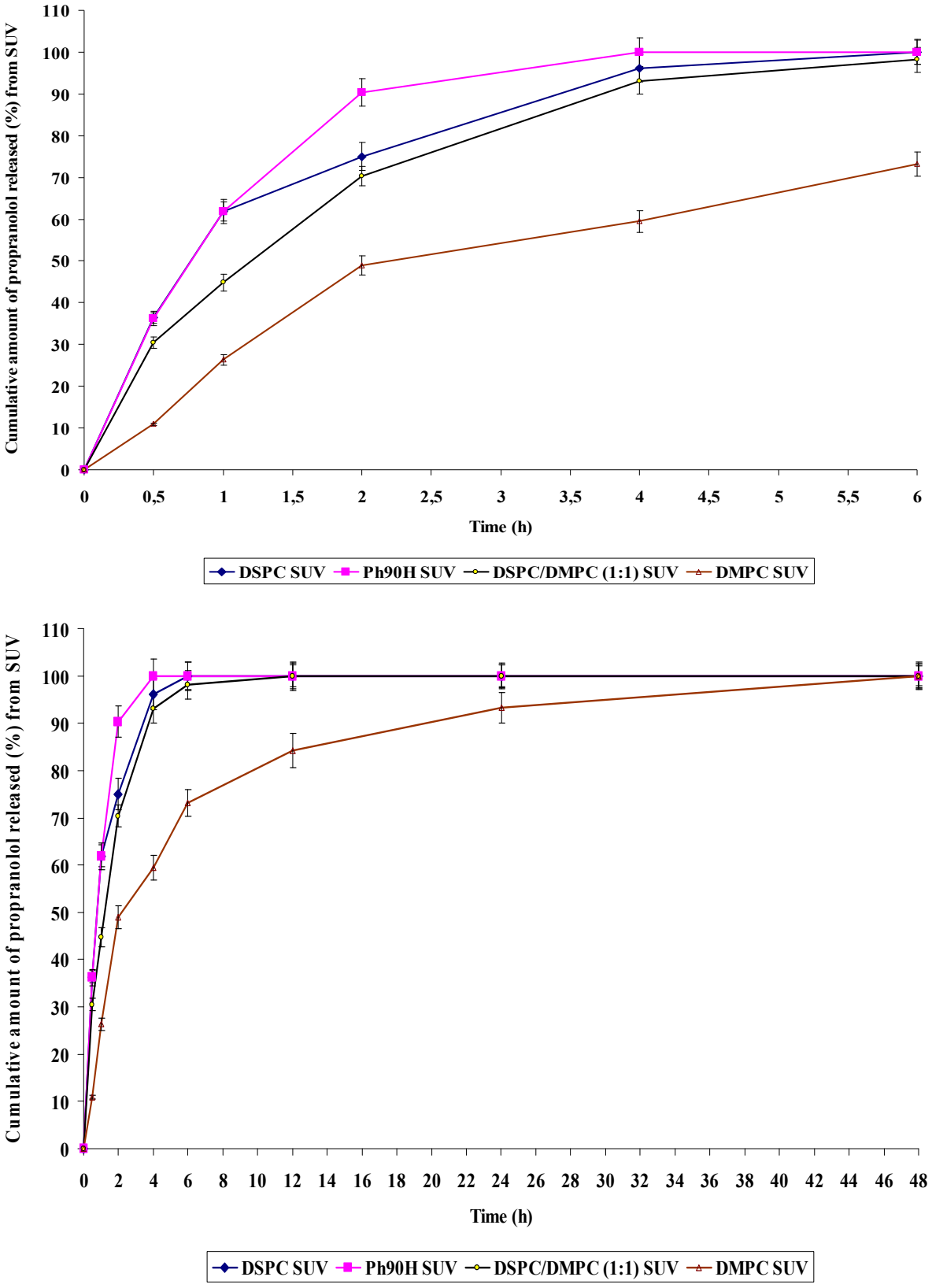

Figure 56: Release pattern of propranolol from SUV liposomes of different lipid compositions into PBS, at pH 7.4, at 37 ± 0.5 °C using dialysismethod. Mean ± S.D., *n* = 3.

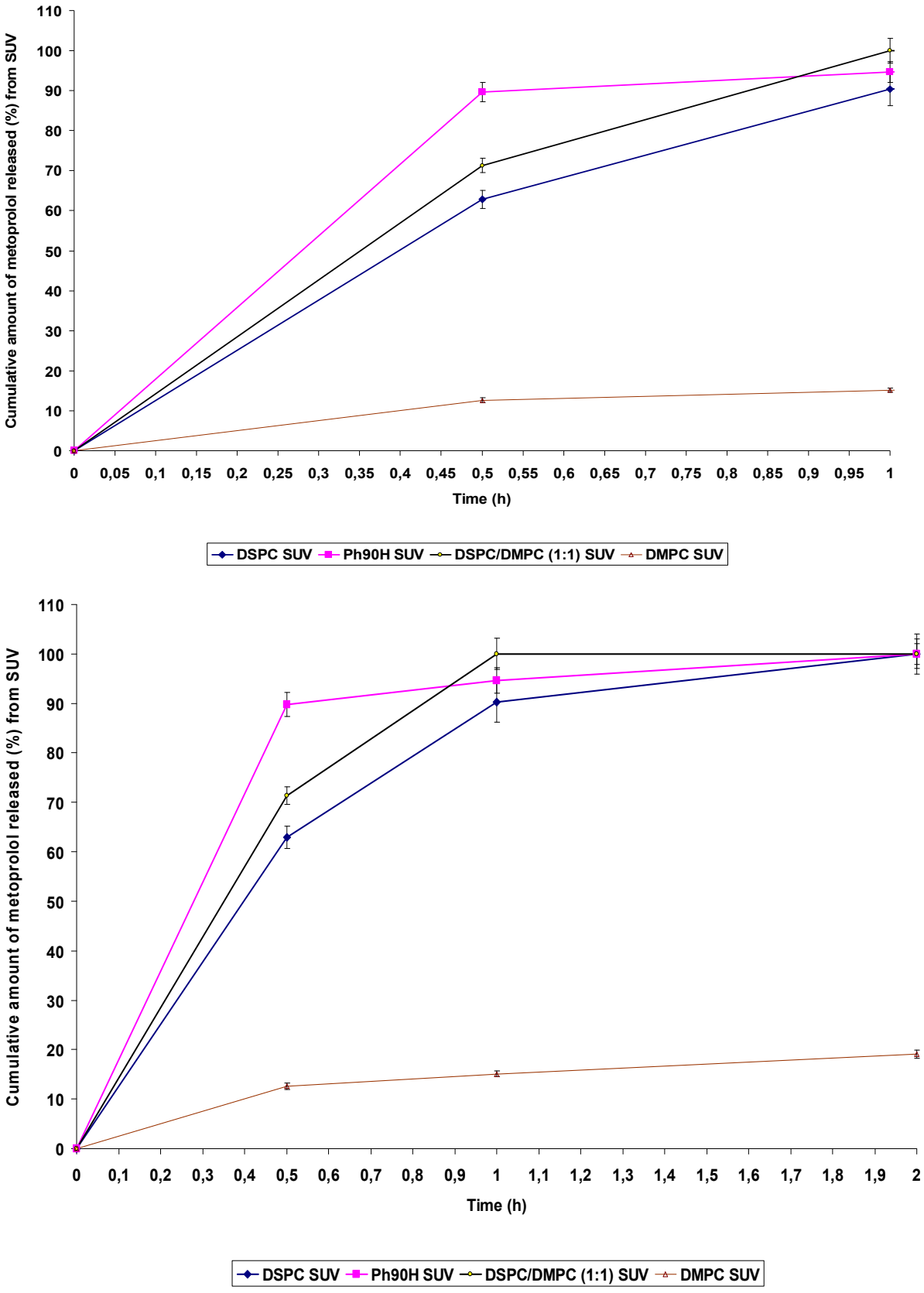

Figure 57: Release pattern of metoprolol from SUV liposomes of different lipid compositions into PBS, at pH 7.4, at 37 ± 0.5 °C using dialysismethod. Mean ± S.D., *n* = 3.

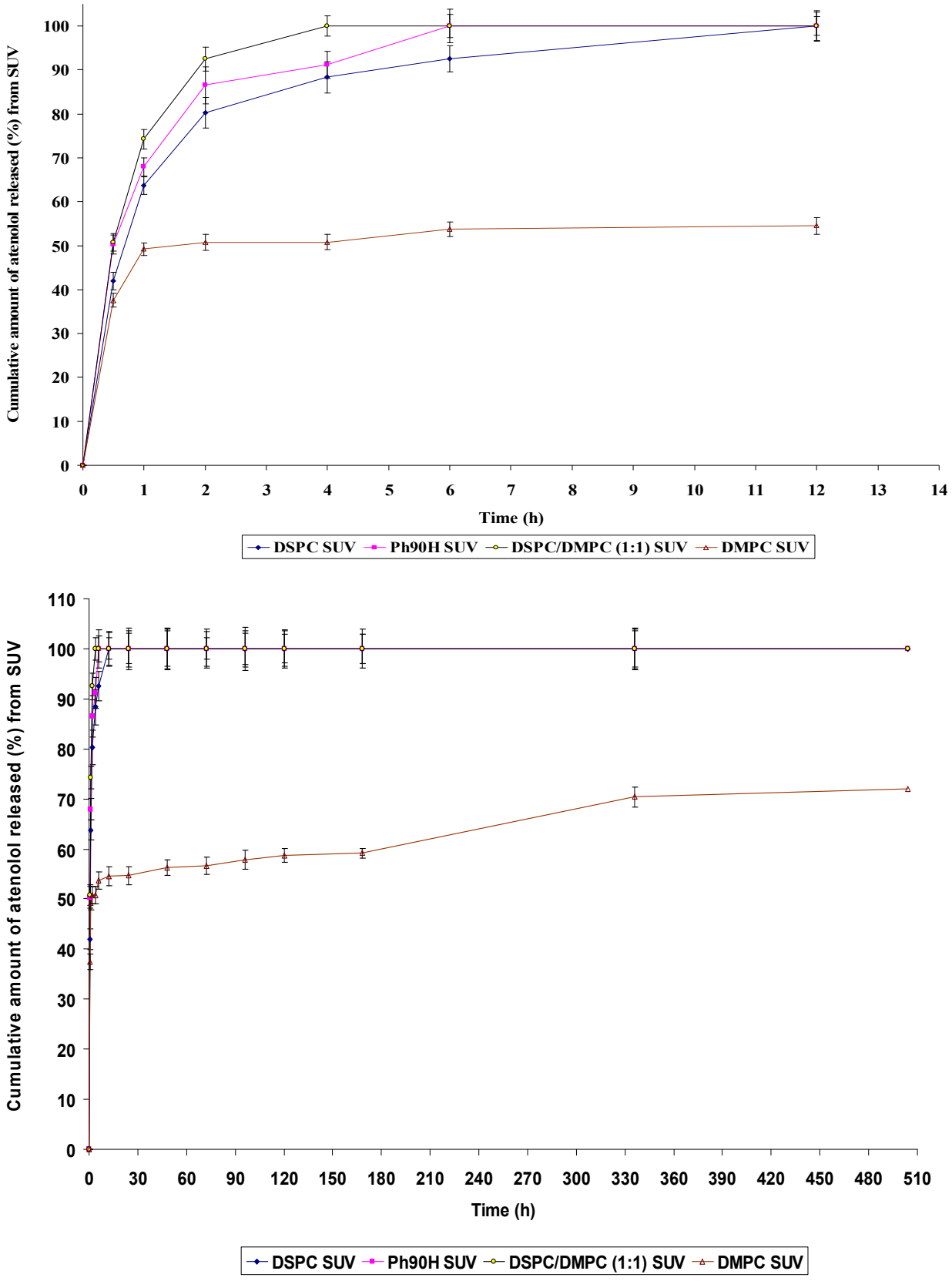

Figure 58: Release pattern of atenolol from SUV liposomes of different lipid compositions into PBS, at pH 7.4, at 37 ± 0.5 °C using dialysismethod. Mean ± S.D., *n* = 3.

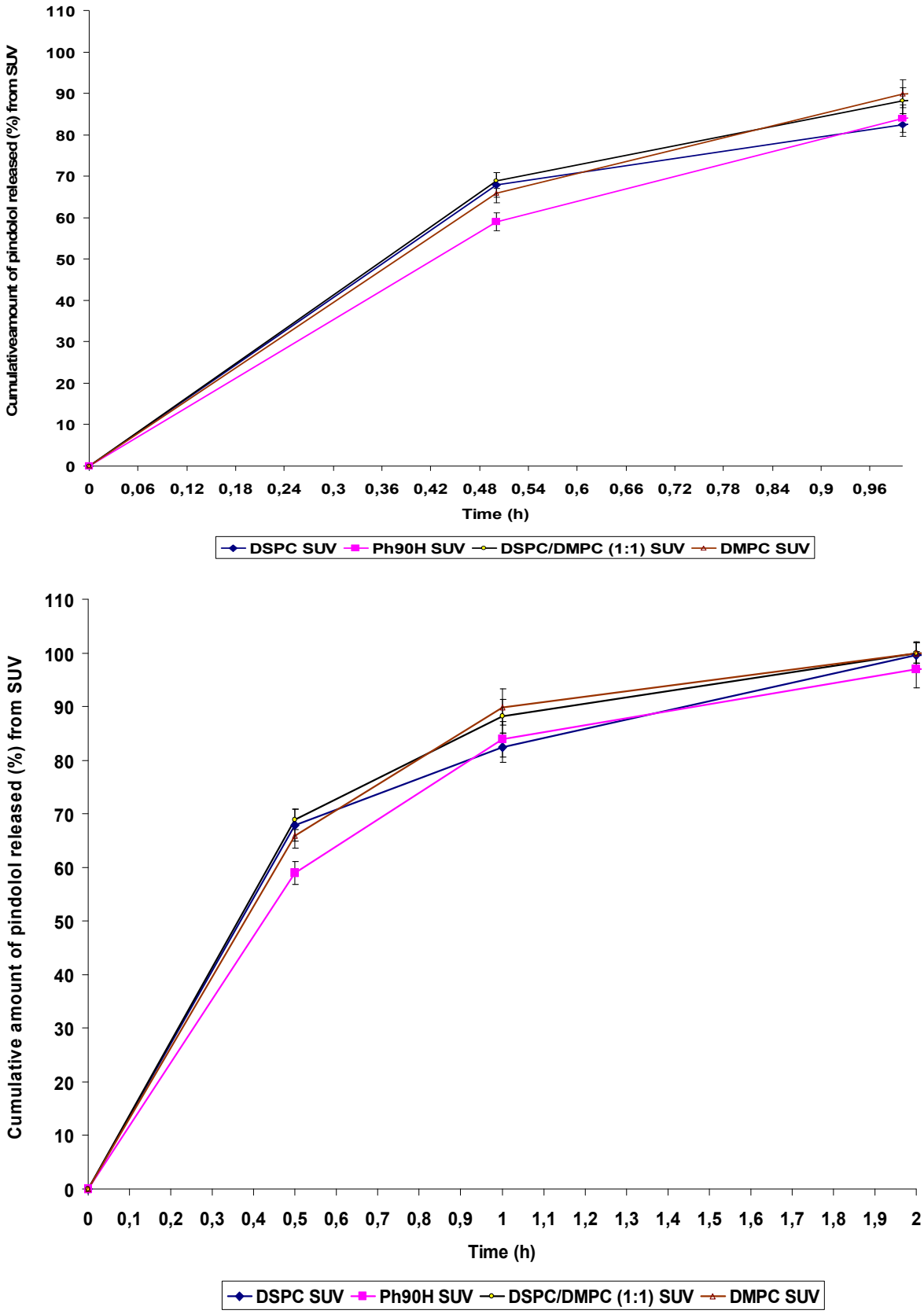

Figure 59: Release pattern of pindolol from SUV liposomes of different lipid compositions into PBS, at pH 7.4, at 37 ± 0.5 °C using dialysismethod. Mean ± S.D., *n* = 3.

III.4.2. In vitro release of β-adrenoceptor antagonists liposomes using a dispersion method

In this thesis, the dispersion method was used only for measurement of the in vitro release of β-adrenoceptor antagonists from MLV liposomes into PBS, pH 7.4 at 37± 0.5 °C. Figures 60, 61, 62 and 63 exhibit the release pattern of β-adrenoceptor antagonists using the dispersion method. By this method the release patterns of β-adrenoceptor antagonists were the same as in case of the dialysis method. In general however it was found that the release rates of the incorporated β-adrenoceptor antagonists were consistently higher when using the dispersion method as compared to the dialysis method.

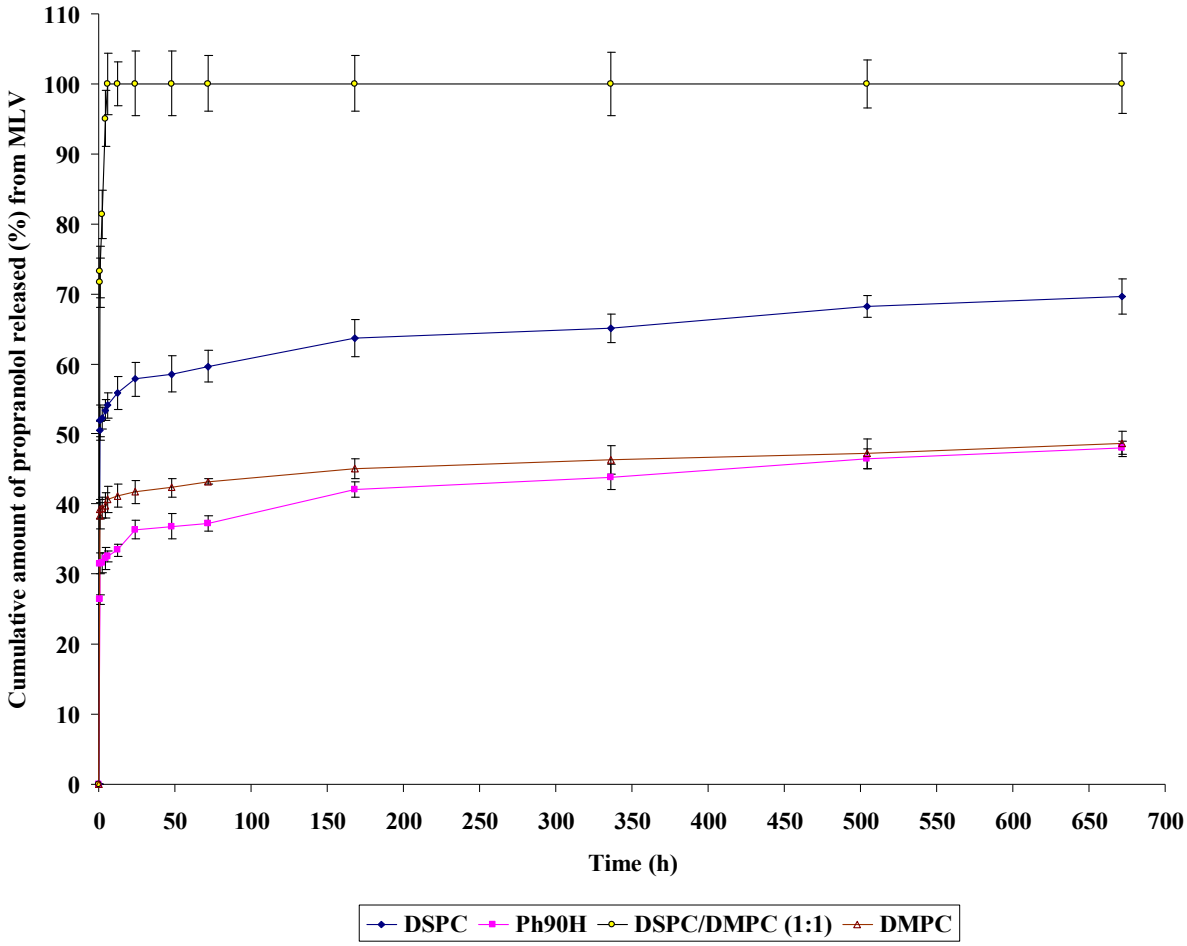

Figure 60: Release pattern of propranolol from MLV liposomes of different lipid compositions into PBS, at pH 7.4, at 37 ± 0.5 °C using dispersion method. Mean ± S.D., *n* = 3.

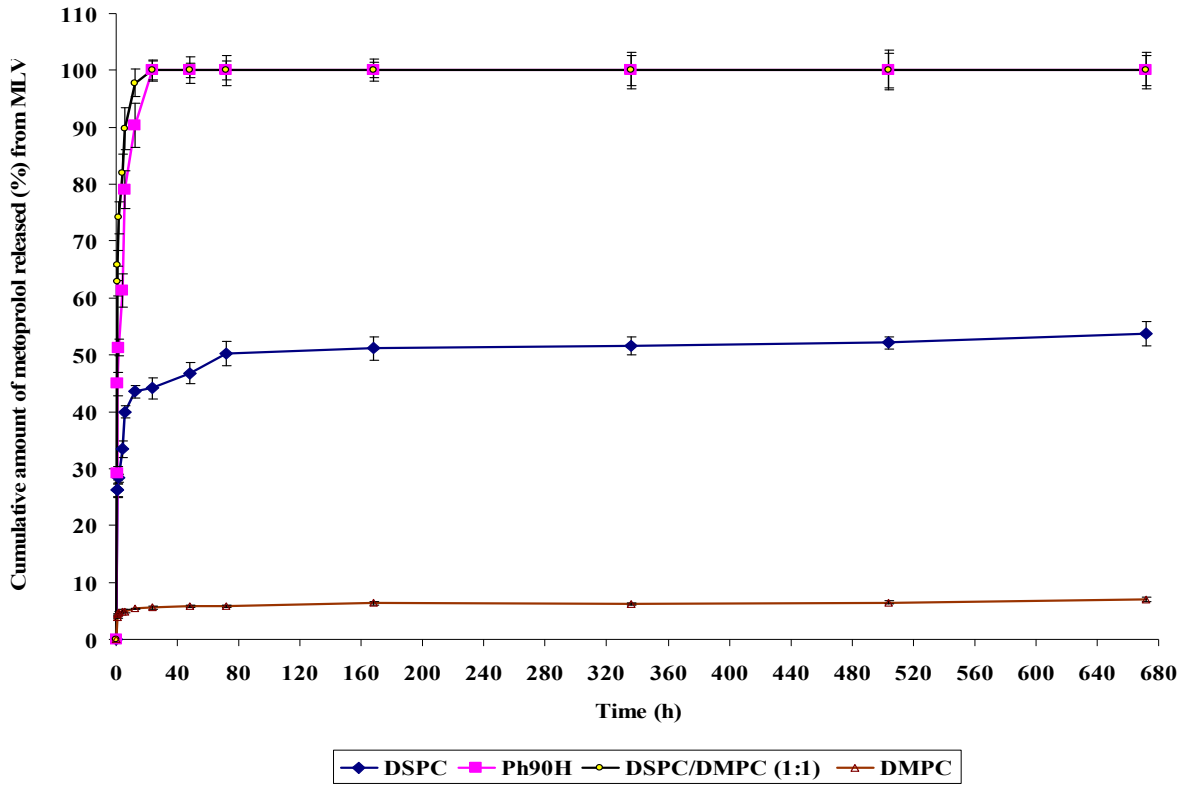

Figure 61: Release pattern of metoprolol from MLV liposomes of different lipid compositions into PBS, at pH 7.4, at 37 ± 0.5 °C using dispersion method. Mean ± S.D., *n* = 3.

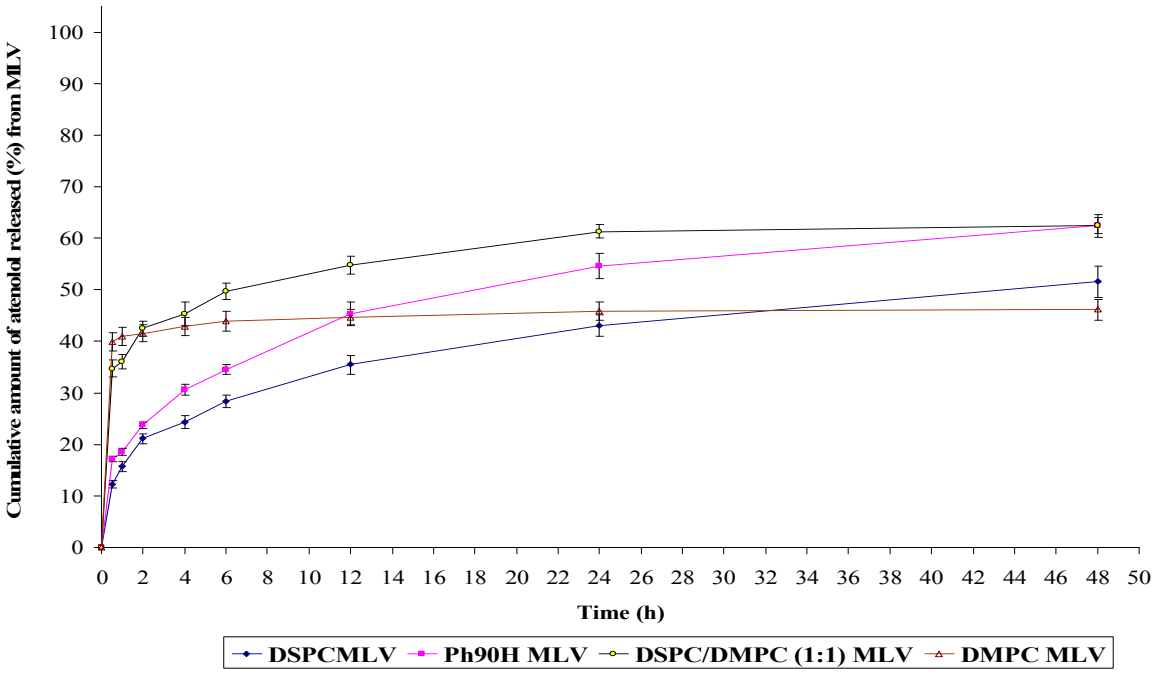

Figure 62: Release pattern of atenolol from MLV liposomes of different lipid compositions into PBS, at pH 7.4, at 37 ± 0.5 °C using dispersion method. Mean ± S.D., *n* =3.

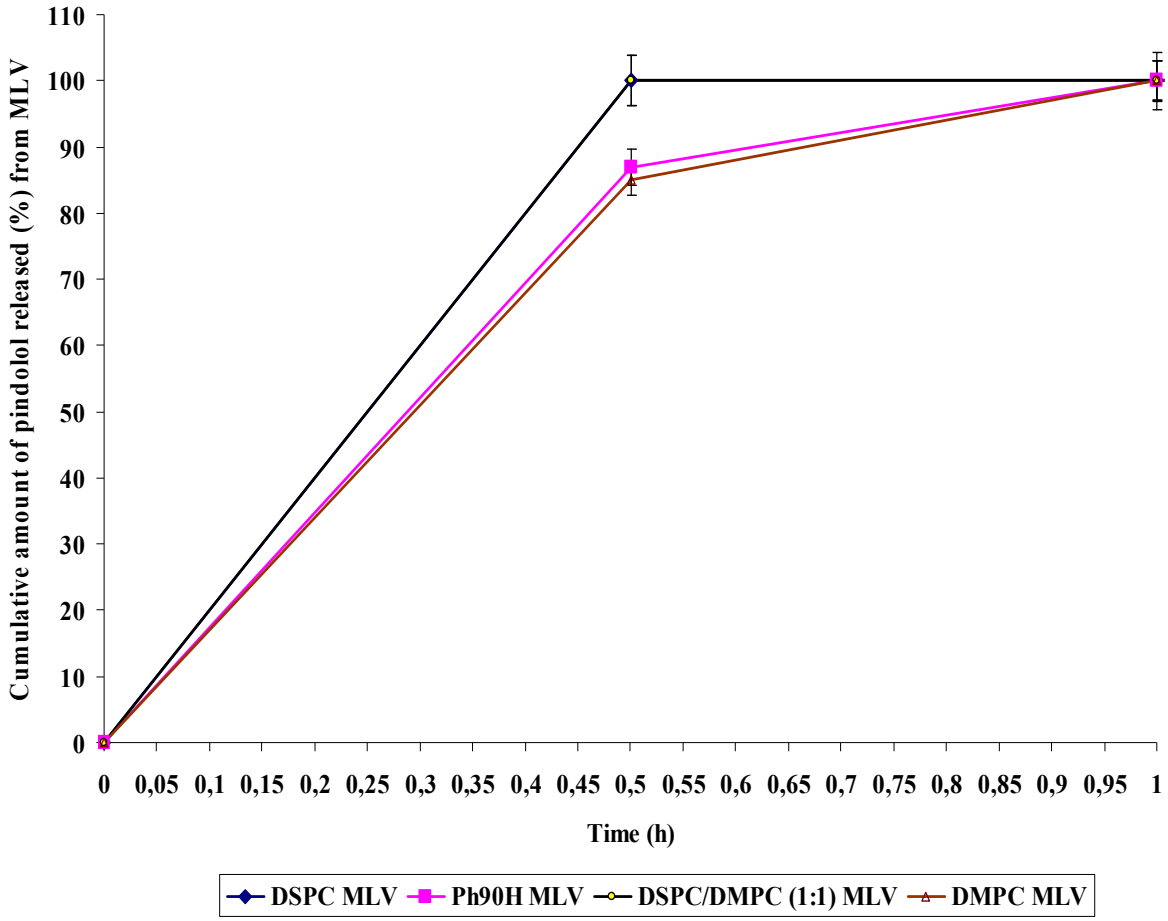

Figure 63: Release pattern of pindolol from MLV liposomes of different lipid compositions into PBS, at pH 7.4, at 37 ± 0.5 °C using dispersion method. Mean ± S.D., *n* =3.

III.5. In vitro release of glucose from liposomes using a dispersion method

III.5.1. In vitro release of glucose from MLV

The in vitro release of glucose from MLV prepared from different lipids (e.g. DSPC, DSPC/DMPC (1:1), DMPC and Ph90H) into PBS, pH 7.4 at 37 ± 0.5 °C using a dispersion method are shown as cumulative percent released over a 96 hour study period and are illustrated in Figure 64. Regarding liposomes prepared from DSPC and Ph90H, the glucose release profiles show an initial burst effect followed by slower release phase.

Concerning DMPC, DSPC/DMPC (1:1) and Syb, the release of glucose was faster reaching 100 % after 1 hour.

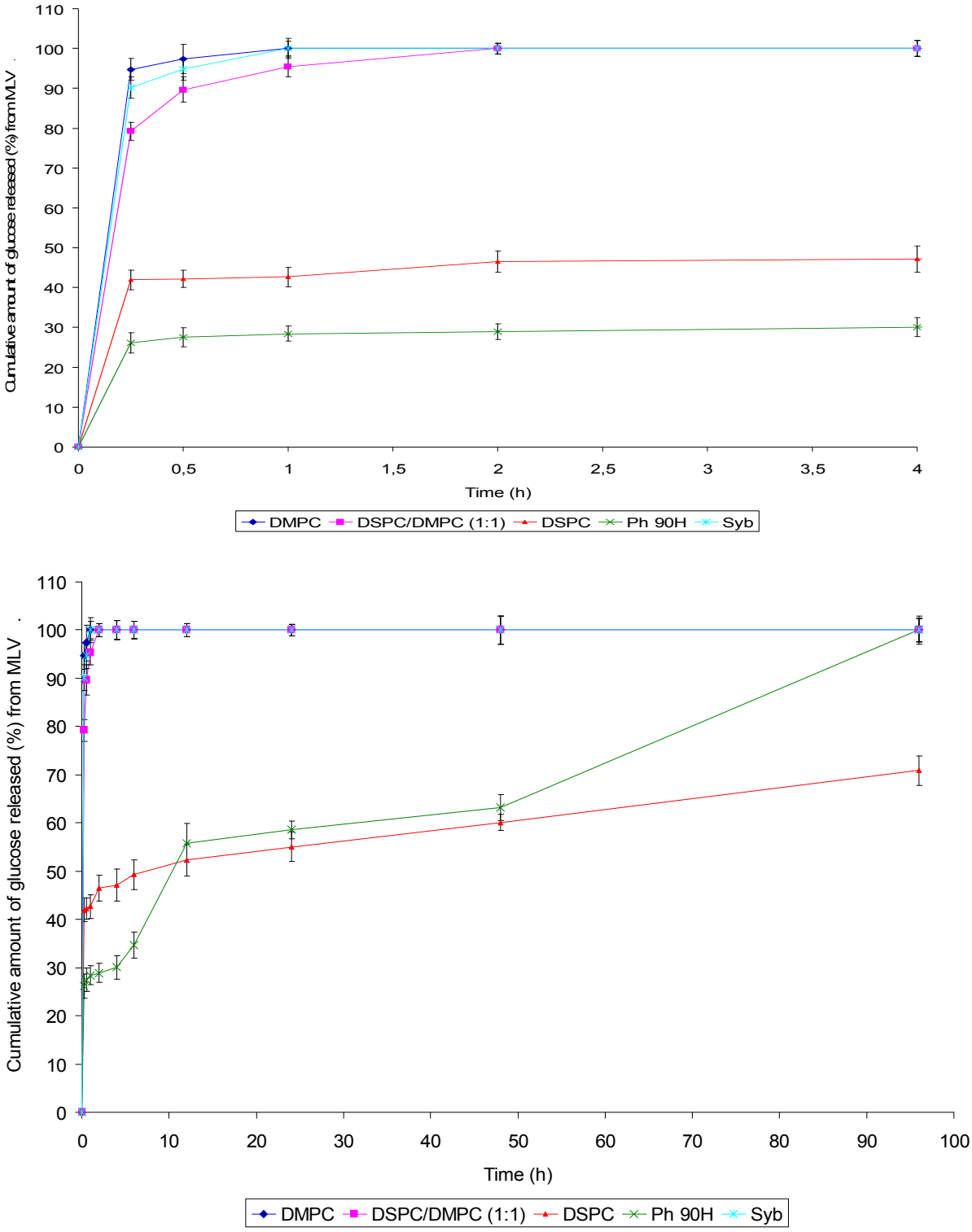

Figure 64: Release pattern of glucose from MLV liposomes of different lipid compositions into PBS, at pH 7.4, at 37 ± 0.5 °C using dispersion method. Mean ± S.D., *n* =3.

III.5.2. In vitro release of glucose from LUV and SUV

Figures 65 and 66 exhibit the in vitro release of glucose as cumulative percent released from LUV and SUV prepared from different lipids (e.g. DSPC, DSPC/DMPC (1:1), DMPC and Ph90H) into PBS, pH 7.4 at 37 ± 0.5 °C using the dispersion method.

It was found that the release of glucose from LUV was in the order DSPC > PH90H > DSPC/DMPC (1:1) > Syb > DMPC. 100 % of glucose released from all formulations was obtained after 2 hours. But in case of SUV, 100 % of glucose released after 0.5 hour.

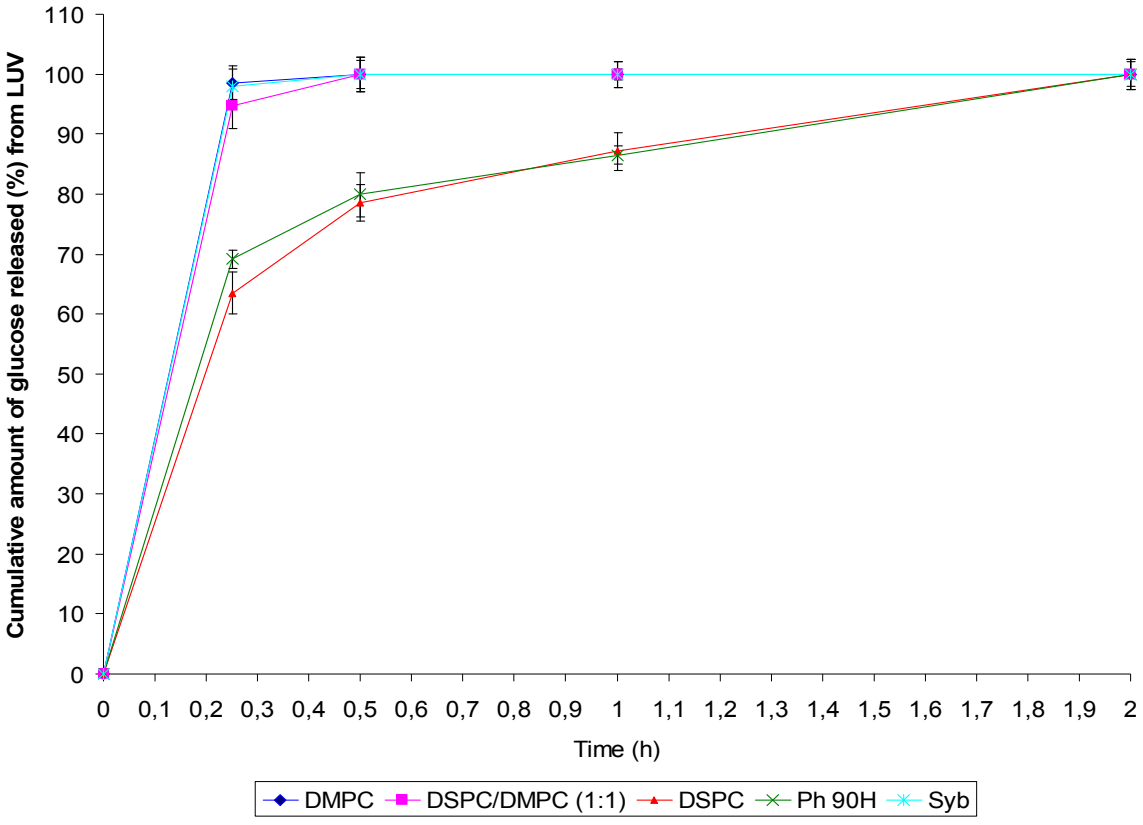

Figure 65: Release pattern of glucose from LUV liposomes of different lipid compositions into PBS, at pH 7.4, at 37 ± 0.5 °C using dispersion method. Mean ± S.D., *n* =3.

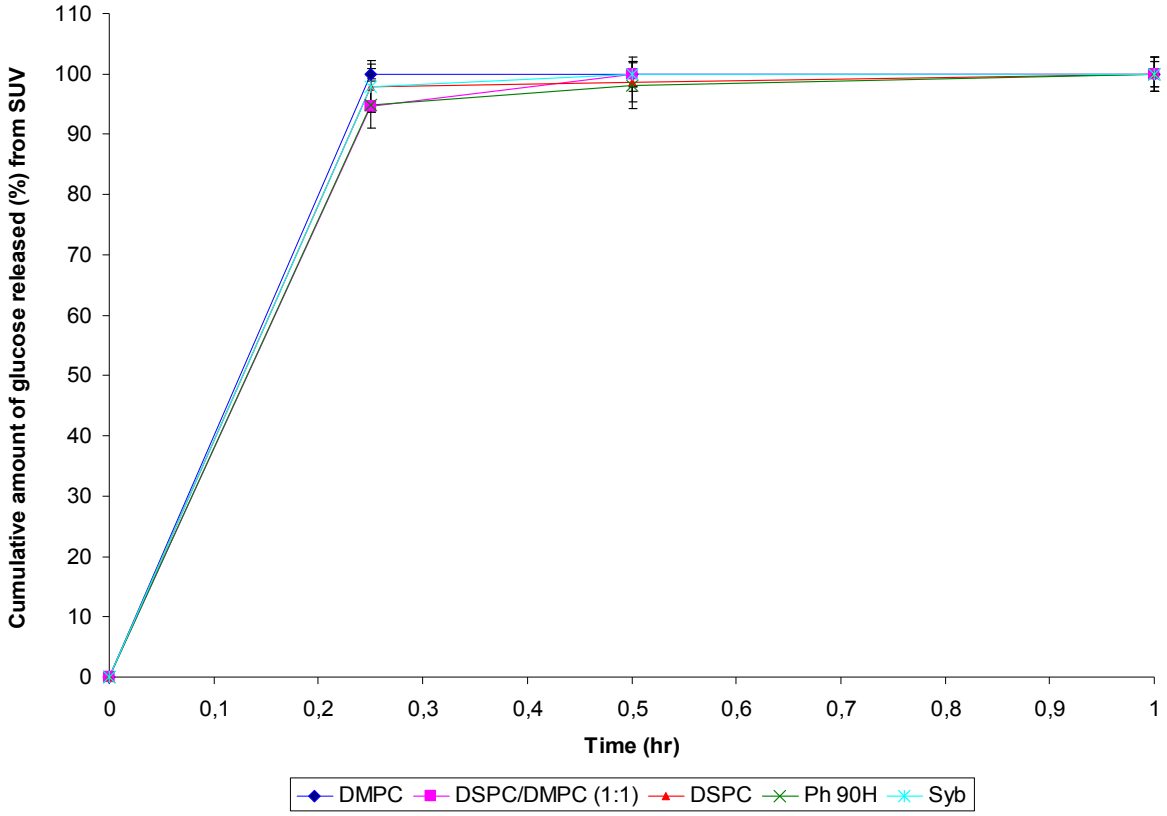

Figure 66: Release pattern of glucose from SUV liposomes of different lipid compositions into PBS, at pH 7.4, at 37 ± 0.5 °C using dispersion method. Mean ± S.D., *n* =3.

III.6. In vitro release of FDG from liposomes using a dispersion method

III.6.1. In vitro release of FDG from MLV

The in vitro release of FDG (represented by plotting of FDG activity (MBq) versus time) from MLV prepared from different lipids (e.g. DSPC, DSPC/DMPC (1:1), DMPC, Syb and Ph90H) into PBS, pH 7.4 at 37 ± 0.5 °C using the dispersion method is presented in Figure 67. From the results it is concluded that the FDG release was increased in the following order Ph90H > DSPC > Syb > DSPC/DMPC (1:1) > DMPC.

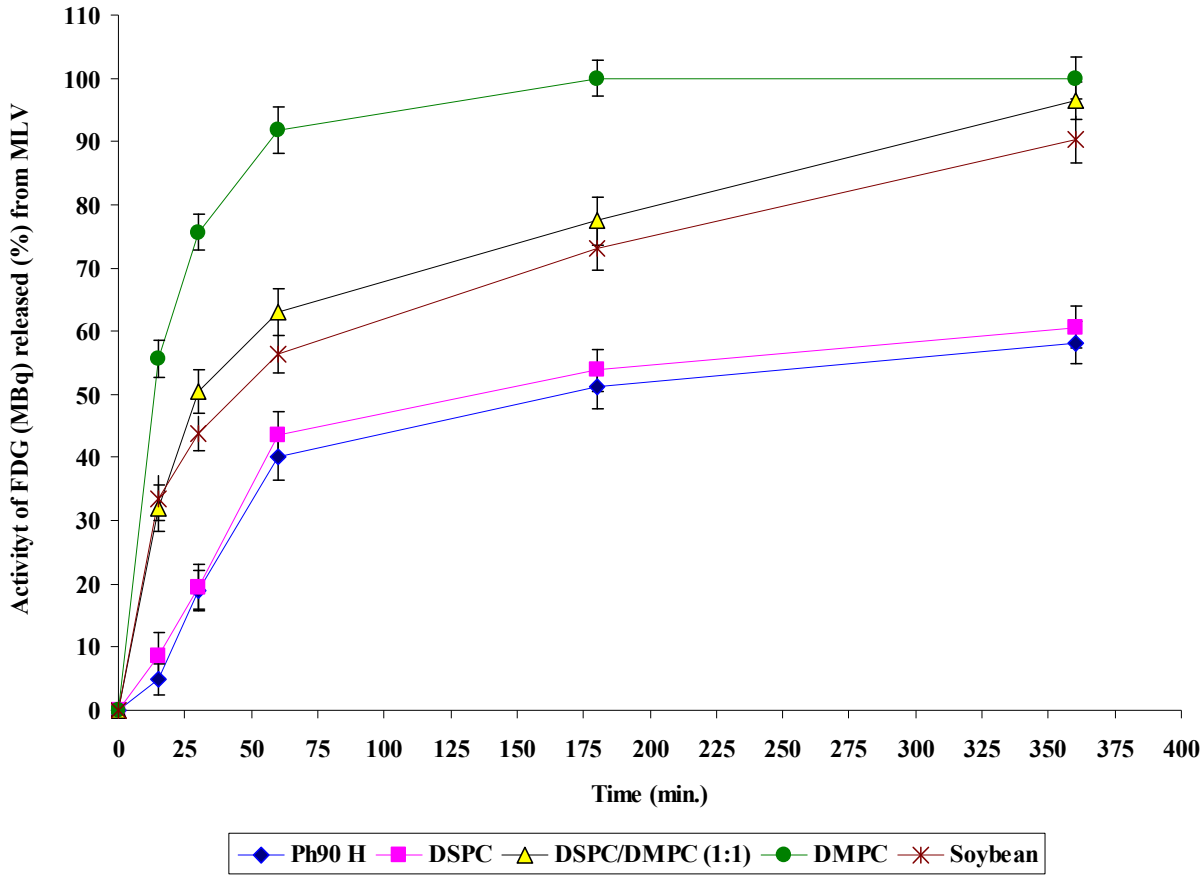

Figure 67: Release pattern of FDG from MLV liposomes of different lipid compositions into PBS, at pH 7.4, at 37 ± 0.5 °C using dispersion method. Mean ± S.D., *n* =3.

III.6.2. In vitro release of FDG from LUV

Figure 68 exhibits the in vitro release pattern of FDG from LUV, presented by plotting the activity of FDG (MBq) released versus time, prepared from Ph90H into isotonic saline solution, pH 7.4 at 37 ± 0.5 °C using the dispersion method. 100 % of FDG was released after 120 minutes.

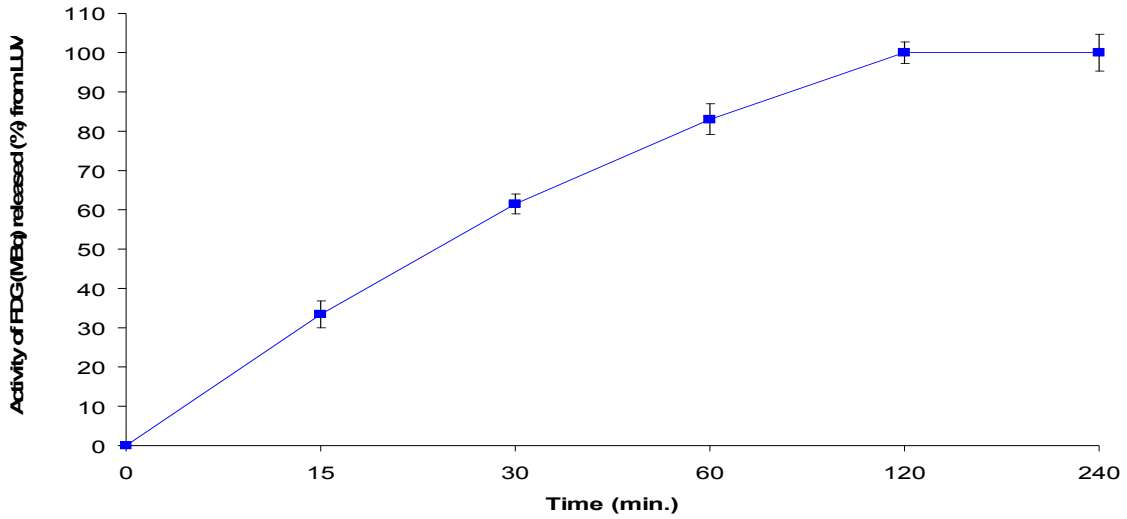

Figure 68: Release pattern of FDG (MBq) from LUV liposomes prepared from Ph90H into isotonic saline solution, pH 7.4, at 37 ± 0.5 °C using dispersion method. Mean ± S.D., *n* =3.

III.6.3. In vitro release of FDG from SUV

The in vitro release pattern of FDG illustrated by plotting the activity of FDG (MBq) released against time, from SUV prepared from Ph90H into isotonic saline solution, pH 7.4 at 37 ± 0.5 °C using the dispersion method is exhibited in Figure 69. FDG was released completely after 120 minutes.

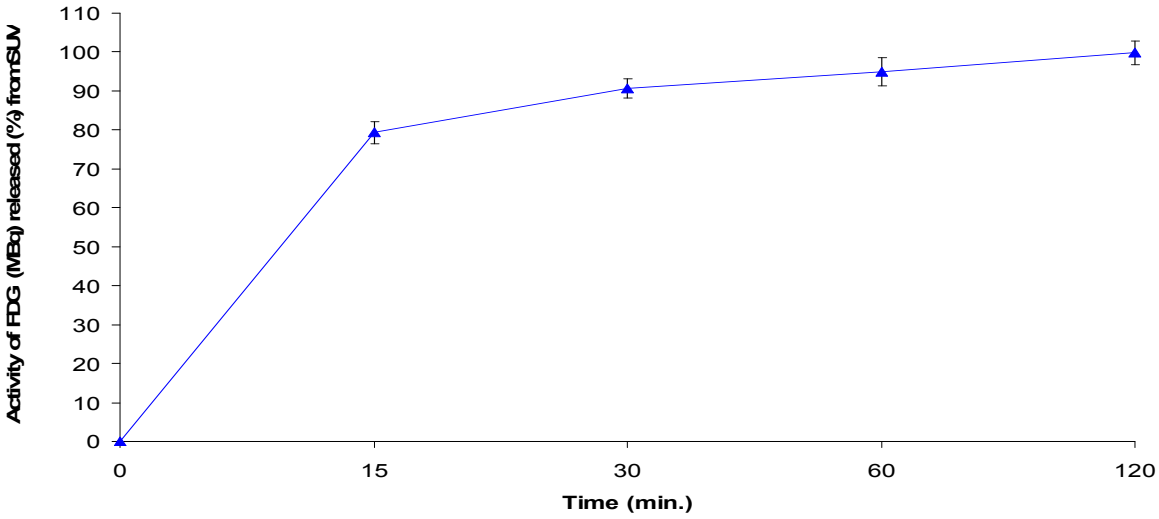

Figure 69: Release pattern of FDG (MBq) from SUV liposomes prepared from Ph90H into isotonic saline solution, pH 7.4, at 37 ± 0.5 °C using dispersion method. Mean ± S.D., *n* =3.

III.7. Effect of the lipophilicity on the in vitro release of β-adrenoceptor antagonists from liposomes

The following Figures 70, 71 and 72 depict the effect of lipophicity on the in vitro release of β-adrenoceptor antagonists, represented by plotting the cumulative percentage of release of β-adrenoceptor antagonists against time, from liposomes (MLV, LUV and SUV respectively) prepared from Ph90H. It was found that the release of β-adrenoceptor antagonists was in the following order pindolol > atenolol > metoprolol > propranolol in case of MLV. However, the release of β-adrenoceptor antagonists from LUV and SUV liposomes was in the following order metoprolol > atenolol > pindolol > propranolol.

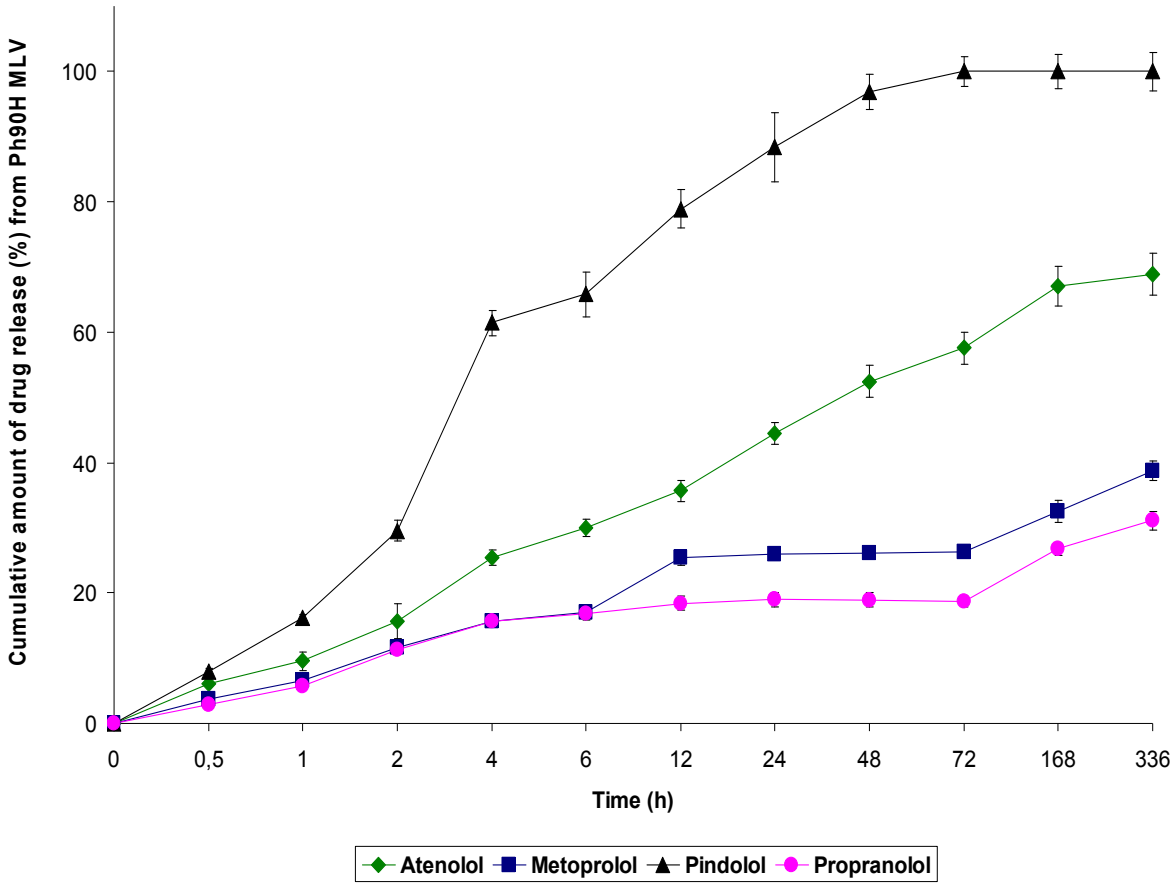

Figure 70: Effect of lipophilicity of β-adrenoceptor antagonists on their in vitro release from MLV liposomes prepared from Ph90H into PBS, pH 7.4, at 37 ± 0.5 °C using dialysis method. Mean ± S.D., *n* =3.

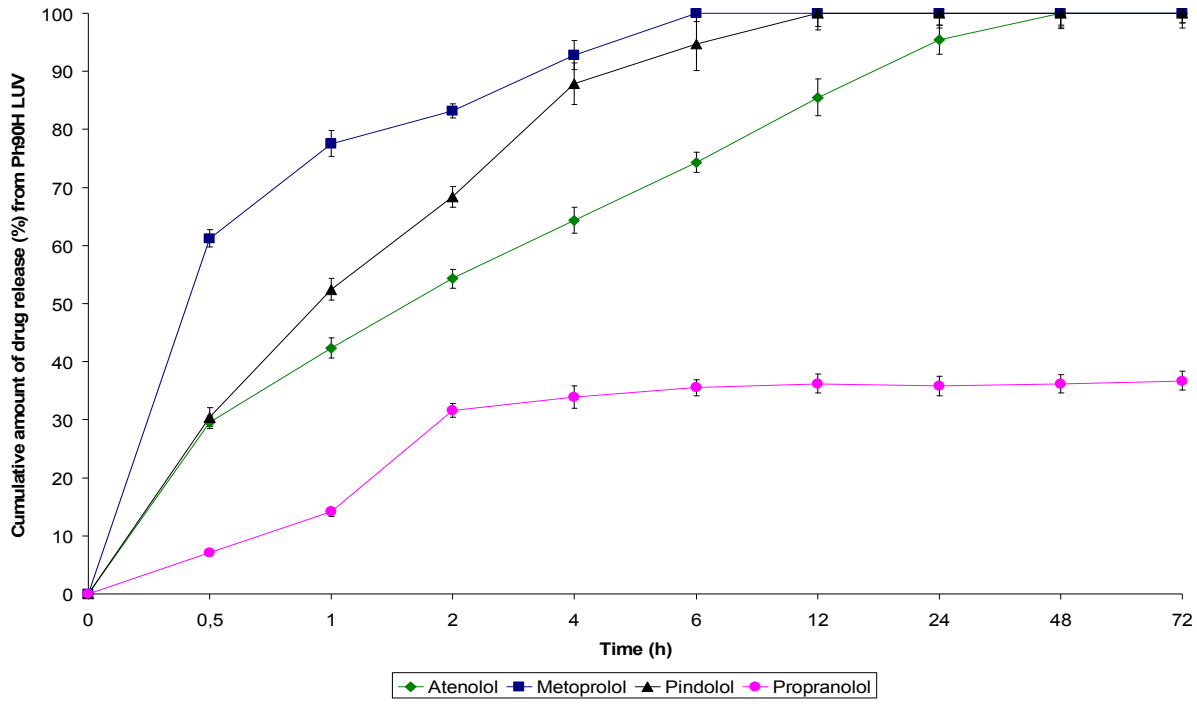

Figure 71: Effect of lipophilicity of β-adrenoceptor antagonists on their in vitro release from LUV liposomes prepared from Ph90H into PBS, pH 7.4, at 37 ± 0.5 °C using dialysis method. Mean ± S.D., *n* =3.

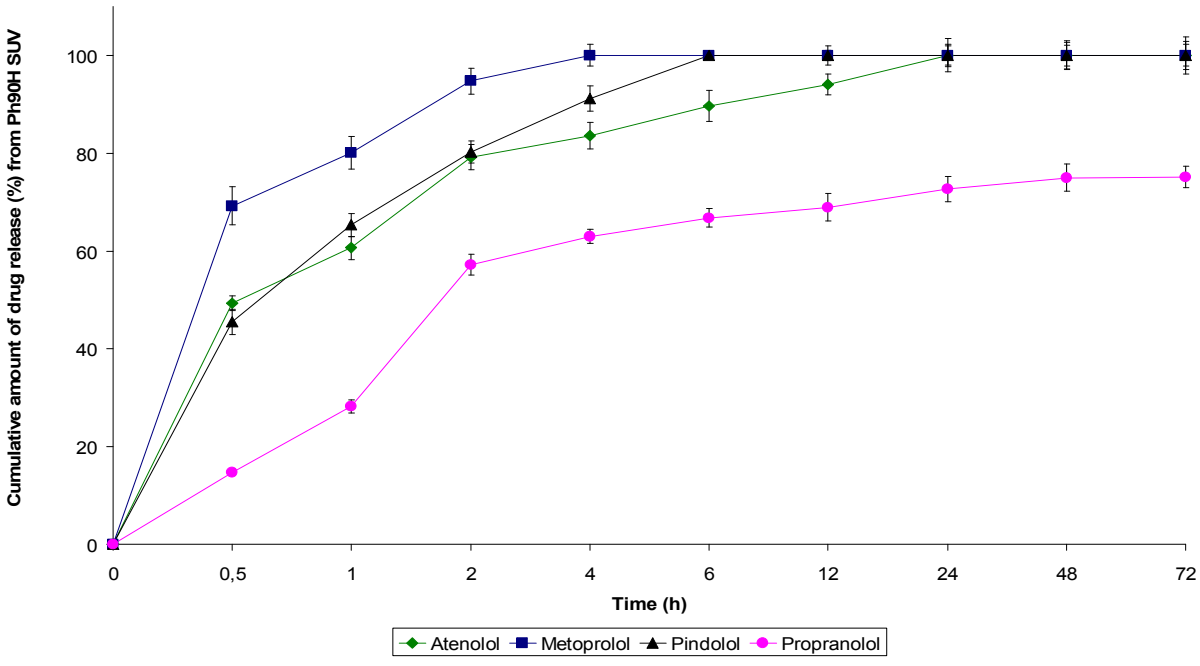

Figure 72: Effect of lipophilicity of β-adrenoceptor antagonists on their in vitro release from SUV liposomes prepared from Ph90H into PBS, pH 7.4, at 37 ± 0.5 °C using dialysis method. Mean ± S.D., *n* =3.

III.8. Effect of liposomal structure on the in vitro release of drugs

III.8.1. Effect of liposomal structure on the in vitro release of β-adrenoceptor antagonists from liposomes

Release data for β-adrenoceptor antagonists from different types of liposomal dispersions into PBS pH 7.4 at 37± 0.5 °C using a dialysis method are shown as cumulative percent released in Figure 73. It was found that the release of β-adrenoceptor antagonists was increased from MLV to LUV to SUV.

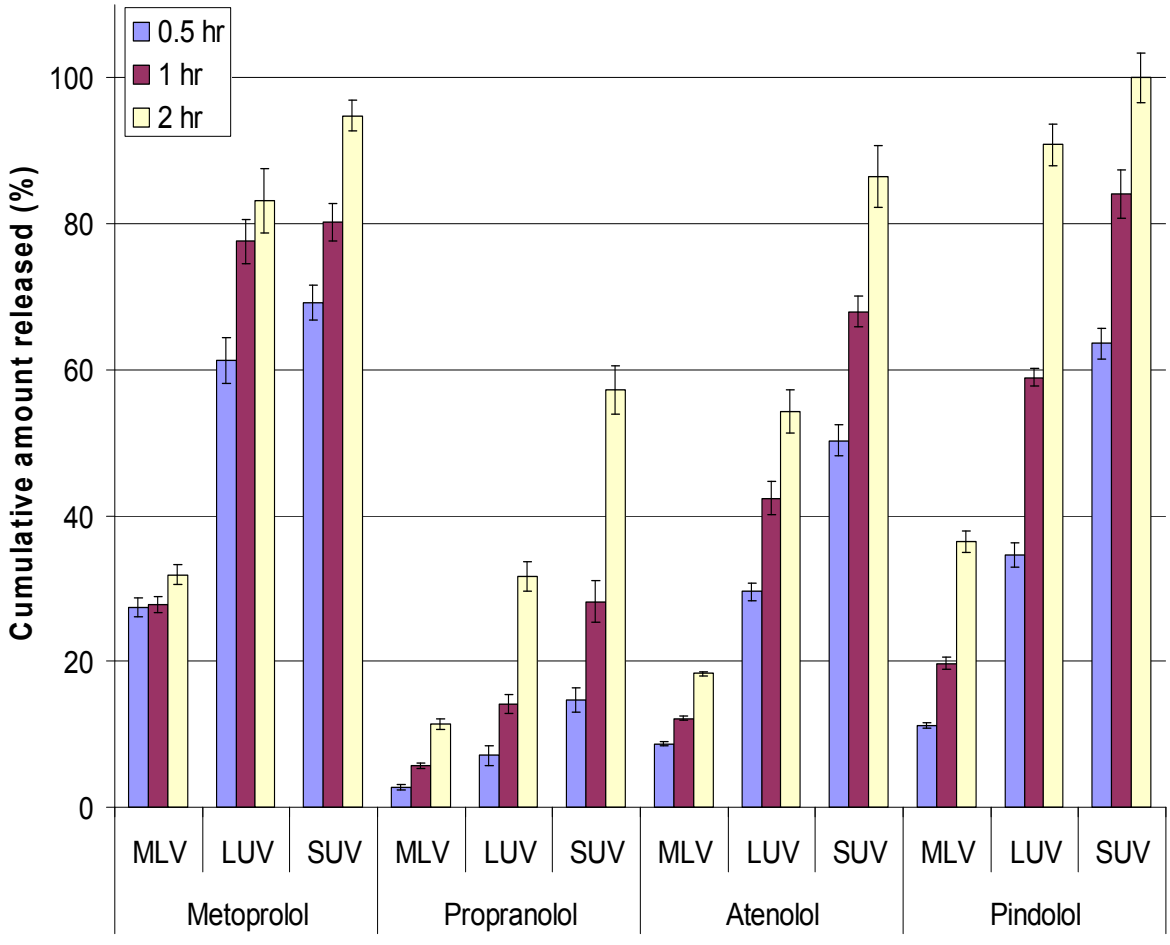

Figure 73: Release pattern of β-adrenoceptor antagonists from different liposomes into PBS, at pH 7.4, at 37 ± 0.5 °C using dialysismethod. Mean ± S.D., *n* =3.

III.8.2. Effect of liposomal structure on the in vitro release of glucose using the dispersion method

Glucose release profiles from different liposomal structures (e.g. MLV, LUV and SUV) using the dispersion method are reported in Figure 74. It was found that the release of glucose was in the following order SUV > LUV > MLV.

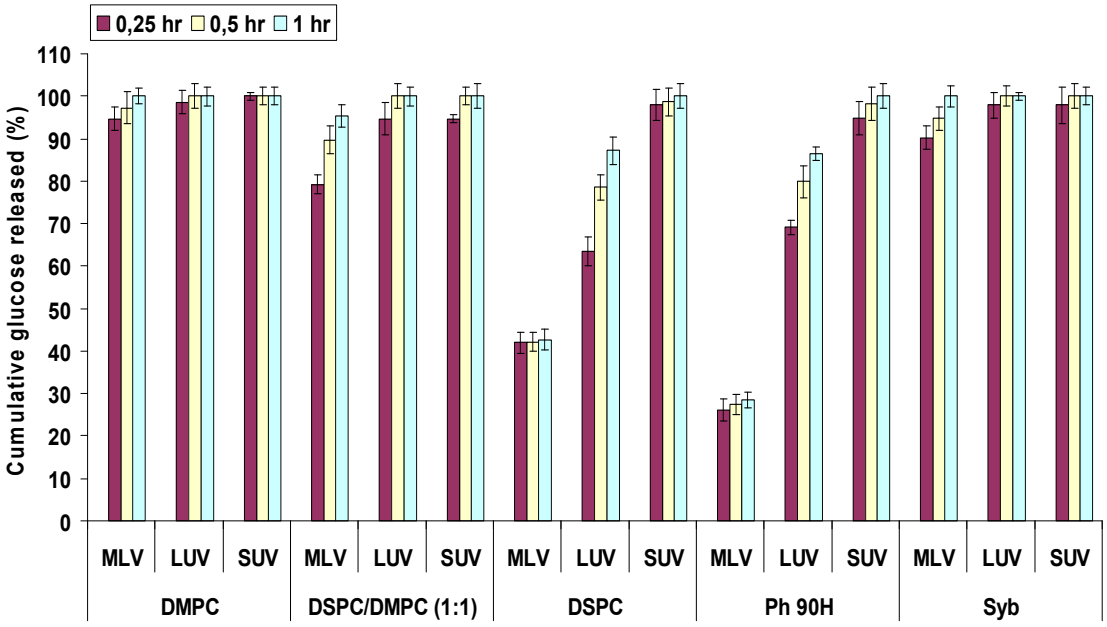

Figure 74: Release pattern of glucose from different liposomes into PBS, at pH 7.4, at 37 ± 0.5°C using dispersion method. Mean ± S.D., *n* =3.

III.9. Effect of lipid concentration on the in vitro release of β-adrenoceptor antagonists from Ph90H liposomes

Figures 75, 76, 77 and 78 show the effect of Ph90H concentration (50 and 100mg/mL) on the vitro release of β-adrenoceptor antagonists (propranolol, metoprolol, pindolol and atenolol respectively) from MLV liposomes into PBS, pH 7.4 at 37± 0.5 °C.

The results were illustrated by plotting the cumulative percentage amount released of β-adrenoceptor antagonists versus time. From the release profiles, it was found that the concentration of 100 mg/ml Ph90H shows slower release of all β-adrenoceptor antagonists used than at 50 mg/ml Ph 90H, that is to say as the concentration of lipid increases, the release of the drug decreases.

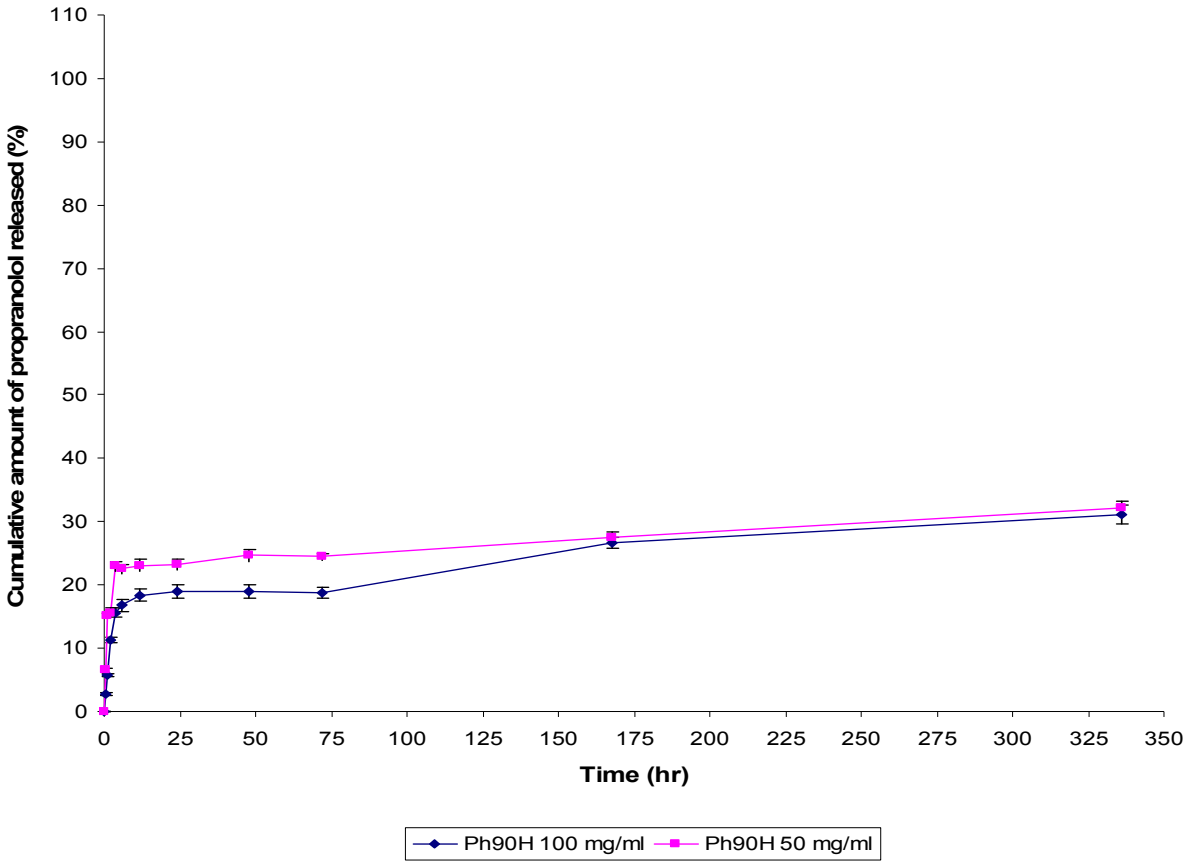

Figure 75: Effect of Ph90H concentration on in vitro release of propranolol from MLV into PBS, at pH 7.4, at 37 ± 0.5 °C using dialysismethod. Mean ± S.D., *n* =3.

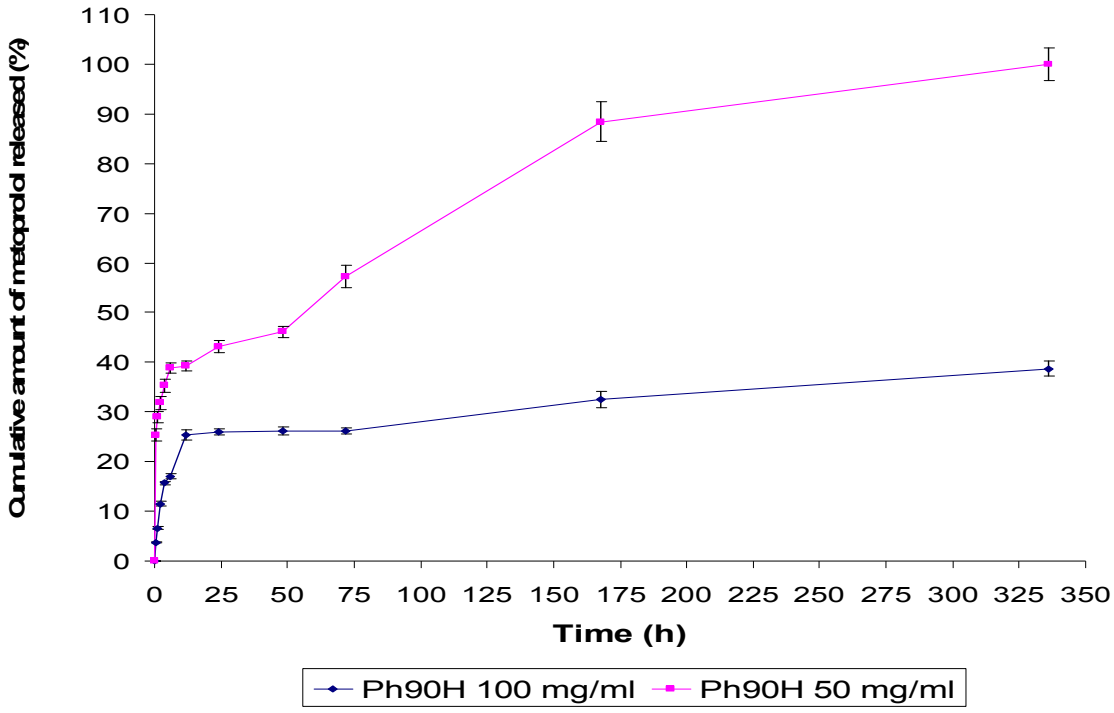

Figure 76: Effect of Ph90H concentration on in vitro release of metoprolol from MLV into PBS, at pH 7.4, at 37 ± 0.5 °C using dialysismethod. Mean ± S.D., *n* =3.

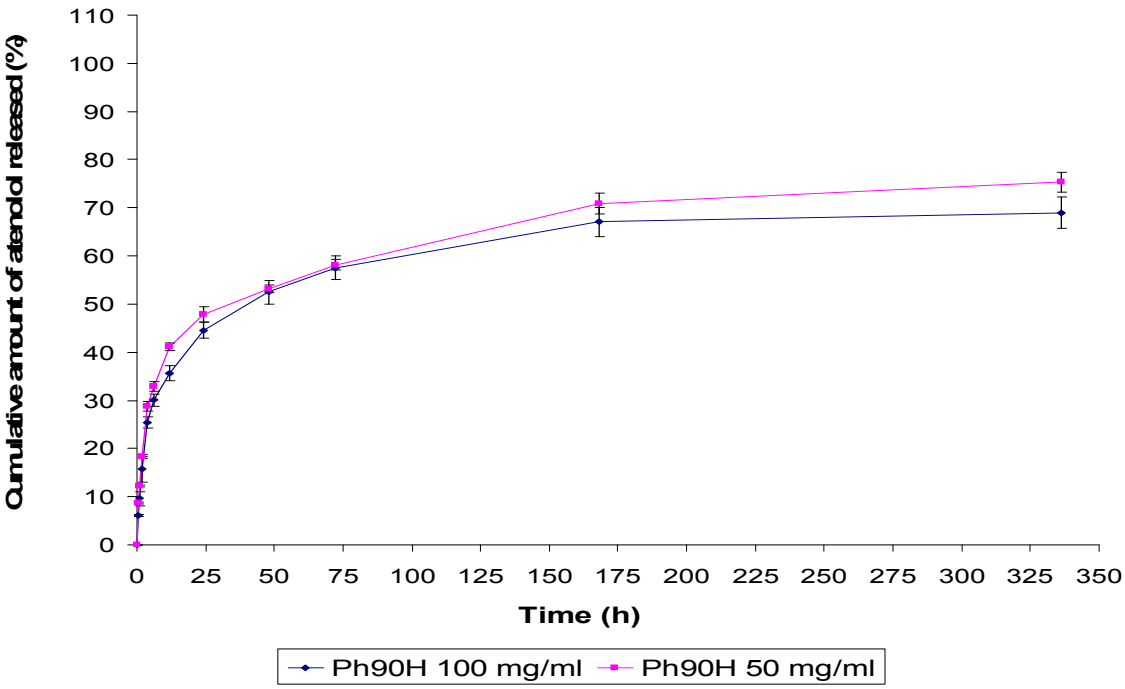

Figure 77: Effect of Ph90H concentration on in vitro release of pindolol from MLV into PBS, at pH 7.4, at 37 ± 0.5 °C using dialysismethod. Mean ± S.D., *n* =3.

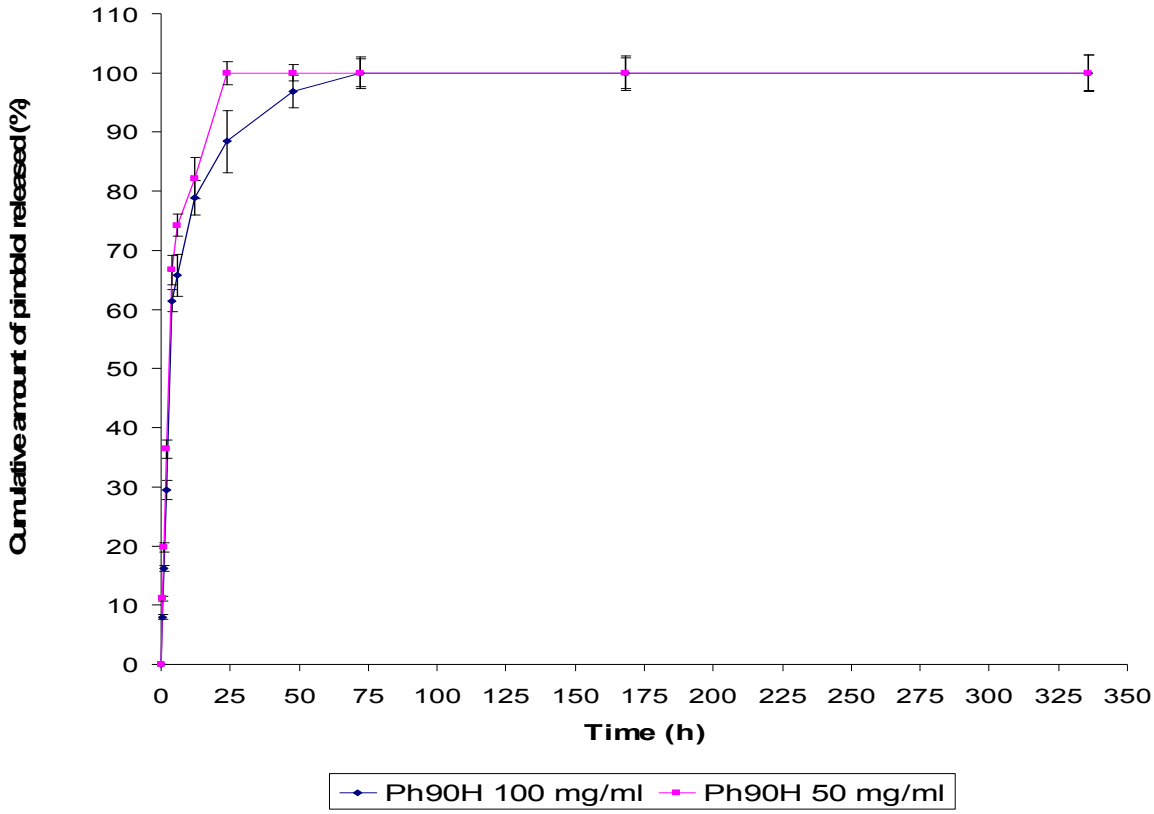

Figure 78: Effect of Ph90H concentration on in vitro release of atenolol from MLV into PBS, at pH 7.4, at 37 ± 0.5 °C using dialysismethod. Mean ± S.D., *n* =3.

III.10. Calculation of the half life ($t_{1/2}$) of the in vitro release

III.10.1. Calculation of the half life ($t_{1/2}$) of the in vitro release of β-adrenoceptor antagonists from liposomes

The half-lives ($t_{1/2}$) of the in vitro release of β-adrenoceptor antagonists from MLV, LUV and SUV was calculated using both Lineweaver-Burk plot (double reciprocal plot) and a plot of the ln (cumulative percentage remained) versus time. The calculated data are presented in Table 12. Figures 79 and 80 represent Lineweaver-Burk plot (double reciprocal plot) and a plot of the ln (cumulative percentage remained) versus time, respectively.

Table 12: Half-lives of release ($t_{1/2}$) of β- adrenoceptor antagonists-containing liposomes

Liposomal type		Half life (h)			
		Propranolol	Metoprolol	Pindolol	Atenolol
MLV	DSPC	1.3	65.0	2.0	9.2
	Ph 90H	6.8	60.0	3.7	7.2
	DSPC/DMPC (1:1)	1.2	3.0	2.9	3.2
	DMPC	2.4	3.8	7.1	1.6
LUV	DSPC	1.5	0.7	0.5	0.9
	Ph 90H	1.8	0.8	1.4	1.9
	DSPC/DMPC (1:1)	1.2	1.3	0.3	1.6
	DMPC	1.9	4.5	0.4	2.2
SUV	DSPC	1.5	0.7	0.8	1.2
	Ph 90H	1.3	0.7	0.7	1.0
	DSPC/DMPC (1:1)	1.3	0.5	0.8	1.0
	DMPC	2.1	4.2	1.3	3.4

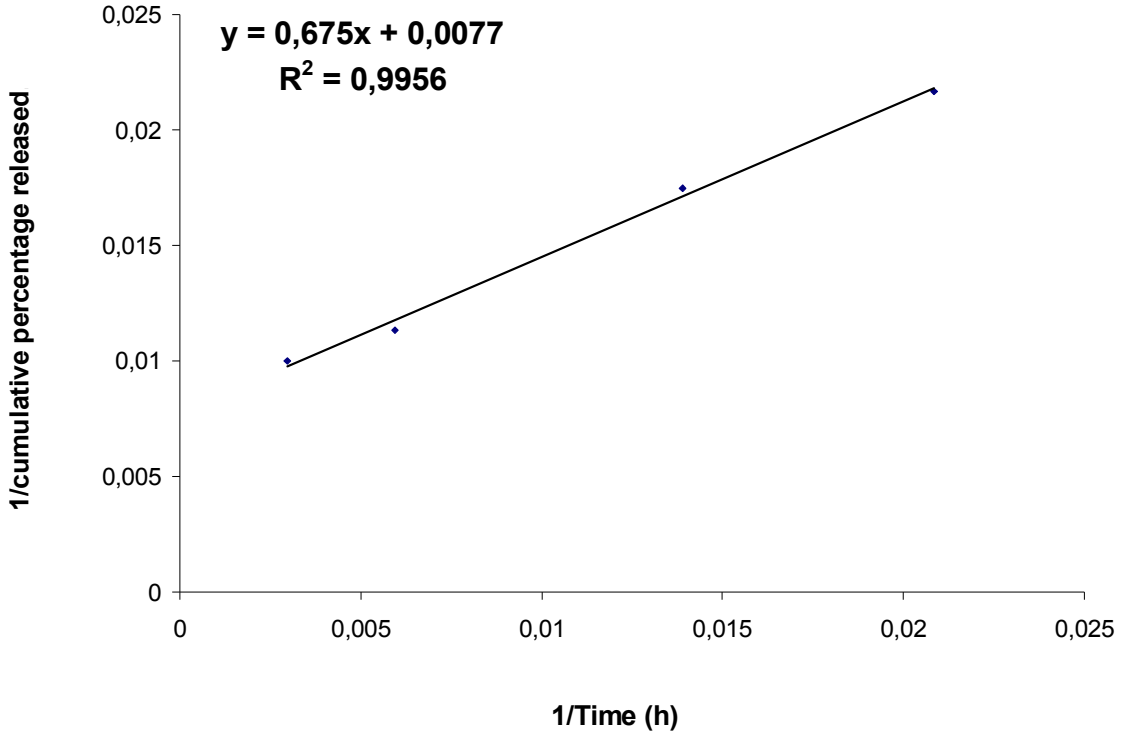

Figure 79: Double reciprocal plot of cumulative percentage of metoprolol released from Ph90H MLV (Lineweaver-Burk plot)

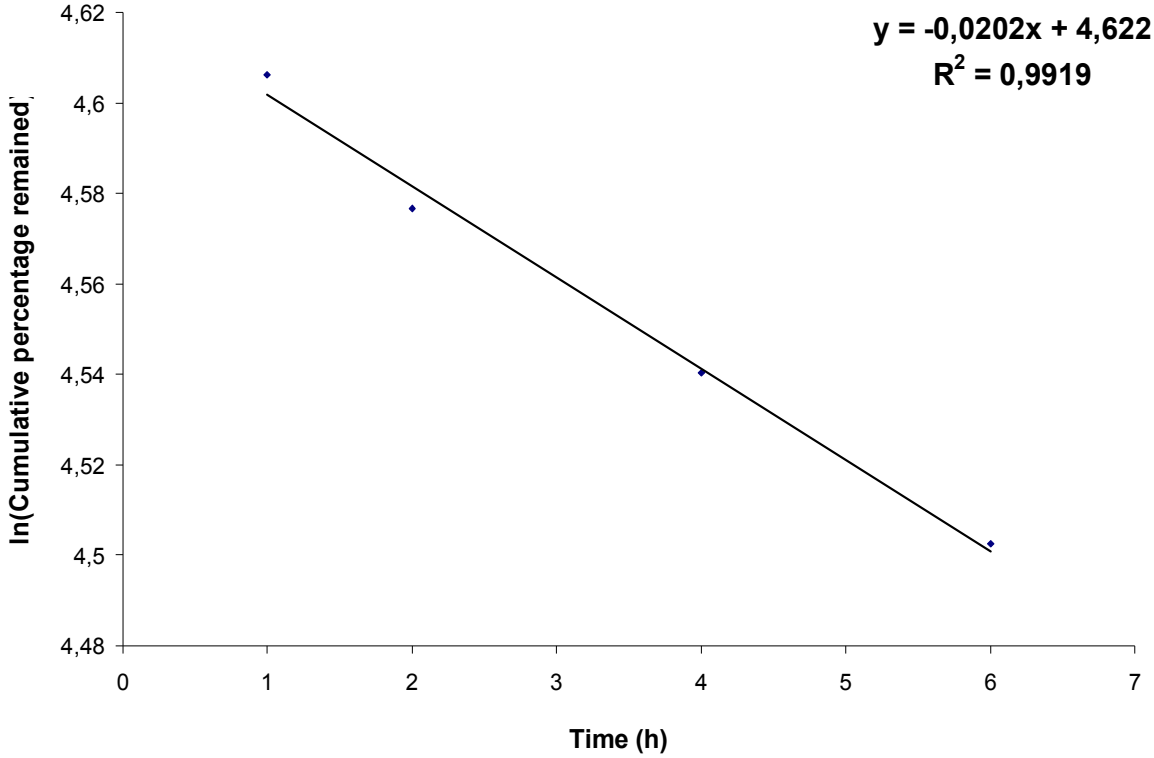

Figure 80: Semi-logarithmic presentation of cumulative percentage Metoprolol remaining in PH90H MLV

III.10.2. Calculation of the half life ($t_{1/2}$) of the in vitro release of glucose from liposomes

The half life ($t_{1/2}$) of the in vitro release of glucose from MLV and LUV was calculated using using both Lineweaver-Burk plot (double reciprocal plot) and a plot of the ln (cumulative percentage remained) versus time. The calculated data are presented in Table 13. Figures 81 and 82 represent Lineweaver-Burk plot (double reciprocal plot) and a plot of the ln (cumulative percentage remaining) versus time, respectively.

Table 13: Half-lives ($t_{1/2}$) of release of glucose-containing liposomes

	DMPC	DSPC/DMPC (1:1)	DSPC	Ph 90H	Syb
MLV	0.34	0.46	0.25	0.39	0.34
LUV	0.56	0.58	0.53	0.46	0.56

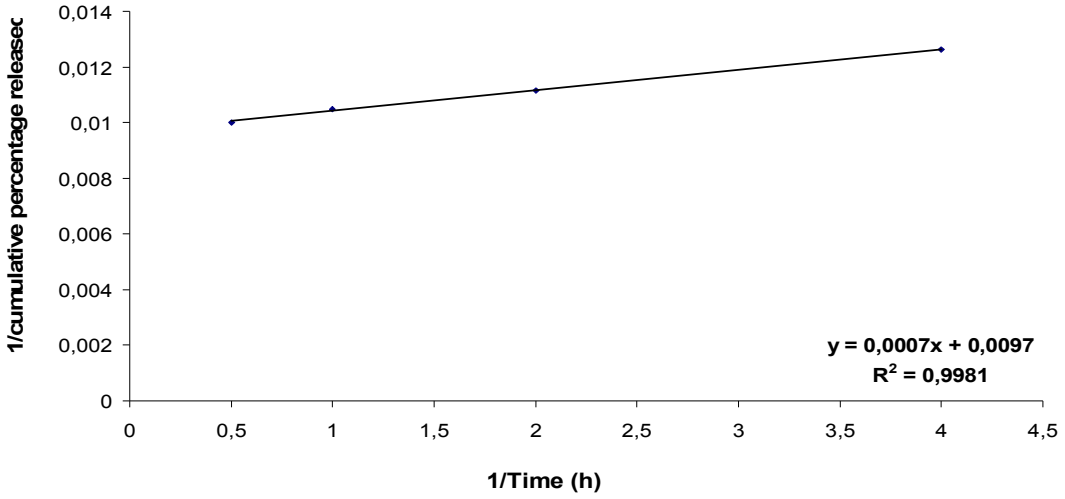

Figure 81: Double reciprocal plot of cumulative percentage of glucose released from DSPC&DMPC (1:1) MLV (Lineweaver-Burk plot)

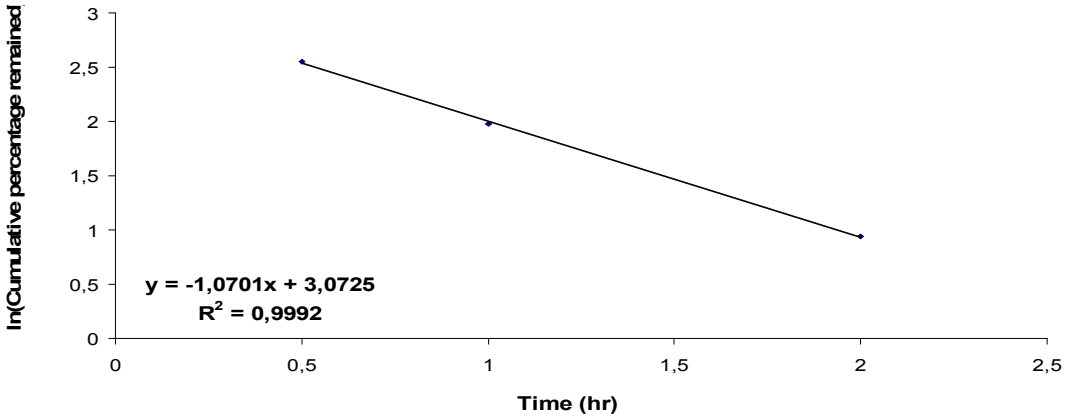

Figure 82: Semi-logarithmic presentation of cumulative percentage glucose remained in DSPC/DMPC (1:1) MLV

III.11. Stability of the Er-DTPA liposomes

III.11.1. Effect of storage temperature on the percentage of residual content of Er-DTPA in SUV

Er-DTPA SUV was stored at three different temperatures i.e. 4, 25 and 37 °C for up to 96 hours. Figures 83, 84 and 85 show the percentage of the amount of Er-DTPA complex retained in SUV prepared from different amounts of soybean lipid (30, 50 and 70 mg/ml respectively).

It was found that the amount retained of Er-DTPA is inversely proportional to the storage temperature, where liposomes maintained at 4 °C exhibits the highest percentage of Er-DTPA retained (13.58 %) than other liposomes stored at 25 and 37 °C (3.28 % and 2.11 % respectively) after 96 hours.

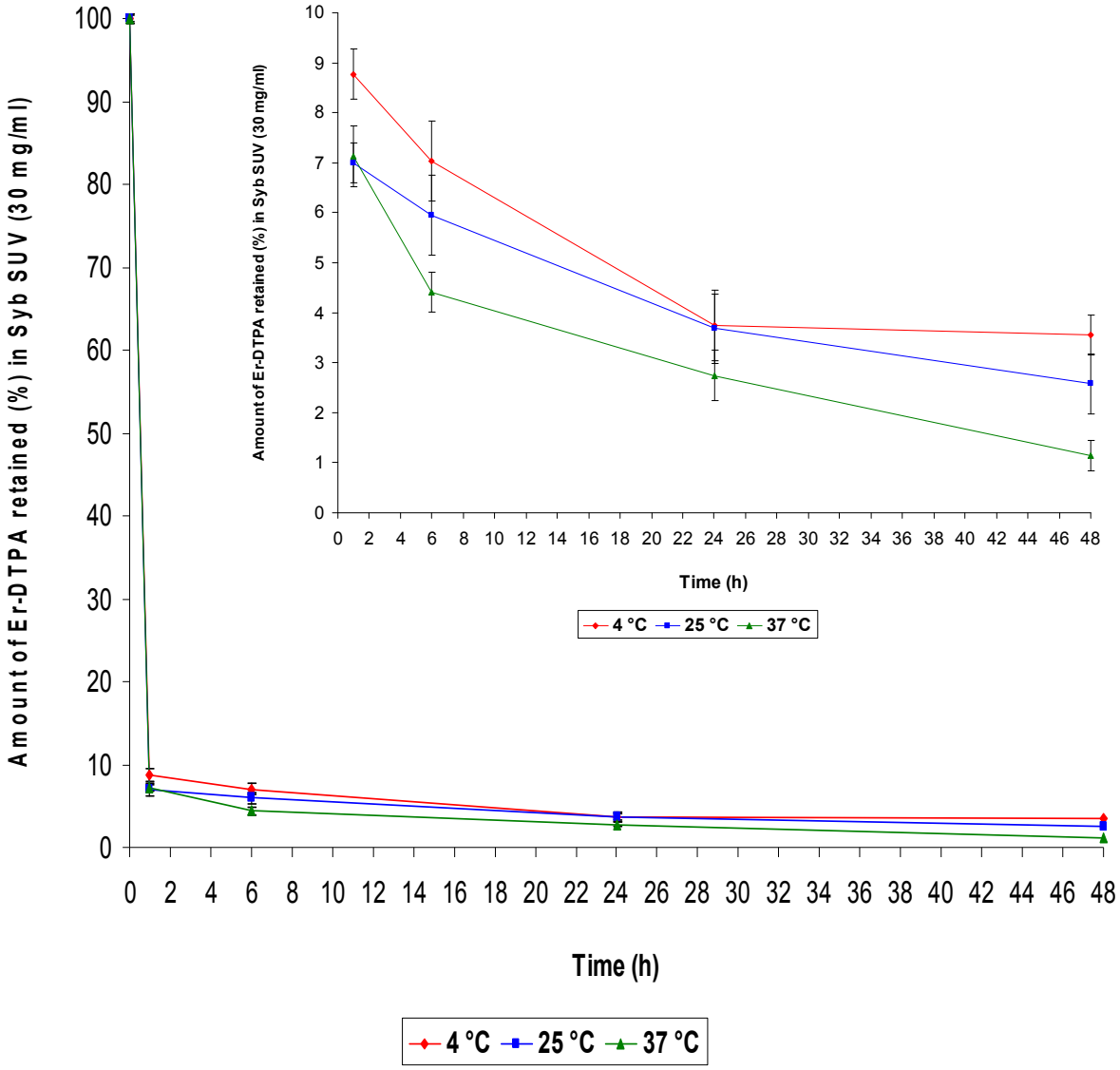

Figure 83: Effect of storage temperature on the percentage of Er-DTPA complex retained in SUV prepared from Syb lipid (30mg/ml)

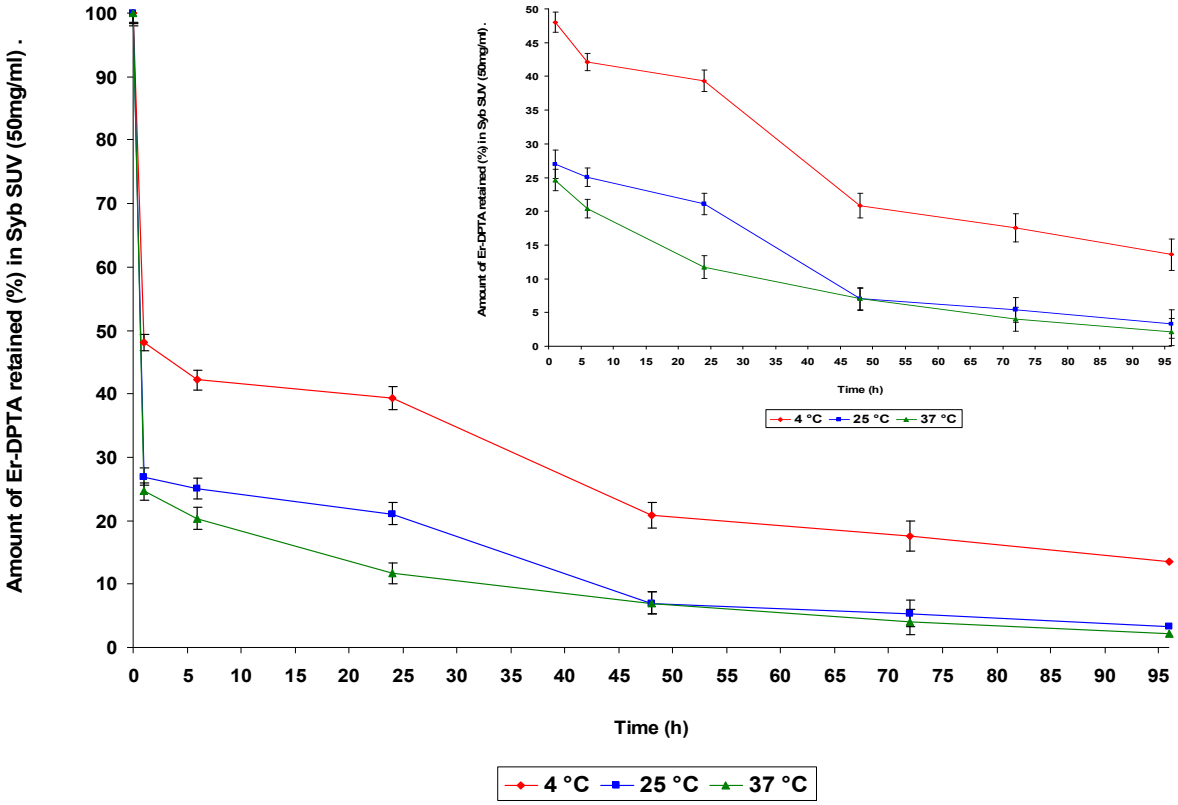

Figure 84: Effect of storage temperature on the percentage of amount of Er-DTPA complex retained in SUV prepared from Syb lipid (50mg/ml)

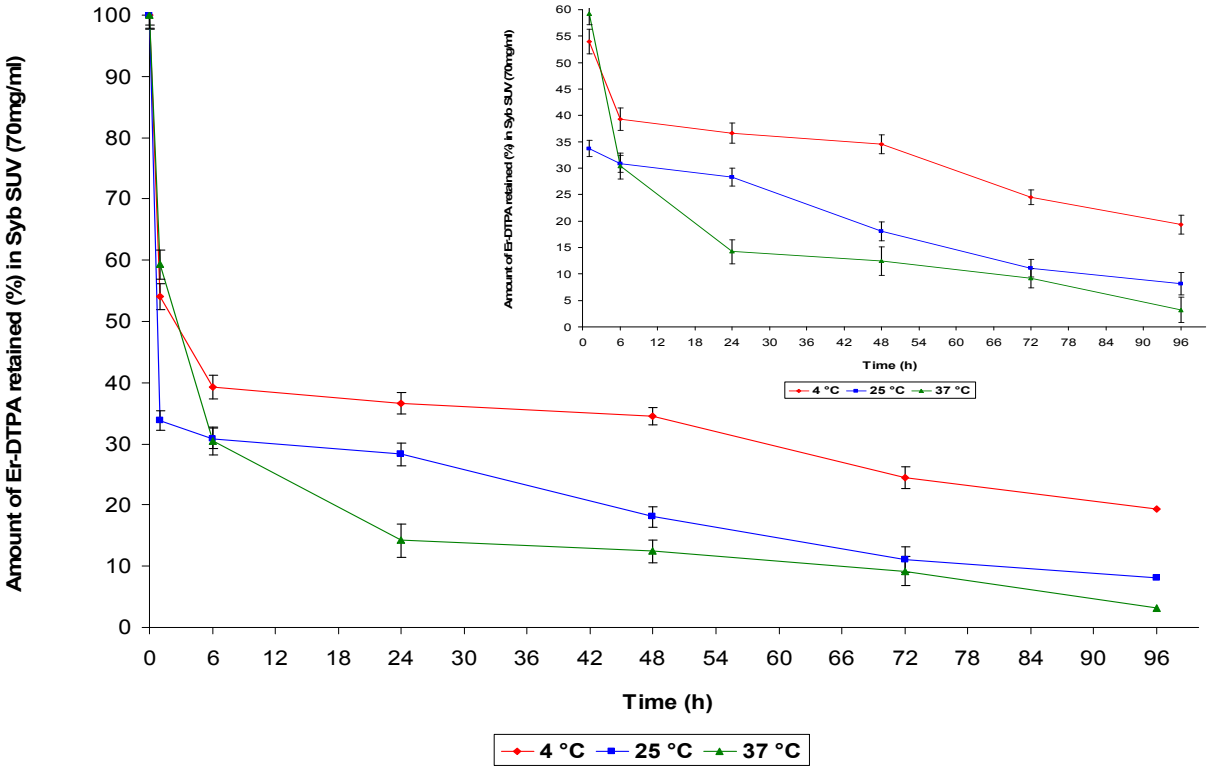

Figure 85: Effect of storage temperature on the percentage of Er-DTPA complex retained in SUV prepared from Syb lipid (70mg/ml)

III.11.2. Effect of soybean lipid concentration on the percentage of retained amount of Er-DTPA in SUV

Three batches of SUV liposomes were prepared with different soybean lipid content (30, 50 and 70 mg/ml). The percentage of Er-DTPA complex retained in SUV was determined and plotted against time (Figure 86). The overall tendency observed was a decrease in the percentage of the amount of Er-DTPA complex retained with decreasing soybean lipid concentration for lipid concentrations of 70, 50 and 30 mg/ml. When comparing soybean lipid concentrations of 30 and 70 mg/ml however a dramatic change was found. Whereas the formulation containing 30 mg/ml of soybean lipid retained about 7 % Er-DTPA complex after one hour and about 2.6 % after 48 hours. While the formulation containing 70% mg/ml soybean lipid retained 33.7 % of Er-DTPA complex after one hour and 18.1 % after 48 hours.

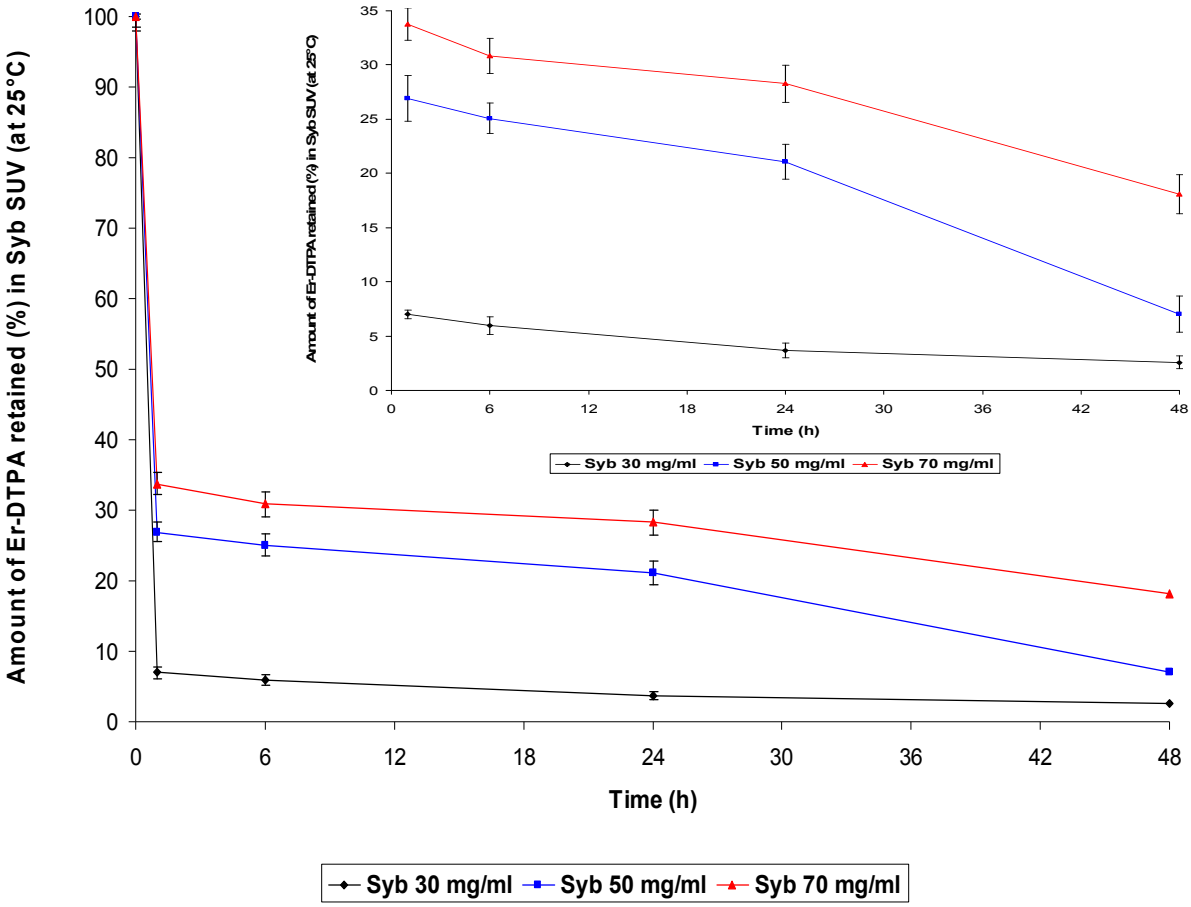

Figure 86: Effect of soybean lipid concentration on the percentage of Er-DTPA complex retained in SUV prepared from Syb lipid

III.12. In vivo imaging of FDG in animal using PET

III.12.1. Biodistribution of FDG in the whole body and the brain of rats

Distribution of FDG from unencapsulated FDG in saline solution, FDG-containing LUV and FDG-containing MLV in the whole body after 2 hours is shown in Figures 87, 88 and 89 respectively. It was concluded that FDG was distributed faster from unencapsulated FDG than from both FDG-containing MLV and FDG-containing LUV. Figures 90 and 92 depict scanning the distribution of FDG from unencapsulated FDG and FDG-containing MLV to the brain at time interval 30, 60, 90 and 120 minutes respectively. Figure 91 exhibits the scanning of the distribution of FDG from FDG-containing LUV to the brain at time interval 30, 60 and 90 minutes. It was found that the release of FDG was fast in case of unencapsulated FDG, moderate in case of FDG-containing LUV and sustained in case of FDG-containing MLV.

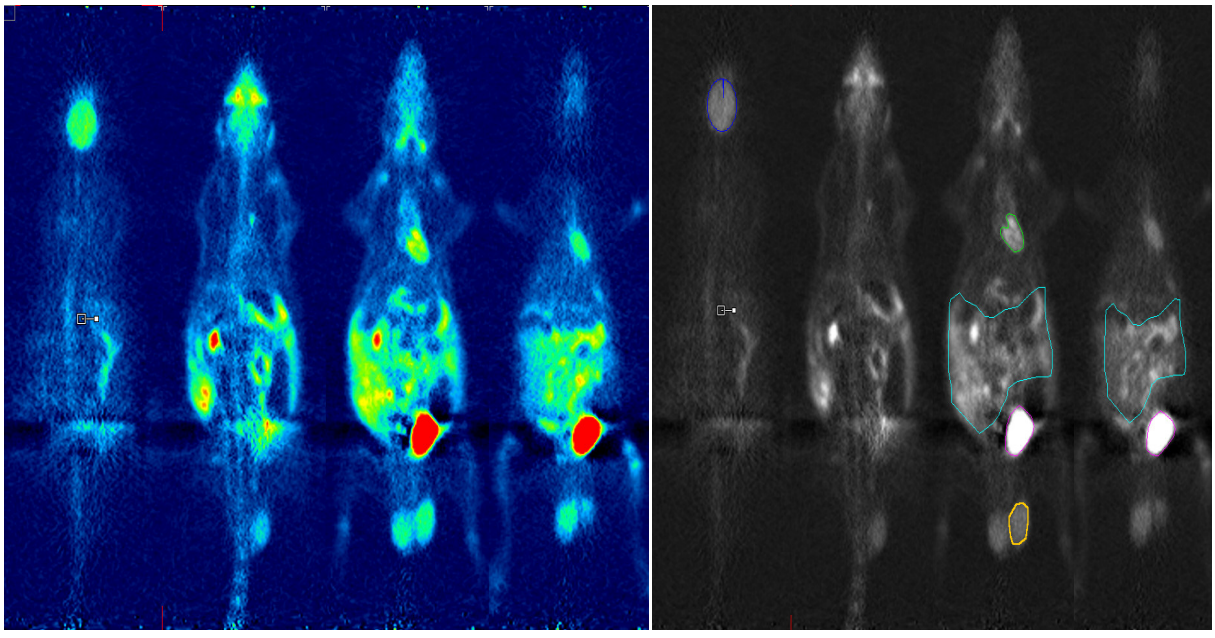

Figure 87: Biodistribution of ^{18}F-FDG from unencapsulated FDG in the whole body of rats showing brain, heart, urinary bladder and testes after 2 hours.

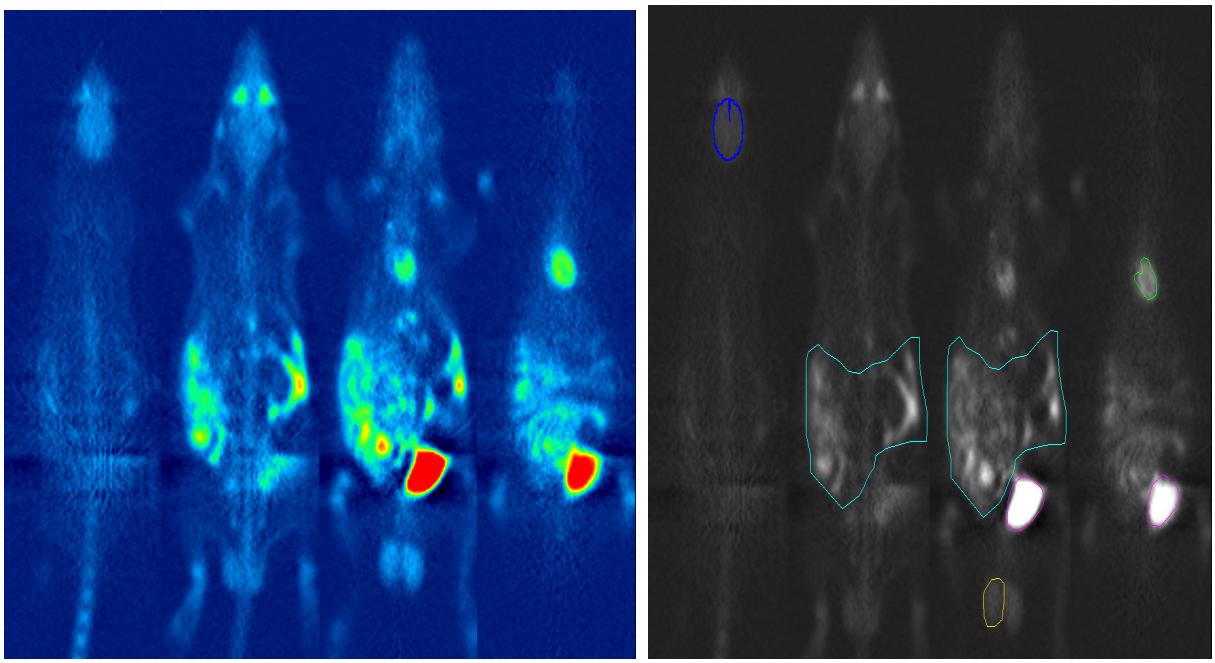

Figure 88: Biodistribution of ^{18}F-FDG from FDG-containing LUV in the whole body of rats showing brain, heart, urinary bladder and testes after 2 hours

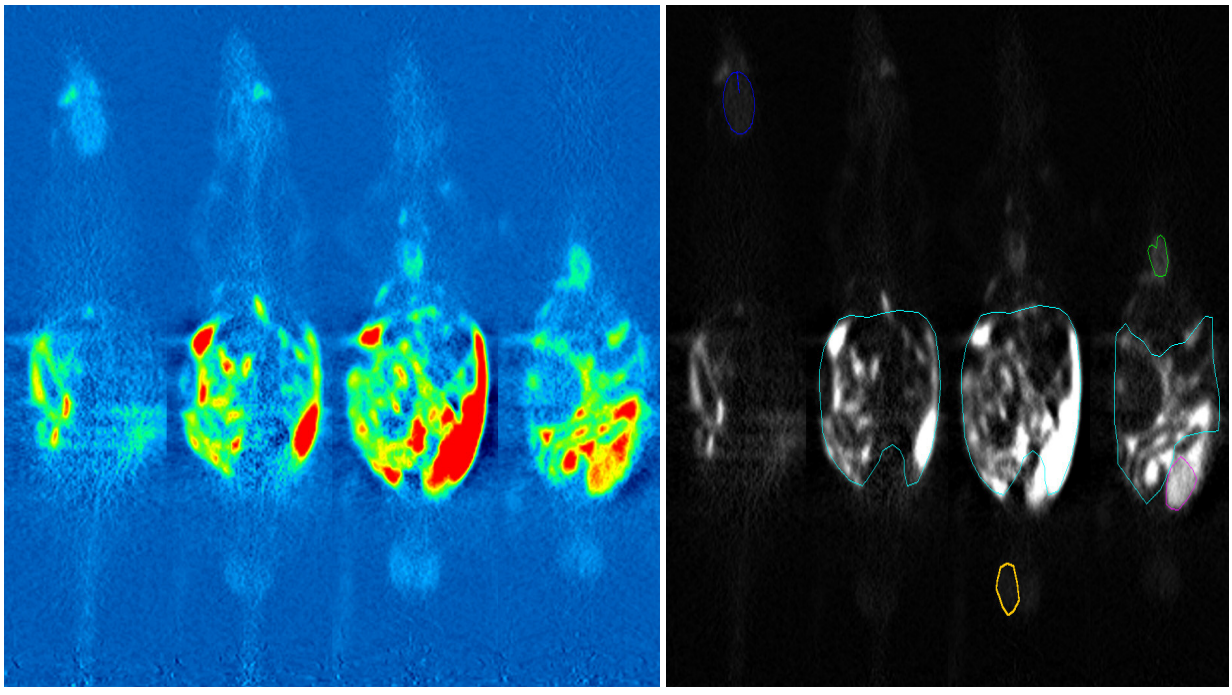

Figure 89: Biodistribution of ^{18}F-FDG from FDG-containing MLV in the whole body of rats showing brain, heart, urinary bladder and testes after 2 hours

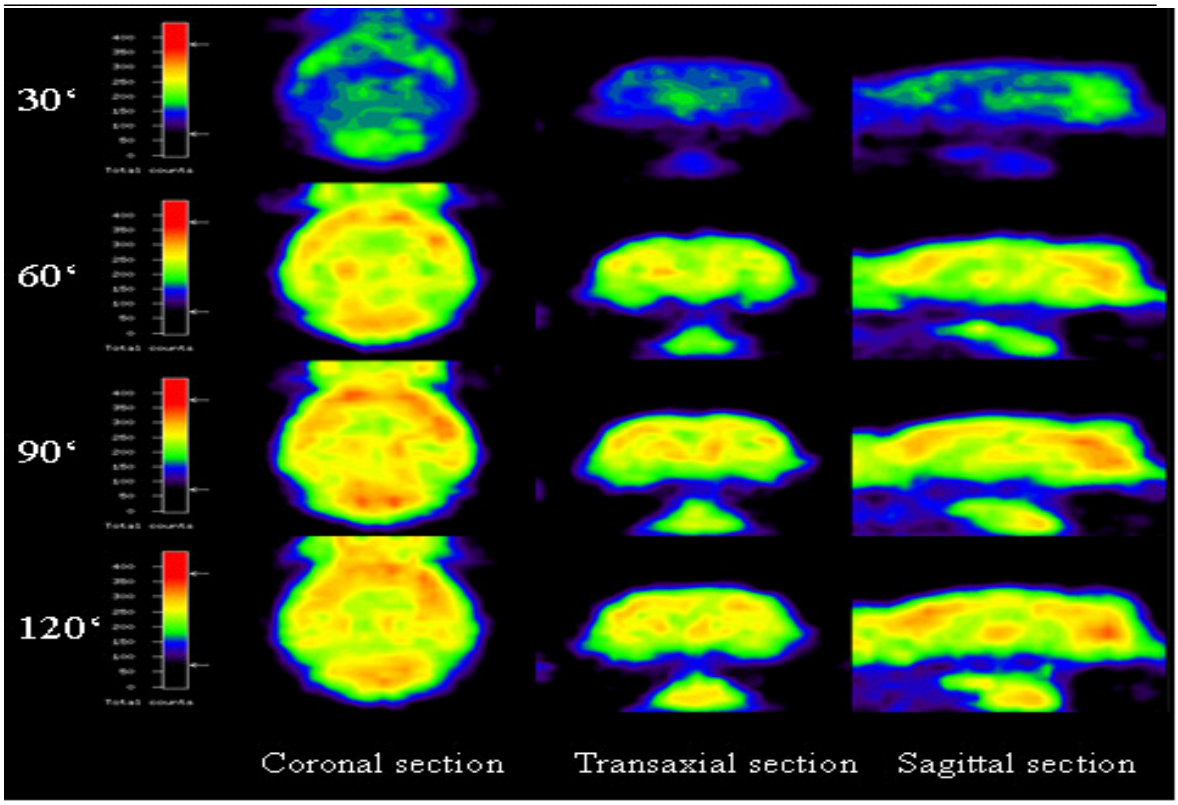

Figure 90: PET images of ^{18}F-FDG from unencapsulated FDG in saline solution in the brain of rats (horizontal, transaxial and sagital sections) at time intervals of 30, 60, 90 and 120 minutes

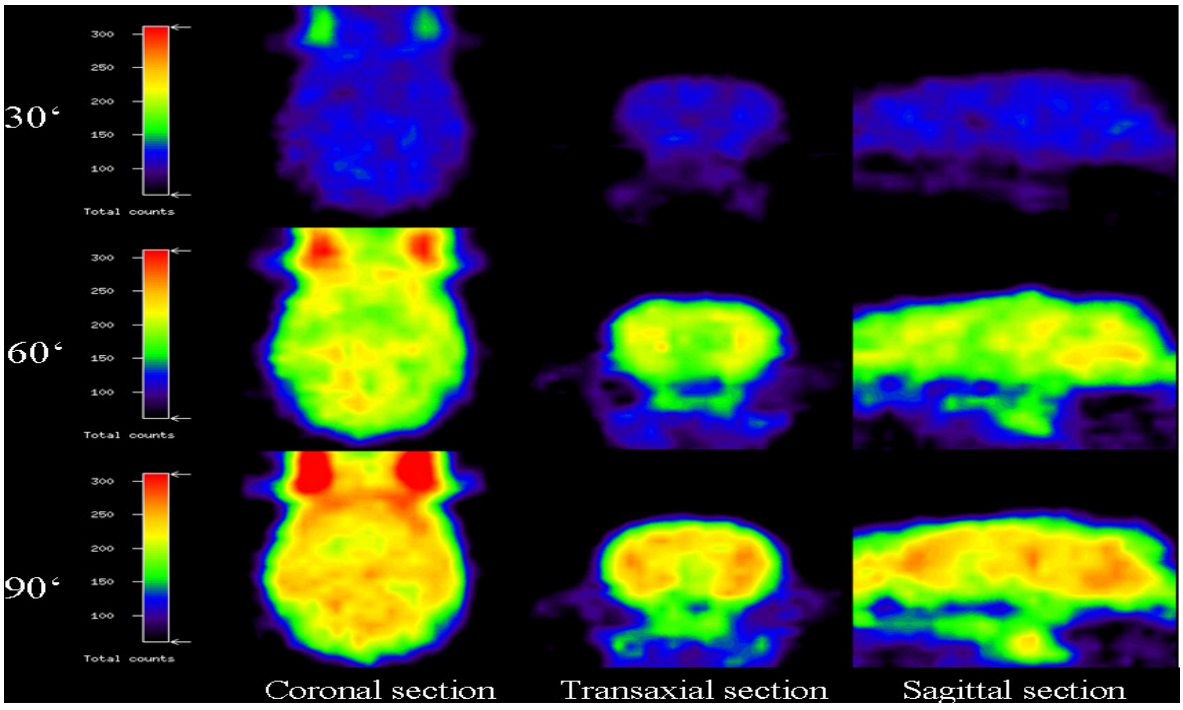

Figure 91: PET images of ^{18}F-FDG from FDG-containing LUV in the brain of rats (horizontal, transaxial and sagital sections) at time intervals of 30, 60 and 90 minutes

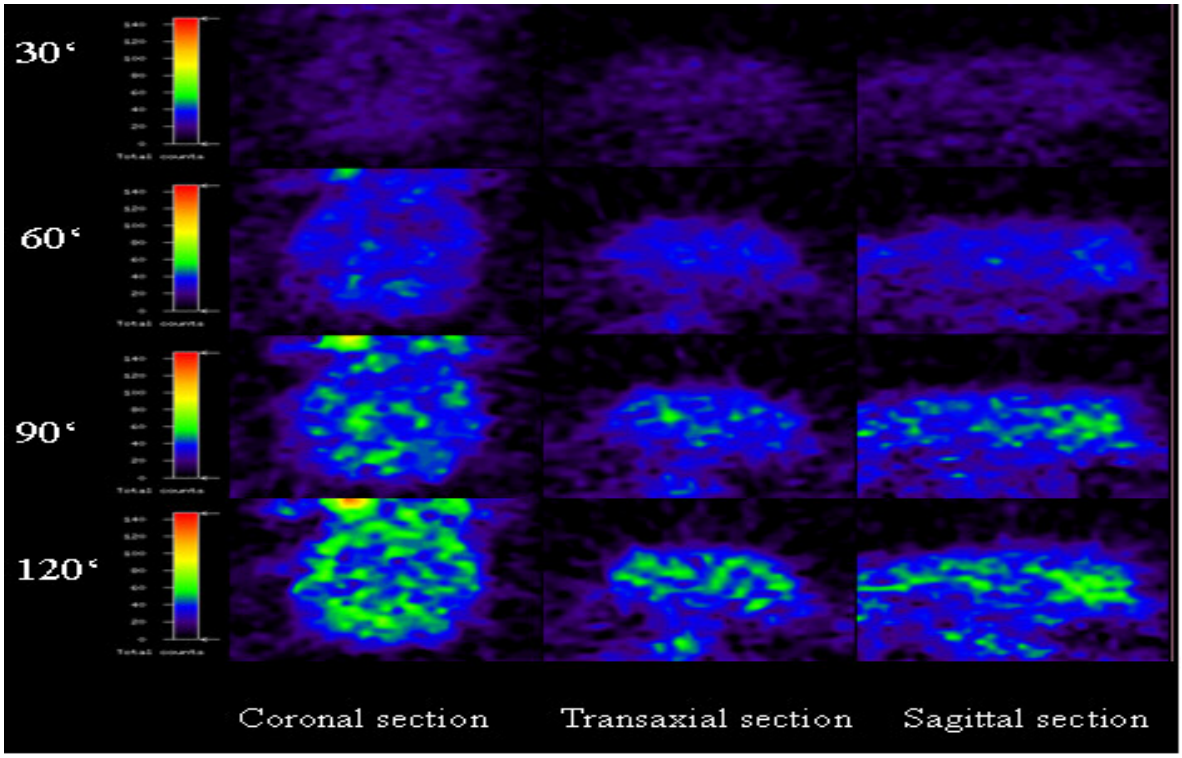

Figure 92: PET images of ^{18}F-FDG from FDG-containing MLV in the brain of rats (horizontal, transaxial and sagital sections) at time intervals of 30, 60, 90 and 120 minutes

III.12.2. Comparison of whole body-regions of interest (WH-ROIs) of FDG from unencaspsulated FDG and FDG-containing liposomes

Table 14 shows a comparison of distribution of FDG from unencapsulated FDG and FDG-containing liposomes (MLV and LUV) in various regions of interest.

Table 14: Comparison of WHb-ROIs of FDG from unencaspsulated FDG and FDG-containing liposomes

Liposomes	Region of Interest (ROIs)	Averaged Activity (MBq)	Ratio to Testes	Ratio of liposomes/ unencapsulated FDG
Unencapsulated FDG	Brain	2.02E-07	1.13	1.00
	Abdomen	2.77E-07	1.55	1.00
	Heart	6.27E-07	3.51	1.00
	Urinary Bladder	2.28E-06	12.75	1.00
	Testes	1.79E-07	1.00	1.00
LUV	Brain	2.02E-07	1.13	0.92
	Abdomen	2.77E-07	1.55	1.36
	Heart	6.27E-07	3.51	2.19
	Urinary Bladder	2.28E-06	12.75	1.18
	Testes	1.79E-07	1.00	0.94
MLV	Brain	5.01E-08	1.33	0.29
	Abdomen	2.40E-07	6.36	1.49
	Heart	1.08E-07	2.86	0.48
	Urinary Bladder	3.93E-07	10.41	0.26
	Testes	3.78E-08	1.00	0.25

III.12.3. Time activity curve (TAC) of FDG

Figure 93 exhibits the % injected dose of FDG for uncapsulated FDG, FDG-containing LUV and FDG-containing MLV against time. This Figure depicts sustained release of FDG in case of FDG-containing MLV, immediate release in case of FDG from FDG-containing LUV and instantaneous distribution of FDG in case of unencapsulated FDG.

III.13. In vitro-In vivo relationship

The in vitro release of FDG from fast, moderate and sustained liposomal formulations is represented in Figure 94. A rank-order relationship is seen between the kinetics of appearance of FDG in rat brain and in vitro release rate of FDG (Figures 93 and 94 respectively).

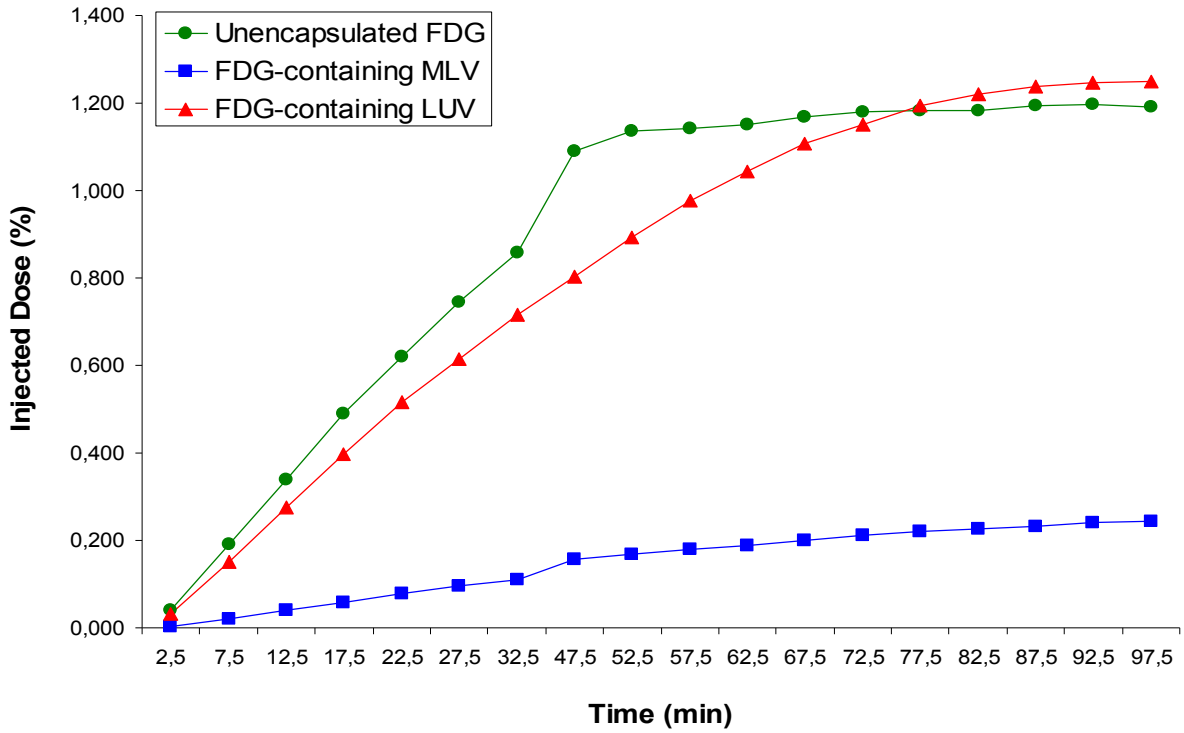

Figure 93: Time activity curve (TAC) of unencapsulated FDG, FDG-containing LUV and FDG-containing MLV

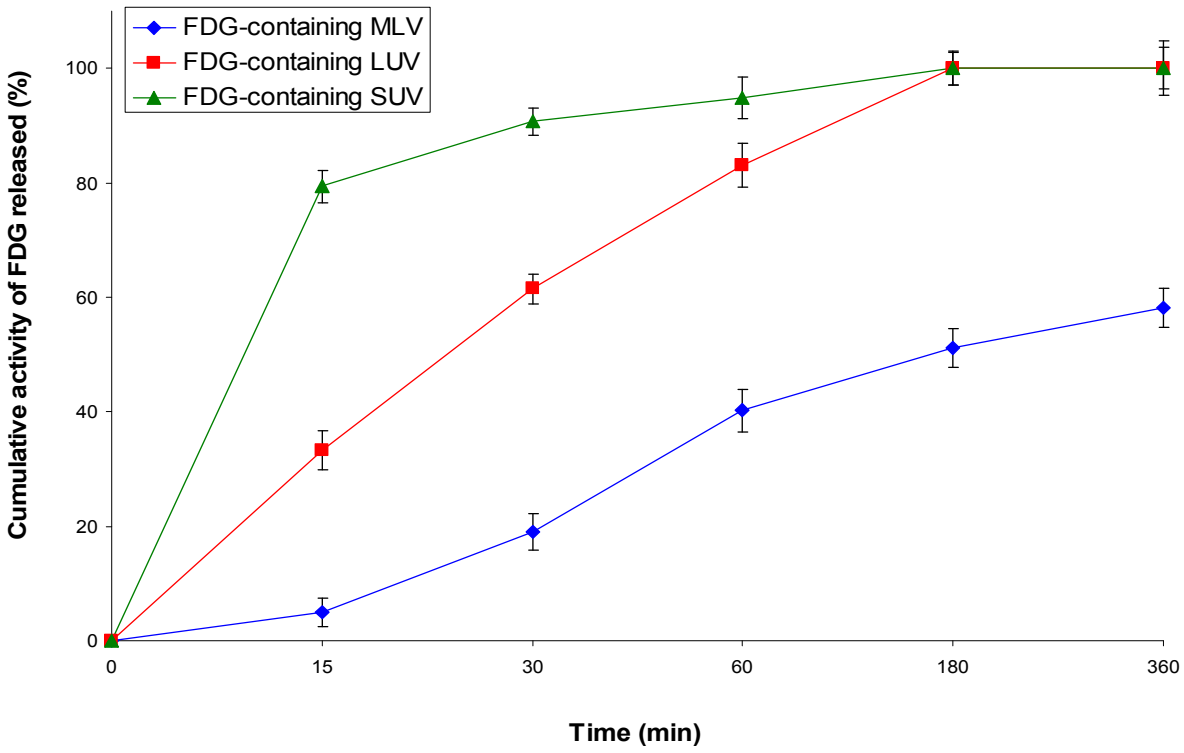

Figure 94: In vitro release of FDG (MBq) from unencapsulated FDG, FDG-containing MLV and FDG-containing LUV

Chapter IV: Discussions

IV.1. Determination of entrapment efficiency

IV.1.1. Entrapment efficiency (EE)of β-adrenoceptor antagonists

The EE of propranolol, metoprolol, pindolol and atenolol in MLV liposomes prepared from different lipids was calculated using the equation stated in materials and methods (page 58). The calculated EE is plotted for each drug as in Figure 39. It was found that the EE differs from one lipid to another. The highest value of EE was found in case of DSPC liposomes and the lowest value was found in case of DMPC. This might be due to the difference in acyl chain length and in the phase transition temperature (Tc). Ph90H and DSPC have longer acyl chain and higher Tc (54 and 54.5 °C respectively) than DMPC which has the shorter acyl chain and low Tc (23 °C). These findings are in agreement with *Anderson and Omri, 2004,* who studied the effect of lipid type on the encapsulation efficiency of inulin. They found that DMPC has lower encapsulation efficiency of inulin than DSPC.

IV.1.2. Entrapment efficiency (EE) of glucose

The EE of glucose in MLV, LUV and SUV liposomes prepared from Ph90H was calculated (Figure 40). SUV vesicles showed the highest value of EE compared with the other types of liposomes (LUV and MLV). This might be attributed to the interaction through hydrogen bonds between glucose and lipid during the sonication process. While in case of LUV some of glucose entrapped was liberated during extrusion.

IV.1.3. Entrapment efficiency of Er-DTPA

Er-DTPA complex, owing to their low affinity and solubility in the lipids which constitute the liposomal membrane, is encapsulated within the internal

aqueous compartments of the liposomes, depending on the encapsulated aqueous volume. Figure 41 shows the encapsulation of erbium in SUV liposomes containing varying amounts of soybean lipids. It was found that the encapsulation efficiency increased by increasing the concentration of soybean lipid from 30 mg/ml to 70 mg/ml of soybean lipid. The increase in EE upon increasing the soybean lipid concentration may be due to an increasing number of vesicles formed.

IV.2. Determination of the particle size

The average particle size determined by both DLS and LDA varies depending on the type of the lipid (DSPC, DMPC, DSPC/DMPC (1:1) and Ph90H) and the type of liposome (MLV, LUV or SUV) (Tables 9 and 10). It was found that there is a different broad size distribution ranging from 0.04 μm to 238 μm depending on the lipid and the liposomal types (Table 10). It was found that the particle size distribution determined by LDA shows unimodal, bimodal and multimodal size distributions depending on the types of both lipids used and liposomes prepared.

Regarding the effect of soybean concentration on the particle size, it was found that increasing the soybean lipid concentration of the formulations from 30 to 70 mg/ml tends to slightly increase the mean particle size and particle agglomeration. This observation is in accordance with (*Szoka, 1996; Pons, et al., 1993*), who reported that when the lipid concentration increases, the resulting vesicle diameter increases as well.

The effect of storage temperature on particle size was studied using LDA. It was found that the liposomal diameter increased with increasing temperatures. The increase in the size could be due to the fusion of liposomes. Similar results were observed by (*Garg, et al., 2007*), who reported that an insignificant difference was found in the vesicle size of all

liposomal formulations stored at 4°C for 30 days. But a significant increase in the vesicular size was observed when the liposomal formulations were stored at 25°C and 40°C up to 30 days.

Regarding storage time, it is obvious that the particle size of liposomes containing Er-DTPA initially decreases and this may be attributed to the release of the encapsulated Er-DTPA complex, which consecutively leads to vesicle collapse. Thereafter the particle size increases again, which may be attributed to fusion of particles. These results are in accordance with those found by *Vermehren, et al., 1999,* who stated that DPPC liposomes showed a minor increase in size from 100 nm to approximately 125 nm during the first week of storage, probably due to fusion and/or aggregation of the particles.

IV.3. In vitro release from β-adrenoceptor antagonist-loaded liposomes

IV.3.1. In vitro release of β-adrenoceptor antagonist-loaded liposomes using a dialysis method

IV.3.1.1. In vitro release of β-adrenoceptor antagonists from MLV

IV.3.1.1.1. In vitro release of propranolol from MLV

The in vitro release profiles of unencapsulted propranolol and propranolol MLV formulations prepared from different lipids are exhibited in Figure 48. It was found that the formulations made from DSPC, Ph90H and DMPC lipids exhibited an initial burst drug release followed by a plateau. This means that either the hydration process of the liposomes in the semi permeable bag or the release of propranolol from the liposomal dispersion after the hydration slows down the overall release. Similar results were previously reported by *Byung-Nak, et al., 1995,* who reported that propranolol was released slowly from proliposomes. There is another explanation, in that there may be an interaction between popranolol and the

lipid, which may slow down the drug release. This is consistent with the results reported by *Ubrich, et al., 2004*, who stated that propranolol hydrochloride-loaded nanoparticles showed initial release followed by a rather stable plateau between 2 and 8 h. The plateau-phase was attributed to the interactions between propranolol hydrochloride and the excipients used. Although DMPC has a short acyl chain and low Tc (23 °C), the release of propranolol was slow and constant up to 504 hours which might be due to sorption of propranolol in DMPC MLV. These results are in accordance with those found by *Cocquyt, et al., 2007*, who reported that the amounts of propranolol were sorbed in DMPC vesicles at pH 7 at 37 °C, where the vesicles are in a liquid-crystalline state and at 4 °C, i.e., in the gel state, the amounts sorbed were slightly less than half of those found in the liquid-crystalline state. In case of DSPC/DMPC (1:1), there was rapid increase of the propranolol concentration in the dissolution medium followed by a slow down of propranolol release. This might be due to the higher diffusion of propranolol from the DSPC/DMPC mixture due to (1) immiscibility of this mixture in the solid state or (2) the miscibility of DSPC and DMPC is not ideal or (3) formation of fractures in the bilayer leading to enhancement of propranolol release. This is in agreement with *Nicolussi, et al., 1982*, who reported that when two lipids mix nonideally, a difference in lipid-lipid interactions may originate which must lead to a preferential formation of either unlike or like lipid pairs. As a consequence, fractures may form in the bilayer, in which the contact between the hydrocarbon chains and the water is increased or where the lipid mobility is increased. In both cases, the solute permeability is greatly enhanced. The release of propranolol from Ph90H MLV is slower than that from DMPC MLV. This could be attributed to the fact that the sorption of propranolol in these vesicles is stronger than in case of DMPC vesicles.

IV.3.1.1.2. In vitro release of metoprolol from MLV

Figure 49 presents the in vitro release of metoprolol MLV formulations prepared from different lipids (DSPC, DMPC, DSPC/DMPC (1:1) or Ph90H). From these release profiles, it was concluded that the unencapsulated metoprolol diffuses completely in about one hour. The formulations made from Ph90H and DSPC show slower release of metoprolol. This could be due to the interaction between metoprolol and these lipids (DSPC and Ph90H). Because the degree of interaction between metoprolol and DSPC is greater than the interaction between metoprolol and Ph90H, the release of metoprolol from DSPC MLV was slower than that from Ph90H. Similar results were previously described by *(Carrozzinol and Khaledi, 2004)*, who reported an interaction between metoprolol and lipid bilayers of liposomes. In case of DSPC/DMPC liposomes, the release rate of metoprolol was faster than in case of DSPC and Ph90H liposomes. This might be due to the separation of DSPC and DMPC layers at 37 °C. Similar results were obtained by (*Giocondi and Grimellec, 2004)*, who found that the mixture of DSPC and DMPC is separated at 32°C. Although DMPC has short acyl chain and low Tc (23 °C), the release of metoprolol was slow and constant up to 672 hours. This might due to the very strong interaction between metoprolol and DMPC MLV. These results are in accordance with *Krill et al., 1998*, who reported that metoprolol exhibits a high degree of affinity to DMPC.

IV.3.1.1.3. In vitro release of atenolol from MLV

The results from the study on in vitro release of atenolol from MLV prepared from different lipids (DSPC, DSPC/DMPC (1:1), DMPC or Ph90H) are exhibited by plotting the percentage cumulative amount released of atenolol versus time (Figure 50). From these results, it was found that the release rate of atenolol from DMPC liposomes is characterized by a sharp initial burst

release during the first 4 hours followed by a plateau up to 504 hours. This may be attributed to the fact that (1) atenolol is a hydrophilic drug; (2) DMPC has a short acyl chain and low Tc (23 °C), (3) a significant portion of the atenolol which is located on and near the surface of DMPC is released at first. After 4 hours the release rate of atenolol from DMPC was very low (plateau). This might be possibly related to an interaction between atenolol and DMPC. *De Sousa et al., 2005* reported that the initial burst of atenolol from atenolol-containing nanoparticles is attributed to the immediate dissolution and release of that portion of the drug located on and near the surface of the particles. The initial release was followed by a rather constant rate over the subsequent hours. This fact is possibly related to an interaction between the drug and the excipient by hydrogen bonding between the functional amine, amide and hydroxyl groups of atenolol and the hydroxyl groups of the excipient. Regarding the release rate of atenolol from the formulations containing Ph90H and DSPC, it is concluded that the release rate of atenolol from formulation containing Ph90H is higher than the release rate from the formulation containing DSPC. This can be attributed to the fact that the interaction of atenolol with DSPC is stronger than with Ph90H. These results were previously reported by *(Carrozzinol and Khaledi, 2004)*, who found significant interactions between atenolol and the lipid bilayers of liposomes. The release rate from formulations containing DSPC/DMPC (1:1) was higher than that containing Ph90H or DSPC. This might be due to the immiscibility of this mixture in the solid state or the nonideal miscibility of DSPC and DMPC or the formation of fractures in the bilayer leading to an enhancement of atenolol release (*Nicolussi, et al., 1982*).

IV.3.1.1.4. In vitro release of pindolol from MLV

The release profiles of pindolol from MLV formulations prepared from different lipids (e.g. DSPC, DSPC/DMPC (1:1), or Ph90H) are exhibited in

Figure 51. The release of pindolol from the formulation made from DMPC was slower than from the other formulations prepared from DSPC, DSPC/DMPC (1:1), or Ph90H. This may be due to the interaction between pindolol and DMPC. As seen in Figure 51, the overall release of pindolol compared to the other β-adrenoceptor antagonists from all formulations was high. This could be related to the nature of the indole group (heterocyclic ring) as an aromatic substituent. The utilization of heterocyclic rings might have an advantage to increase the hydrophilicity of β-adrenoceptor antagonists. This result is somewhat expected based on the findings of *Tashiro et al., 2001*, who reported that pindolol exhibited a higher absorption through the lipid skin barriers than other β-adrenoceptor antagonists.

IV.3.1.2. In vitro release of β-adrenoceptor antagonists from LUV

IV.3.1.2.1. In vitro release of propranolol from LUV

From the release pattern of propranolol from LUV formulations prepared from different lipids (e.g. DSPC, DMPC, DSPC/DMPC (1:1) or Ph90H) (Figure 52), it was found that the release rate of propranolol was slower in case of the formulation made from DMPC than the formulations made from DSPC, DSPC/DMPC (1:1) or Ph90H. This might due to the interaction and sorption of propranolol with DMPC vesicles at pH 7.4 at 37 °C. These results are in accordance with those found by *Cocquyt et al., 2007*, who reported that the propranolol was sorbed in DMPC. The release of propranolol from formulations containing DSPC and Ph90H (100%) was higher than the release rate from the formulation containing DSPC/DMPC (1:1) (80%) after 6 hours. This might be due to the fact that extrusion of DSPC/DMPC (1:1) MLV to form LUV at 63 ° C forms a miscible mixture of both lipids. So the release of propranolol was retarded as compared to the other formulations. But still due to the immiscibility of the excipients, the

release of propranolol is higher than the release from the formulation containing only DMPC. These results are in agreement with *Matubayasit et al., 1986*, who reported that unilamellar vesicles were used and miscibility in binary systems between dimyristoyl-, and distearoyl-phosphatidylcholines was evaluated using differential scanning microcalorimetry and optical absorbance methods. It was found that dimyristoyl- and distearoyl-phosphatidylcholines, where the difference in the lipid chain-length is four carbon atoms, mixed well even at pretransition temperature.

IV.3.1.2.2. In vitro release of metoprolol from LUV

Figure 53 depicts the release profiles of metoprolol from LUV formulations prepared from different lipids (DSPC, DMPC, DSPC/DMPC (1:1) or Ph90H). As shown in Figure 51, it was found that the release of metoprolol from formulation made from DMPC was slower than the formulations made from other lipids. This might be due to the higher interaction of metoprolol with DMPC vesicles at pH 7.4 at 37 °C. This strong interaction between metoprolol and DMPC could be due to the number of extrusions performed (11 times) at higher temperature (at 63 °C) and thus the intimate mixing of the components. The release of metoprolol from the formulation made from DSPC/DMPC (1:1) is slower than the formulations made from either DSPC or Ph90H. This may be attributed to the interaction of metoprolol and DMPC. These results are in accordance with *Katz et al., 2006*, who reported that metoprolol shows a high interaction with DMPC.

IV.3.1.2.3. In vitro release of atenolol from LUV

Figure 54 show the release pattern of atenolol from LUV formulations prepared from different lipids (DSPC, DMPC, DSPC/DMPC (1:1) or Ph90H). From the data, it becomes obvious that the formulation made from DMPC exhibits the lowest release of atenolol among the formulations made

from DSPC, DSPC/DMPC (1:1) or Ph90H. This could be attributed to the interaction between atenolol and DMPC. These results are similar to those of *Betageri and Parsons, 1992*, who reported that the release rate of atenolol from DMPC liposomes was slower than that from DSPC liposomes. The release rate of atenolol in case of the formulation made from Ph90H was higher than that from the formulation made from DSPC, which might be due to the fact that the interaction of atenolol with Ph90H is lower than the interaction of atenolol with DSPC. In case of DSPC/DMPC (1:1), the release rate of atenolol was slower than that of Ph90H and DSPC. This might be attributed to the interaction between atenolol and DMPC (*Betageri and Parsons, 1992*).

IV.3.1.2.4. In vitro release of pindolol from LUV

Release profiles of pindolol were obtained from LUV formulations prepared from different lipids (DSPC, DMPC, DSPC/DMPC (1:1), Ph90H) (Figure 55). It was found that 100% of pindolol release was obtained from DSPC, Ph90H, DSPC/DMPC (1:1) and DMPC LUV after 4 hours. This can be related to the nature of indole group (heterocyclic ring) as an aromatic substituent (see discussion section IV.3.1.1.4, page 137-138).

IV.3.1.3. In vitro release of β-adrenoceptor antagonists from SUV

IV.3.1.3.1. In vitro release of propranolol from SUV

The in vitro release of propranolol from SUV prepared from different lipids (DSPC, DMPC, DSPC/DMPC (1:1) or Ph90H) is exhibited in Figure 56. It was found that the lowest cumulative percentage of propranolol was released from the formulation made from DMPC lipid. This might due to the sorption of propranolol in DMPC lipid as explained before in section section IV.3.1.1.1, page 134-135.

IV.3.1.3.2. In vitro release of metoprolol from SUV

From the release profiles of metoprolol SUV liposomes prepared from different lipids (DSPC, DMPC, DSPC/DMPC (1:1) or Ph90H (Figure 57), it is concluded that the slowest metoprolol release was exhibited from DMPC vesicles. This release kinetics might due to the higher interaction of metoprolol with DMPC vesicles at pH 7.4 at 37 °C as explained before in section section IV.3.1.1.2, page 136.

IV.3.1.3.3. In vitro release of atenolol from SUV

From Figure 58, which shows the in vitro release data of atenolol SUV liposomes prepared from different lipids (DSPC, DMPC, DSPC/DMPC (1:1) or Ph90H), it is concluded that atenolol exhibits the slowest release from DMPC SUV among DSPC/DMPC (1:1) SUV, Ph90H, and DSPC. The delayed release of atenolol from DMPC might due to the higher interaction of atenolol with DMPC vesicles in pH 7.4 buffer at 37 °C. These results are similar with that of *Zhao and Feng, 2004* who reported that paclitaxel interacts more readily with the lipids of shorter chain length, which is DMPC. In case of DSPC/DMPC, the release rate of atenolol was faster than from other liposomes. This might be due to higher diffusion of atenolol from DSPC/DMPC mixture (*Nicolussi, et al., 1982)*. The release rate from Ph90H was slightly higher than that from DSPC due to difference in acyl chain length and Tc.

IV.3.1.3.4. In vitro release of pindolol from SUV

It is concluded from the release rate of pindolol from SUV liposomes prepared from different lipids (e.g. DSPC, DMPC, DSPC/DMPC (1:1) or Ph90H), as shown in Figure 59, that the release of pindolol was 100 % from all preparations after 4 hours.

This could be related to the nature of the indole group (heterocyclic ring) as an aromatic substituent. For explanation see discussion section IV.3.1.1.4, page 137-138.

IV.3.2. In vitro release of β-adrenoceptor antagonists from liposomes using a dispersion method

In comparison of the dialysis and dispersion methods for measurement of in vitro release of β-adrenoceptor antagonists from MLV liposomes (Figures 60, 61, 62 and 63), it was found that the release rate of the incorporated β-adrenoceptor antagonists was consistently higher when using the dispersion method as compared to the dialysis method. This might be due to (1) differences in the hydrodynamics of the system when comparing the liposomal formulation within the dialysisto the formulation dispersed within a flask. These differences relate to variations in the shear-effect exerted upon the formulation; (2) the density of the liposomal vesicles in their aqueous dissolution medium is higher in the dialysis method when compared to the dispersion method. Given that the probability of vesicle to vesicle contacts will increase with higher density, it may be postulated that the surface area of the vesicles available for contact with the dissolution medium should be higher in case of the dispersion method. Consequently, under sink conditions, this mechanism should explain the higher release rate of the drug under the conditions of the dispersion method; (3) the membrane permeability of the dialysis membrane. These results are in agreement with those reported by *Saarinen-Savolainen, et al., 1997*, who stated that, the drug release from the dialysisis affected by the stirring inside the bag as well as the membrane permeability.

IV.4. In vitro release of glucose from liposomes using a dispersion method

IV.4.1. In vitro release of glucose from MLV

Figure 64 depicts the in vitro release of glucose (as described under materials and methods, section II.2.3.2, page 67) from MLV prepared from different lipids (e.g. DSPC, DSPC/DMPC (1:1), DMPC, Ph90H or Syb). As seen in Figure 64, glucose release from liposomes made from DSPC and Ph90H shows an initial burst effect followed by a slower release phase. The initial fast rate of release is commonly ascribed to glucose detachment from liposomal surface while the latter slow release results from sustained glucose release from the inner lamellae. This slow release can be attributed to the interaction between glucose and phospholipid through hydrogen bonding. Similar results were obtained by *Nounou, et al., 2006*, who found that release of 5-fluorouracil, a water-soluble drug, shows fast release followed by slow release. Concerning liposomes made from DMPC, DSPC/DMPC (1:1) or Syb, the release of glucose was faster than from other liposmes (DSPC and Ph90H). This may be attributed to the alkyl hydrocarbon chain length: as the hydrocarbon chain length is increased, van der Waals interactions between the lipid chains become stronger requiring more energy to disrupt the ordered packing, and the drug release decreases (*Mohammed, et al., 2004*).

IV.4.2. In vitro release of glucose from LUV and SUV

From the in vitro release profiles of glucose from LUV and SUV liposomes (Figures 65 and 66 respectively) prepared from different lipids (e.g. DSPC, DSPC/DMPC (1:1), DMPC, Syb or Ph90H), it was concluded that DMPC liposomes show faster release than liposomes prepared from other lipids. This can be attributed to the fact that DMPC has the lowest hydrocarbon chain length compared to the other lipids (*Mohammed, et al., 2004*).

IV.5. In vitro release of FDG from liposomes using a dispersion method

IV.5.1. In vitro release of FDG from MLV

The in vitro release of FDG from MLV, prepared from different lipids (e.g. DSPC, DSPC/DMPC (1:1), DMPC, Syb or Ph90H) (Figure 67), was increased in the following order Ph90H < DSPC < Syb < DSPC/DMPC (1:1) < DMPC. This behaviour may be explained by the fact that DMPC has the lowest alkyl chain and transition temperature (C14, Tc = 23°C) among the lipids. These results are similar to those found by *Anderson and Omri, 2004*, who stated that the DSPC liposomes that have the highest phase Tc among the three lipids tested, is more stable and has greater drug retention than DPPC (Tc = 41.5◦C) and DMPC (Tc = 23◦C).

IV.5.2. In vitro release of FDG from LUV and SUV

The in vitro release patterns of FDG from LUV and SUV prepared from Ph90H into isotonic saline solution, pH 7.4 at 37 ± 0.5 °C using the dispersion method were showed in Figures 68 and 69 respectively. It was found that 100 % of FDG was released from both LUV and SUV liposomes after 120 minutes. But LUV exhibits slower release of FDG than SUV liposomes.

IV.6. Effect of the lipophilicity on the in vitro release of β-adrenoceptor antagonists from liposomes

The effect of lipophilicity on the release pattern from MLV, LUV and SUV liposomes prepared from PH90H was represented in Figures 70, 71 and 72 respectively. In case of MLV liposomes it was found that pindolol shows the highest release followed by atenolol, metoprolol and propranolol. This could be related to the nature of the indole group (heterocyclic ring) as an aromatic substituent. For explanation see discussion IV.3.11.4, page 123. It was stated

that propranolol is more lipophilic than metoprolol, atenolol and pindolol (*Landray et al., 2002*). This high lipophilicity enhances the residence of propranolol and metoprolol in liposomes compared to atenolol and pindolol, which are less lipophilic. The same results were obtained by *Shigenori, et al. 1998*, who found that the accumulated amount in the intact skin was the greatest for propranolol, which has the largest lipophilicity among the other tested β-blockers.

Regarding the differences between LUV and SUV liposomes it was found that metoprolol exhibits the highest release followed by pindolol, atenolol and propranolol. This could be attributed to the fact that metoprolol has the least partitioning into LUV and SUV as compared to the other β-adrenoceptor antagonists. This is in accordance with *Liu, et al., 2001*, who reported that the partitioning of propranolol, atenolol and pindolol into small and large unilamelar liposomes was higher than metoprolol.

IV.7. Effect of liposomal structure on the in vitro release of drugs

IV.7.1. Effect of liposomal structure on the in vitro release of β-adrenoceptor antagonists from liposomes using a dialysis method

Regarding the release of β-adrenoceptor antagonists from different types of liposomal dispersions using the dialysis method (Figure 73), it was concluded that their release was increased from MLV to LUV to SUV. This behaviour could be a consequence of a decreasing surface area to volume ratio from SUV to LUV to MLV. Moreover, SUV possess only a single bilayer, which could have been altered more easily than those of multilamellar vesicles. These results are in agreement with a report by *Manconi, et al., 2002*, who found that tretinoin delivery efficiency always improved from MLV to LUV to SUV. Also this difference in drug release

may be due to the higher bilayer curvature of SUV, as compared to LUV and MLV. This is in accordance with *Moreira, et al., 1996*, who reported hat LUV present significantly lower membrane permeability than SUV and this difference may be due to the higher bilayer curvature of SUV, as compared to LUV, which make SUV thermodynamically less stable than LUV.

IV.7.2. Effect of liposomal structure on in the vitro release of glucose using a dispersion method

Glucose release profiles from different liposomal structures (e.g. MLV, LUV and SUV) are presented in Figure 74. As expected, liposome formulations gave rise to fast and prolonged glucose release. Different glucose release profiles were observed, depending on the vesicle characteristics. In particular, MLV vesicles showed the slowest glucose release with respect to the other liposomal formulations at all the examined times. This could be due to the presences of several lamellae, which retained the glucose. On the contrary, the fastest glucose release was observed from SUV liposomes. This may be attributed to their smaller size. An intermediate behaviour was observed for LUV. Such a result can be explained by the substantially analogous multilamellar structure of these liposomes. These results are similar to those found by *Faure, et al., 2006*, who reported that glucose release from SUV was faster than from MLV and LUV.

IV.8. Effect of lipid concentration on the in vitro release of β-adrenoceptor antagonists from Ph90H liposomes

Two concentrations of Ph90H (50 and 100mg/mL) were used for preparation of MLV liposomes loaded with propranolol, metoprolol, pindolol or atenolol, and the in vitro release rates of these drugs were compared (as shown in Figures 75, 76, 77 and 78, respectively). From the release profiles, it was found that MLV liposomes made from 100 mg/ml Ph90H show

slower release rate for the tested drugs than MLV liposomes made from 50 mg/ml Ph90H, i.e. the higher concentration of Ph90H, the slower the release of the drug. This could be attributed to the higher viscosity in case of the concentration of Ph90H of 100 mg/ml compared to the lower viscosity at a concentration of Ph90H of 50 mg/ml. This result is consistent with that obtained by *Bhalerao and Harshal, 2003*, who reported that salicylic acid releases rapidly by decreasing concentration of PC. This also may be attributed to the formation of more vesicular lamella when the lipid concentration increases. The same results were observed by *Brandl, et al., 1997*, who reported that the release rate decreases with increasing lipid concentration.

IV.9. Stability of the Er-DTPA liposomes

IV.9.1. Effect of storage temperature on the percentage of residual content of Er-DTPA in SUV

The effect of storage temperature on the stability of Er-DTPA in SUV was studied and is presented in Figures 83, 84 and 85. It was found that the amount retained of Er-DTPA is inversely proportional to the storage temperature. Liberation of Er-DTPA from SUV stored at 37 °C was faster than that stored at lower temperatures of 25 and 4 °C. This may be attributed to the effect of temperature on the gel to liquid transition of lipid bilayers together with possible chemical degradation of the phospholipids, leading to defects in the membrane packing. These results are similar to that reported by *Bhatia, 2004,* who found that tamoxifen released faster from liposomes maintained at 37 °C than from liposomes maintained at room temperature. Also *Fan, et al., 2007* found that Salidroside liposomes showed higher release when the temperature increased.

IV.9.2. Effect of soybean lipid concentration on the percentage of retained amount of Er-DTPA in SUV

The effect of different soybean lipid content (30, 50 and 70 mg/ml) on the stability of Er-DTPA complex in SUV was studied at 25 °C and the percentage of Er-DTPA retained was plotted against time (Figure 86). The overall tendency observed was a decrease in the percentage of the amount of Er-DTPA complex retained with decreasing soybean lipid concentration for lipid concentrations 70, 50 and 30 mg/ml. This can be explained by either the higher viscosity at high lipid concentration or the lower concentration gradient in case of the higher lipid concentration. These results are in accordance with those done by *Brandl, et al., 1997*, who found that the fraction of the marker (calcein) released from liposome of higher lipid concentration was much smaller than from that of lower lipid concentration .

IV.10. In vivo imaging of FDG in rats using PET

IV.10.1. Biodistribution of FDG in both the whole body and the brain of rats

After intraperitoneal injection and microPET scanning of unencapsulated FDG, FDG-containing LUV and FDG-containing MLV (Figures 87, 88 and 89, respectively), FDG is distributed in the whole body especially to the brain, testes, urinary bladder and heart. In comparing the biodistribution of unencapsulated FDG, FDG-containing LUV and FDG-containing MLV, we found that the unencapsulated FDG is distributed rapidly to the brain, testes, heart and urinary bladder followed by biodistribution of FDG from FDG-containing LUV and FDG-containing MLV, which shows sustained release of FDG.

Figures 90 and 92 show the scanning of distribution of FDG from unencapsulated FDG and FDG-containing MLV at time intervals 30, 60, 90 and 120 minutes. Figure 91 depicts the scanning of distribution of FDG from FDG-containing LUV at time intervals 30, 60 and 90 minutes. It is evident that the distribution of FDG into the brain was higher in case of unencapsulated FDG (fast distribution) than in case of both FDG-containing LUV (moderate distribution) and FDG-containing MLV (sustained distribution). This sustained release of FDG from MLV can be explained by the substantially analogous multilamellar structure of these liposomes. But the moderate FDG release obtained from LUV liposomes is attributable to their unilamellar structure. Similar results were reported by *Maestrelli, et al., 2006*, using ketoprofen, which exhibited faster release from SUV liposomes than from MLV.

V. Conclusions

- The entrapment efficiency (EE) of β-adrenoceptor antagonists, glucose and Er-DTPA in the prepared liposomes varies depending on the lipid used.
- The apparent average particle size and particle size distribution of the prepared liposomes using dynamic light scattering and laser diffraction analyzer differ from one formulation to another depending on the type of lipid used and type of liposomes.
- The release of β-adrenoceptor antagonists from the dispersion method was higher than from the dialysis method.
- The in vitro release of β-adrenoceptor antagonists and glucose was improved from MLV to LUV to SUV.
- The percentage of Er-DPTA retained in all formulations is temperature dependent, whereby formulations maintained at 4 °C showed higher percentage of the amount of Er-DPTA retained than the other formulation maintained at 25 and 37 °C. The amount of Er-DPTA retained also depends on the concentration of soybean lipid. Whereas formulations containing 70 mg/ml of soybean lipid exhibited higher amount retained of Er-DPTA than other formulations (30 and 50 mg/ml).
- The in vitro release of FDG (through measuring the activity of FDG) from the liposomes prepared differs from one lipid to another.
- The in vivo distribution of FDG to the whole body especially to the brain is very fast from unencapsulated FDG, moderate from FDG-containing LUV and sustained from FDG-containing MLV.
- In vitro-In vivo correlation was studied using the in vitro release data of FDG from liposomes and in vivo absorption data of FDG from injected liposomes using PET.

VII. References

Anderson M. and Omri A. (2004). The effect of different lipid component on the in vitro stability and release kinetics of liposome formulations. *Drug Delivery*, 11: 33-39.

Baldeschwieler J., Schmidt P, 1997. Liposomal drugs: From setbacks to success. *Chemtech*, 27(10): 34-42.

Bangham, A. D., Standish, M. M. and Watkins, J. C. (1965). Diffusion of univalent ions across the swollen phospholipids. *J. Mol. Biol*, 13: 238-252.

Bertz J., Giersiepen K., Haberland J., Hentschel S., Kaatsch P., Katalinic A., Stabenow R., Stegmaier C., Ziegler H (2006). *Krebs in deutschland häufigkeiten und trends*. Gesellschaft der epidemiologischen Krebsregister in Deutschland e.V. (GEKID) in Zusammenarbeit mit dem Robert Koch-Institut (RKI).

Betageri G.V. and Parsons D.L. (1992). Drug encapsulation and release from multilamellar and unilamellar liposomes. *Int. J. Pharm.,* 81: 235-241.

Beyer GJ, Miederer M, Vranjes-Duric S, Comor JJ, Kunzi G, Hartley O, Senekowitsch-Schmidtke R, Soloviev D, Buchegger F (2004). Targeted alpha therapy in vivo: direct evidence for single cancer cell kill using 149Tb-rituximab. *Eur. J. Nucl. Med. Mol. Imaging,* 3: 547-54.

Bhalerao S.S. and Harshal R.A. (**2003**). Preparation, optimization, characterization, and stability studies of salicylic acid liposomes. *Drug Dev. Ind. Pharm.*, 29(4): 451–467.

Bhatia A. (**2004**). Tamoxifen in topical liposomes: development, characterization and in-vitro evaluation. *J. Pharm. Pharmaceut. Sci.,* 7(2):252-259).

Brandl M., Tardi C., Drechsler M., Bachmann D., Reszka R., Bauer K.H., Schubert R. (**1997**). Three-dimensional liposome networks: freeze fracture electron microscopical evaluation of their structure and in vitro analysis of release of hydrophilic markers. *Adv. Drug Delivery Rev.,* 24(2-3): 161-164.

Byung-Nak A., Shin-Keum K., Chang-Koo S. (**1995**). Proliposomes as an intranasal dosage form for the sustained delivery of propranolol. *J. Controlled Release*, 34: 203-210.

Cancer Research UK (2007). UK cancer incidence statistics by age. Retrieved on 2007-06-25. http://en.wikipedia.org/wiki/Cancer

Cardot J-M. , Beyssac E., and Alric M. (2007). In vitro–in vivo correlation importance of dissolution in IVIVC. *Dissolution Technologies*, 14(1): 15-19.

Carrozzino1 J.M. and Khaledi M.G. (2004). Interaction of basic drugs with lipid bilayers using liposome electrokinetic. *Chromatography Pharmaceutical Research,* 21(12): 2327-2335.

Chu B. (1991). Laser light scattering: Basic principles and practice. Academic press, Boston.

Cocquyt J., Saveyn P., Van der Meeren P., and De Cuyper M. (2007). Evaluation of the interaction of propranolol with 1, 2-Dimyristoyl-*sn*-glycero-3-phosphocholine (DMPC) liposomes: The partitioning model. *Langmuir*, 23: 1959-1964.

Daniels R. Galenic Principles of Modern Skin Care Products', Issue 25, Skin Care Forum. (http://www.scf-online.com/english/25_e/galenic_25_e.htm)

De Sousa A. and de Sousa E.M.B. (2005). Ordered mesoporous silica carrier system applied in nanobiothecnology. *Braz. Arch. Biol. Technol.,* 48: 243-250.

Dhe-Paganon S., Magrath J., and Abeles R.H. (1994). Mechanism of mevalonate pyrophosphate decarboxylase: Evidence for a carbocationic transition state. *Biochemistry***,** 33: 13355- 13362.

Duncan R. and Thanou M. (2003). Polymer-protein and polymer-drug conjugates in cancer therapy. *Curr. Opin. Investig. Drugs*, 4(6):701-709.

Emami J. (2006). In vitro - In vivo correlation: From theory to applications. *J. Pharm. Pharmaceut. Sci.* 9 (2): 31-51.

Fan M., Xu S., Xia S., Zhang X. (2007). Effect of different preparation methods on physicochemical properties of salidroside liposomes. *J. Agric. Food Chem.*, 55: 3089-3095.

Faure C., Nallet F., Roux D., Milner S., Gauffre F., Olea D. and Lambert O. (2006). Modeling leakage kinetics from multilamellar vesicles for membrane permeability determination: Application to glucose. *Biophys. J.*, 91: 4340–4349.

Ferlay J., Autier P., Boniol M., Heanue M., Colombet M., and Boyle P. (2007). Estimates of the cancer incidence and mortality in Europe in 2006. *Ann. Oncol.,* 18(3):581-592.

Garg M., Dutta T., Jain N. (2007). Stability Study of Stavudine-Loaded O-Palmitoyl-Anchored Carbohydrate-Coated Liposomes. *AAPS PharmSciTech*. 8(2): article 38 (E_1-E_8).

Gelperina S., Kisich K., Iseman M. D., and Heifets L. (2005). The Potential Advantages of Nanoparticle Drug Delivery Systems in Chemotherapy of Tuberculosis. *American journal of respiratory and critical care medicine*, 172: 1487-1490.

Gillespie W.R. (1997). Convolution-based approaches for in vitro-in vivo correlation modelling in: Young D, DeVane J, Butler J, eds. In vitro-In vivo correlations. New York, NY: Plenum Press, 423:53-65.

Giocondi C. M. and Grimellec C. (2004). Temperature Dependence of the Surface Topography in Dimyristoylphosphatidylcholine/ Distearoylphosphatidylcholine Multibilayers. *Biophys. J.,* 86: 2218–2230.

Gorman S., Brown P. (2003). *The Drug Delivery Companies Report*, Spring/Summer: 31-34.

Guidance for industry (1997). extended release oral dosage forms: development, evaluation and application of an in vitro/in vivo correlation. FDA, CDER.

Gulati M., Grover M., Singh S. and Singh M. (1998). Lipophilic drug derivatives in liposomes. *Int. J. Pharm*., 165:129–168.

Hope M.J., Bally M.B., Webb G. and Cullis P.R. (**1985).** Production of large unilamellar vesicles by a rapid extrusion procedure. Characterization of size distribution, trapped volume and ability to maintain a membrane potential. *Biochim. Biophys. Acta*, 812: 55-65.

Hsieh Y., Chen L., Wang Y., Chang J., and Chang H. (2002). Properties of liposomes prepared with various lipids. *J. Food Sci.*, 67(8): 2808-2813.

Katz M., Ben-Shlush I., Kolusheva S. and Jelinek R.(2006). Rapid colorimetric screening of drug interaction and penetration through lipid barriers. *Pharm. Res*., 23(3): 580-588.

Kawano K., Takayama K., Nagai T., et al. (2003). Preparation and pharmacokinetics of pirarubicin loaded dehydration–rehydration vesicles. *Int. J. Pharm*., 252 (1-2): 73-79.

Khelfallah N., Gunari N., Fischer K., Gkogkas G., Hadjichristidis N., Schmidt M. (2005). Micelles Formed by Cylindrical Brush-Coil Block Copolymersa. *Macromol. Rapid Commun.*, 26: 1693–1697.

Knight C. G. (1981). In "Research monographs in cell and tissue physiology" (Dingle J. T., Gordon J. L.), Vol. 7, Elsevier/ North-Holland Biomedical Press, Amsterdam, New York and Oxford.

Krill S.L., Lau K.Y., Plachy W.Z., and Rehfeld S.J. (1998). Penetration of dimyristoylphosphatidylcholine monolayers and bilayers by model *β*-Blocker agents of varying lipophilicity. *J. Pharm. Sci.*, 87(6): 751-755.

Landray M. J., Toescu V. and Kendall M. J. (2002). The cardioprotective role of β-blockers in patients with diabetes mellitus. *J. Clin. Pharm. Ther.,* 27: 233–242.

Lasic, D.D. and Templeton, N.S. (1996). Liposomes in gene therapy. *Adv. Drug Deliv. Rev.,* 20: 221–266.

Lee H.Y., Jee H.W., Seo S.M., Kwak B.K., Khang G., Cho S.H. (2006). Diethylenetriaminepentaacetic acid-gadolinium (DTPA-Gd)-conjugated polysuccinimide derivatives as magnetic resonance imaging contrast agents. *Bioconjug. Chem.*, 17(3):700-6.

Liu X., Yanga Q., Kamo N., Miyake J. (2001). Effect of liposome type and membrane fluidity on drug–membrane partitioning analyzed by immobilized liposome chromatography. *J. Chromatogr. A*, 913: 123–131.

MacDonald R.C., MacDonald R.I., Menco B.Ph. M., Takeshita K., Subbarao N.K. and Hu lan-rong (**1991**)**.** Small volume extrusion apparatus for preparation of large unilamellar vesicles*, Biochim. Biophys. Acta,* 1061: 297-303.

Maestrelli F., Gonz´alez-Rodr´ıguez M. L.B., Rabasco A.M., Muraa P. (2006). Effect of preparation technique on the properties of liposomes encapsulating ketoprofen–cyclodextrin complexes aimed for transdermal delivery. *Int. J. Pharm*., 312: 53–60.

Mahato, R.I., Rolland, A. and Tomlinson, E. (1997). Delivery systems: Pharmaceutical perspectives. *Pharm. Res.,* 14: 853–859.

Manconi M., Sinico C., Valenti D., Loy G., Fadda A.M. (**2002**). Niosomes as carriers for tretinoin. I. Preparation and properties. *Int. J. Pharm.,* 234: 237–248.

Matubayasit N., Shigematsu T., Leharat T., Kamaya H., and Ueda I. (1986). Miscibility of phosphatidylcholine binary mixtures in unilamellar vesicles. *J. Membr. Biol*., 90: 37-42.

Mohammed A.R., Weston N., Coombes A.G.A., Fitzgerald M., Perri Y. (2004). Liposome formulation of poorly water soluble drugs: optimisation of drug loading and SEM analysis of stability. *Int. J. Pharm.*, 285: 23–34.

Moreira J. N., L. M. Almeida, C. F. Geraldes, M. L. Costa (1996). Evaluation of in vitro stability of large unilamellar liposomes coated with a modified polysaccharide (O-palmitoylpullulan). *J. Mater. Sci. - Mater. Med.,* 7: 301-303.

Nawroth T., Buch P., Glube N., Peters T., Shazly G., Langguth P., Pairet B., Decker H., Schmidberger H., Alexiou C. , Le Duc G., Bravin A., May R.P. (2007). Nanoparticles for Indirect Radiation Therapy of Cancer IRT. *DPhG Deutsche Pharmazeutische Gesellschaft Erlangen*, 10.-12. 10. 2007.

Nicolussi A., Massari S., and Colonna R. (1982). Effect of Lipid Mixing on the Permeability and Fusion of Saturated Lecithin Membrane. *Biochemistry,* 21: 2134-2140.

Nounou M., El-Khordagui L., Khalafallah N. (2006). In vitro release of hydrophilic and hydrophobic drugs from liposomal dispersions and gels. *Acta Pharm.*, 56: 311–324.

Patty P.J. and Frisken B.J. (2003). The Pressure-Dependence of the size of extruded vesicles. *Biophys. J.,* 85: 996–1004.

Pitcher W.H. III and Huestis W.H. (**2002**). Preparation and analysis of small unilamellar phospholipids vesicles of a uniform size. *Bioch. Biophy. Res. Comm.,* 296: 1352–1355.

Pons M., Foradada M. and Estelrich J. (1993). Liposomes obtained by the ethanol injection method. *Int. J. Pharm.,* 95(1-3): 51-56.

Port R., Schuster C., Port C. and Bachert P. (**2006).** Simultaneous sustained release of fludarabine monophosphate and Gd-DTPA from an interstitial liposome depot in rats: potential for indirect monitoring of drug release by magnetic resonance imaging. *Canc. Chemoth. Pharmaco.*, 58 (5): 607-617.

Prescott F., Nimmo S. (1989). Novel drug delivery and its therapeutic application, John Wiley & Sons Ltd., Chichester & New York.

Prestidge C. A., Barnes T., Simovic S. (2004). Polymer and particle adsorption at the PDMS droplet-water interface. *Adv. Coll. Interface Sci*., 108-109: 105-118.

Quon A. and Gambhir S.S. (2005). FDG-PET and beyond: Molecular breast cancer imaging. *J. Clin. Oncol.*, 23(8): 1664-1673.

Roberts J. R., Xiao J., Schliesman B., Parsons D. J., and Shaw C. F., (1996). Kinetics and mechanism of the reaction between serum albumin and auranofin (and its isopropyl analogue) in vitro. *Inorg. Chem.,* 35: 424-433.

Saarinen-Savolainen P., Järvinen T., Taipale H., and Urtti A. (1997). Method for evaluating drug release from liposomes in sink conditions. *Int. J. Pharm.,* 159: 27–33.

Shigenori Y., Kazuki N., Yuji K., Toshikiro K. (1998). Factors determining drug residence in skin during transdermal absorption: Studies on β-blocking agents. *Biol. Pharm. Bull.*, 16(1): 1195-1201.

Storm G. and Crommelin J.A. (1998). Liposomes. *Pharm. Sci. Techno. Today*, 1(1):19-31.

Szoka F.J. (1996). Preparation of liposomes and lipid complex compositions. United States Patent, patent number 5: 567,434.

Tashiro Y., Sami M, Shichibe S., Kato Y., Hayakawa E., and Itoh K. (2001). Effect of lipophilicity on in vivo iontophoretic delivery. II. b-Blockers. *Biol. Pharm. Bull.,* 24(6): 671—677.

Ubrich N., Bouillot P., Pellerin C., Hoffman M., Maincent P. (2004). Preparation and characterization of propranolol hydrochloride nanoparticles: a comparative study *J. Controlled Release,* 97: 291–300.

United States Pharmacopoeia (2008). In vitro and in vivo evaluations of dosage forms, 27th edition, Revision, Mack Publishing Co., Easton, PA.

Vermehren C., Jørgensen K., Frokjaer S. (1999). Influence of lipopolymer concentration on liposome degradation and blood clearance. *Int. J. Pharm.*, 183: 13–16.

Vingerhoeds, M.H., Storm, G. and Crommelin, D.J.A (1994). Immunoliposomes in vivo. *Immunomethods*, 4: 259-272.

Yoshiyuki H., Hidetoshi A., Yuji M., Fumitoshi H., and Kaneto U. (2006). Preparation and pharmaceutical evaluation of liposomes entrapping salicylic acid γ-cyclodextrin conjugate. *Chem. Pharm. Bull*. 54(1): 26-32.

Zhao L. and Feng S. (**2004**). Effects of lipid chain length on molecular interactions between paclitaxel and phospholipid within model biomembranes. *J. Colloid Interface Sci.,* 274: 55–68.

VI. Summary

Liposomes were discovered about 40 years ago by *A. Bangham* and since then they became very versatile tools in biology, biochemistry and medicine. Liposomes are the smallest artificial vesicles of spherical shape that can be produced from natural untoxic phospholipids and cholesterol. Liposome vesicles can be used as drug carriers and become loaded with a great variety of molecules, such as small drug molecules, proteins, nucleotides and even plasmids. Due to the variability of liposomal compositions they can be used for a large number of applications.

In this thesis the β-adrenoceptor antagonists propranolol, metoprolol, atenolol and pindolol, glucose, ^{18}F-Fluorodeoxyglucose (FDG) and Er-DTPA were used for encapsulation in liposomes, characterization and in vitro release studies. Multilamellar vesicles (MLV), large unilamellar vesicles (LUV) and smaller unilamellar vesicles (SUV) were prepared using one of the following lipids: 1,2-Dimyristoyl-*sn*-Glycero-3-Phosphocholine (DMPC), 1,2-Distearoyl-*sn*-Glycero-3-Phosphocholine (DSPC), Phospholipone 90H (Ph90H) or a mixture of DSPC and DMPC (1:1). The freeze thawing method was used for preparation of liposomes because it has three advantages (1) avoiding the use of chloroform, which is used in other methods and causes toxicity (2) it is a simple method and (3) it gives high entrapping efficiency.

The percentage of entrapping efficiencies (EE) was different depending on the type and phase transition temperature (Tc) of the lipid used. The average particle size and particle size distribution of the prepared liposomes were determined using both dynamic light scattering (DLS) and laser diffraction analyzer (LDA).

The average particle size of the prepared liposomes differs according to both liposomal type and lipid type. Dispersion and dialysis techniques were used for the study of the in vitro release of β-adrenoceptor antagonists. The in vitro release rate of β-adrenoceptor antagonists was increased from MLV to LUV to SUV.

Regarding the lipid type, β-adrenoceptor antagonists exhibited different in vitro release pattern from one lipid to another.

Two different concentrations (50 and 100mg/ml) of Ph90H were used for studying the effect of lipid concentration on the in vitro release of β-adrenoceptor antagonists. It was found that liposomes made from 50 mg/ml Ph90H exhibited higher release rates than liposomes made at 100 mg/ml Ph90H.

Also glucose was encapsulated in MLV, LUV and SUV using 1,2-Dimyristoyl-*sn*-Glycero-3-Phosphocholine (DMPC), 1,2-Distearoyl-*sn*-Glycero-3-Phosphocholine (DSPC), Phospholipone 90H (Ph90H), soybean lipid (Syb) or a mixture of DSPC and DMPC (1:1). The average particle size and size distribution were determined using laser diffraction analysis. It was found that both EE and average particle size differ depending on both lipid and liposomal types. The in vitro release of glucose from different types of liposomes was performed using a dispersion method. It was found that the in vitro release of glucose from different liposomes is dependent on the lipid type.

^{18}F-FDG was encapsulated in MLV 1,2-Dimyristoyl-*sn*-Glycero-3-Phosphocholine (DMPC), 1,2-Distearoyl-*sn*-Glycero-3-Phosphocholine (DSPC), Phospholipone 90H (Ph90H), soybean lipid (Syb) or a mixture of DSPC and DMPC (1:1). FDG-containing LUV and SUV were prepared using Ph90H lipid. The in vitro release of FDG from the different types of lipids was accomplished using a dispersion method. Results similar to that of glucose release were obtained.

In vivo imaging of FDG in both uncapsulated FDG and FDG-containing MLV was performed in the brain and the whole body of rats using PET scanner. It was found that the release of FDG from FDG-containing MLV was sustained. In vitro-In vivo correlation was studied using the in vitro release data of FDG from liposomes and in vivo absorption data of FDG from injected liposomes using microPET.

Erbium, which is a lanthanide metal, was used as a chelate with DTPA for encapsulation in SUV liposomes for the indirect radiation therapy of cancer. The liposomes were prepared using three different concentrations of soybean lipid (30, 50 and 70 mg/ml). The stability of Er-DTPA SUV liposomes was carried out by storage of the prepared liposomes at three different temperatures (4, 25 and 37 °C). It was found that the release of Er-DTPA complex is temperature dependent, the higher the temperature, the higher the release. There was an inverse relationship between the release of the Er-DTPA complex and the concentration of lipid.

VI. Zusammenfassung

Liposomen wurden vor ca. 40 Jahren von *A. Bangham* entdeckt und Seitdem werden sie als vielseitige Werkzeuge in der Biologie, Biochemie und Medizin verwendet. Liposomen sind die kleinsten künstlichen Hohlräume von Kugelformen, die sich aus natürlichen Phospholipiden und Cholesterin herstellen lassen. Liposomale Vesikel können als Arzneistoff-Carrier, die mit einer großen Vielzahl von Molekülen, wie zum niedermolekularen Wirkstoffen, Proteinen, Nukleotiden oder Plasmiden beladen sind, eingesetzt werden. Liposomen sind extrem vielseitig und können aufgrund der Variabilität ihrer Zusammensetzung für eine Vielzahl von Anwendungen verwendet werden.

In dieser Arbeit werden die β-Adrenozeptor-Antagonisten Propranolol, Metoprolol, Atenolol und Pindolol, ferner Glucose, ^{18}F-Fluorodeoxyglucose (FDG)- und Er-DTPA in Liposomen eingebracht. Verschiedene Arten von Liposomen z. B. MLV, LUV und SUV wurden durch eine der folgenden Lipide hergestellt: 1,2-Dimyristoyl-sn-glycero-3-Phosphocholine (DMPC), 1,2-Distearoyl-sn-glycero-3-Phosphocholine (DSPC), Phospholipon 90H (Ph90H) oder eine Mischung aus DSPC und DMPC (1:1). Die Einfrier-Auftau-Methode wurde für die Herstellung von Liposomen als Multi-Lamellare-Vesikl (MLV) verwendet, weil sie drei Vorteile hat: (1) Vermeidung der Verwendung von Chloroform, das in anderen Methoden verwendet wird und toxisch ist; (2) Es ist eine einfache Methode und (3) Es ergibt sich allgemin eine hohe Einschluss- Effizienz (EE). Die durchschnittliche Teilchengröße und Teilchengrößenverteilung der vorbereiteten Liposomen wurden mit, der dynamischen Lichtstreuung (DLS) und dem Laser-Beugungs Analyzator (LDA) gemessen.

Die durchschnittliche Partikelgröße der vorbereiteten Liposomen unterscheidet sich in Abhängigkeit von der Art der Liposomen und dem Lipid-Typ. Dispersions- und Dialyse-Techniken wurden für die In-vitro-Freisetzung von β-Adrenozeptor-Antagonisten verwndet. Die In-vitro-Freisetzungs geschwindigkeit von β-Adrenozeptor-Antagonisten wurde von MLV zu LUV zu SUV größer. Ebenfalls konte eindeutlicher Einfluß des Lipid-Typs auf die Freisetzungsgeschwindigkeit von β-Adrenozeptor-Antagonisten festgestellt werden.

Zwei verschiedene Konzentrationen (50 und 100mg/ml) von Ph90H wurden für die Untersuchung des Einflußes der Lipid-Konzentration auf die In-vitro-Freisetzung von β-Adrenozeptor-Antagonisten verwendet.
Es wurde festgestellt, dass Liposomen, die aus 50 mg / ml Ph90H hergestellt wurden, rascher den inkorporierten Wirkstoff freisetzten, als die, die mit 100 mg / ml Ph90H hergestellt wurden.

Glucose wurde ebenfalls MLV, LUV und SUV mit 1,2-Dimyristoyl-sn-glycero-3-Phosphocholine (DMPC), 1,2-Distearoyl-sn-glycero-3-Phosphocholine (DSPC), Phospholipone 90H (Ph90H), Soja-Lipid-(SYB) und einer Mischung aus DSPC und DMPC (1:1) eingekapselt und die entstandenen Produkte bezüglich durchschnittlicher Teilchengröße und Teilchengrößenverteilung charakterisiert. Es wurde festgestellt, dass EE und mittlere Partikelgröße sich in Abhängigkeit von Lipid-und Liposomen-Typ unterscheiden. Die In-vitro-Freisetzung von Glucose aus verschiedenen Arten von Liposomen wurde mit Hilfe der Dispersions-Methode gemessen.

^{18}F-FDG wurde in MLV-Liposomen mit 1,2-Dimyristoyl-sn-glycero-3-Phosphocholine (DMPC), 1,2-Distearoyl-sn-glycero-3-Phosphocholine (DSPC), Phospholipone 90H (Ph90H), Soja-Lipid-(SYB) oder der Mischung aus DSPC und DMPC (1:1) eingekapselt. FDG-haltige LUV und SUV wurden durch die Verwendung von Ph90H Lipiden vorbereitet. Die In-vitro-Freisetzung von FDG aus den verschiedenen Liposomen wurde mit der Dispersions-Methode ausgeführt. Ergebnisse, ähnlich wie die der Freisetzung von Glukose, wurden erhalten. Die In-vivo Freisetzung von FDG aus SUV und MLV wurde vergleich zu einer FDG Lösung in Ratten mittelsPositronen-Emissions-Tomographie (PET) untersucht. Dabei wurde die Anflutung von FDG im Gehirn als Maß der In-vivo Freisetzungsgeschwindigkeit verwendet. Es konnte eine Beziehung zwischen der In-vitro und der In-vivo Freisetzungsgeschwindigkeit festgestellt werden (In-vitro/In-vivo Korrelation).

Erbium, welches ein Lanthanid-Metall ist, sollte als Chelat mit DTPA für die Verkapselung in SUV-Liposomen für die indirekte Strahlungs-Therapie von Krebs hergestellt werden. Die Liposomen wurden unter Verwendung drei unterschiedlicher Konzentrationen von Sojabohnen Lipiden (30, 50 und 70 mg / ml) vorbereitet. Die Stabilität der Er-DTPA SUV-Liposomen wurde durch Lagerung der vorbereiteten Liposomen bei drei verschiedenen Temperaturen (4, 25 und 37 ° C) gemessen. Es wurde festgestellt, dass die Freisetzung von dem Er-DTPA Komplex temperaturabhängig ist, je höher die Temperatur, desto höher ist die Freigabe. Es wurde eine inverse Beziehung zwischen der Freigabe des Er-DTPA Komplexes und der Konzentration von Lipiden festgestellt.

Publications and poster presentations

G Shazly and P. Langguth (2007). Lipid composition and structure affect drug release from liposomes. Annual Conference of German Pharmaceutical Society, 10-13.10.2007, Erlangen.

T. Nawroth, P. Buch, N. Glube, T. Peters, G. Shazly, P. Langguth, B. Pairet, H. Decker, H. Schmidberger, Ch. Alexiou, G. LeDuc, A. Bravins, R. P. May (2007). Nanoparticles for Indirect Radiation Therapy of cancer IRT. Annual Conference of German Pharmaceutical Society, 10-13.10.2007, Erlangen.

G. Shazly, T. Nawroth, and P. Langguth (2008). Comparison of dialysis and dispersion methods for in vitro release determination of drugs from multilamellar liposomes. *Dissolution Technologies,* May 2008, 7-10.

T. Nawroth, P. Buch, N. Glube, T. Peters, G. Shazly, P. Langguth, B. Pairet, H. Decker, H. Schmidberger, Ch. Alexiou, G. LeDuc, A. Bravin, P. Boesecke, R.P. May (2008). Nanoparticles for cancer therapy, liposomes, lipoid particles and ferrofluids. International workshop of mechanical and electrical properties of artificial and cellular membranes at the conference of the German Biophysical Society, 31.03-02.04.2008.

G. Shazly, T. Nawroth, and P. Langguth (2008). In vitro release methods affect the drug release from multilamellar liposomes. Assiut University 6th International Pharmaceutical Science Conference, Faculty of Pharmacy, Assiut, Egypt, March, 12&13, 2008.

T. Nawroth, N. Glube, T. Peters, P. Buch, K. Buch, G. Shazly, P. Langguth, B. Pairet, H. Decker, D. Bickes-Kelleher, P. Vaupel, Schmidberger, M. Konerding, Ch. Alexiou, St. Corde, R. Gähler, B. Lauss, M. Jentsche, R.P. May, P. Boesecke, A. Bravin, G. LeDuc (2008). Nano-IRT: Indirect Radiation Therapy with Nanoparticles Liposomes, Lipoid particles and Ferrofluids. The SYRAD conference on "brain tumor radiotherapy with synchrotron radiation", Grenoble 2008, 2.-4.6.2008

T. Nawroth, T. Peters, N. Glube, P. Buch, G. Shazly,P. Langguth, B. Pairet, H. Decker , B. Lauss , M. Jentschel, R.P. May, P. Callow, P. Boesecke (2008). Structure dynamics of liposomes and lipoid particles: SAXS, SANS, DLS- Nanoparticles for bio-membrane research and cancer therapy. Biomolecular Dynamics Neutron scattering workshop Feldafing-Munich, 24.-26.9. 2008

T. Peters, N. Glube, G. Shazly, T. Nawroth, H. Schmidberger, P. Langguth (2008). Manufacture and Characterization of Nanoparticles for the Improvement of Radiation Therapy. Annual Conference of German Pharmaceutical Society, 08-11.10.2008, Bonn.

T. Nawroth, G. Shazly, T. Peters, D. Palm, P. Langguth. Estimation of heveay metal content and release of Erbium-Chelate of liposomes for nanotherapy by light absorption spectroscopy (in preparation).